Dissertation zur Erlangung des Doktorgrades
der Fakultät für Chemie und Pharmazie
der Ludwig-Maximilians-Universität München

Multinary Lithium (Oxo)nitridosilicates: Syntheses, Structures and their Materials Properties

Katrin Horky, geb. Rudolf

aus

Selb, Deutschland

2017

Erklärung

Diese Dissertation wurde im Sinne von § 7 der Promotionsordnung vom 28. November 2011 von Herrn Prof. Dr. W. Schnick betreut.

Eidesstattliche Versicherung

Diese Dissertation wurde eigenständig und ohne unerlaubte Hilfe erarbeitet.

München, den 22.09.2017

…….

(Katrin Horky)

Dissertation eingereicht am	11.10.2017
1. Gutachter	Prof. Dr. W. Schnick
2. Gutachter	Prof. Dr. Oliver Oeckler
Mündliche Prüfung am	06.11.2017

Für meine Familie

Acknowledgement

Mein erster und ganz besonderer Dank gilt Herrn Prof. Dr. Wolfgang Schnick für die Möglichkeit, meine Doktorarbeit in seinem Arbeitskreis anzufertigen. Für die gegebene Freiheit bei der Bearbeitung des interessanten Forschungsthemas sowie für die hervorragenden Arbeitsbedingungen bin ich ebenfalls sehr dankbar.

Besonderer Dank gilt auch Herrn Prof. Dr. Oliver Oeckler für die Bereitschaft das Koreferat für diese Dissertation zu übernehmen und für die Hilfsbereitschaft bei Fragestellungen.

Frau Prof. Dr. Lena Daumann, sowie den Herrn Prof. Dr. Konstantin Karaghiosoff, Prof. Dr. Hans-Christian Böttcher und Prof. Dr. Schmahl danke ich für die Bereitschaft, mir als weitere Prüfer zur Verfügung zu stehen.

Herrn Dr. Peter Mayer, Herrn Dr. Constantin Hoch, Herrn Peter Wagatha und Herrn Thomas Miller danke ich für die zahlreichen Einkristallmessungen. Großer Dank gilt dabei vor allem Herrn Dr. Constantin Hoch für sein offenes Ohr und seine Hilfsbereitschaft bei kristallographischen Problemen. Herrn Christian Minke danke ich für die zahlreichen Stunden am REM und den damit verbundenen netten und unterhaltsamen Gesprächen.

Frau Olga Lorenz, Herrn Thomas Miller und Herrn Wolfgang Wünschheim danke ich für ihre stete Unterstützung bei allerhand organisatorischer, computertechnischer und sicherheitsrelevanten Fragen.

Meinen Praktikanten Kathrin Grieger, Kathrin Baader, Alexander Landel, Chantal von der Heide und Alicia Dufter danke ich für ihr Interesse an meinem Forschungsgebiet, ihre Arbeit und Unterstützung. Besonders Alicia wünsche ich für Ihre Doktorarbeit noch alles erdenklich Gute.

Ebenfalls danken möchte ich all meinen Laborkollegen für die schöne Zeit und die gute Atmosphäre in D2.103. Allen weiteren ehemaligen und aktuellen Kollegen der Arbeitsgruppen Schnick, Johrendt, Lotsch, Oeckler und Hoch für die nette Stimmung und eine tolle Zeit im zweiten Stock.

Frau Dr. Dajana Durach danke ich ganz besonders, dass sie immer für mich da war, mich von Anfang an durchweg tatkräftig unterstützt, mich immer wieder ermutigt und an mich geglaubt hat. Ich bin sehr dankbar dafür, dass uns der Arbeitskreis Schnick zueinander geführt hat. Danke für die unvergessliche Zeit in München und dass sich an unserer Freundschaft auch danach nichts geändert hat und wir weiterhin gemeinsam durch Dick und Dünn gehen.

Frau Dr. Christine Pösl möchte ich ebenfalls sehr danken, dass sie mir seit meiner gesamten Studienzeit in München immer eine treue Begleiterin ist und alle Hürden während dieser Zeit mit mir gemeistert hat. Sie hatte immer ein offenes Ohr für mich, wir haben uns immer gut verstanden und hatten stets viel zu Lachen. Danke dafür, dass dies auch weiterhin so ist.

Frau Marina Zelger danke ich ebenfalls ganz besonders für Ihre treue Freundschaft und stete Unterstützung. Auch hier hat die Studienzeit dafür gesorgt, dass wir zusammengefunden haben und seitdem immer zusammenhalten. Danke, dass sie von Beginn an immer für mich da war, dass wir so vieles gemeinsam durchgestanden und erlebt haben und für die wunderschöne Zeit in München.

Allergrößter Dank gilt meiner kompletten Familie und ganz besonders meinen Eltern, ohne deren Hilfe, Unterstützung und Glauben an mich wäre das alles nicht möglich gewesen und ich wäre nicht da, wo ich heute bin.

Von ganzem Herzen danke ich aber meinem Mann Stefan, dafür dass ich mich immer auf ihn verlassen und auf ihn bauen kann, dass er mich immer unterstützt, schützt, an mich glaubt und schon mein halbes Leben stets an meiner Seite ist und alles mit mir meistert. Ich freue mich sehr auf unsere gemeinsame Zukunft!

„Unsere größte Leistung besteht nicht darin, niemals zu fallen,

sondern immer wieder aufzustehen!“

(Konfuzius)

Table of Contents

1 Introduction 1

2 Lithium (Oxo)nitridosilicates and their Structural Diversity 8

2.1 Introduction 8

2.2 Investigations into the Synthesis of Ternary and Quaternary Lithium (Oxo)nitridosilicates 15

2.2.1 Introduction 15

2.2.2 Experimental Part 15

2.2.2.1 General 15

2.2.2.2 Ampoule reactions 15

2.2.2.3 Crucible reactions 16

2.2.2.4 High-pressure reactions 16

2.2.2.5 Elemental Analysis 16

2.2.2.6 Powder X-ray Diffraction 16

2.2.2 Results and Discussion 17

2.2.3 Conclusion 24

2.3 $Ba_{32}[Li_{15}Si_9W_{16}N_{67}O_5]$- a Ba-containing Oxonitridolithotungsto-silicate with a Highly Condensed Network Structure 26

2.3.1 Introduction 27

2.3.2 Results and Discussion 29

2.3.2.1 Synthesis and Chemical Analysis 29

2.3.2.2 Single-Crystal Structure Analysis 30

2.3.2.3 Structure Description 33

2.3.2.4 Lattice-Energy Calculations (MAPLE) 37

2.3.2.5 UV-VIS Spectroscopy 39

2.3.3 Conclusions 40

2.3.4 Experimental Section 41

2.3.4.1 General 41

2.3.4.2 Synthesis of $Ba_{32}[Li_{15}Si_9W_{16}N_{67}O_5]$ 41

2.3.4.3 SEM and EDX Spectroscopy 41

2.3.4.4 Single-crystal X-ray diffraction 42

2.3.4.5 Powder X-ray diffraction 42

2.3.4.7 UV-Vis Spectroscopy 43

2.3.4.8 FT-IR Spectroscopy 43

2.3.5 References 44

2.4 $LiCa_4Si_4N_8F$ and $LiSr_4Si_4N_8F$ – Nitridosilicate Fluorides with a BCT-Zeolite Type Network Structure 48

2.4.1 Introduction 49

2.4.2 Results and Discussion 51

2.4.2.1 Synthesis and Sample Characterization 51

2.4.2.3 Lattice-Energy Calculations (MAPLE) 58

2.4.3 Conclusions 60

2.4.4 Experimental Section 61

2.4.4.1 General 61

2.4.4.3 Synthesis of $LiSr_4Si_4N_8F$ 61

2.4.4.4 SEM and EDX Spectroscopy 61

2.4.4.5 Single-crystal X-ray diffraction 62

2.4.5 References 63

3 Lithium (Oxo)nitridosilicates and their Material Properties 66

3.1 Introduction 66

3.2 $Li_{24}Sr_{12}[Si_{24}N_{47}O]F:Eu^{2+}$ - Structure and Luminescence of an Orange Phosphor 71

3.2.1 Introduction 72
3.2.2 Experimental Section 74
3.2.2.1 Synthesis 74
3.2.2.2 SEM and EDX Spectroscopy 74
3.2.2.3 Single-Crystal X-ray Diffraction 75
3.2.2.4 Powder X-ray Diffraction 75
3.2.2.5 Luminescence 75
3.2.2.6 FTIR Spectroscopy 75
3.2.3 Results and Discussion 76
3.2.3.1 Synthesis and Chemical Analysis 76
3.2.3.2 Single-Crystal Structure Analysis 77
3.2.3.3 Crystal Structure Description 79
3.2.3.4 Investigations with PLATON 82
3.2.3.5 Lattice Energy Calculations 83
3.2.3.6 Luminescence 84
3.2.4 Conclusion 88
3.2.5 References 89
3.3 Li^+ ion Conductivity Investigations of Li_2SiN_2:Ca,Mg^{2+} 92
3.3.1 Introduction 92
3.3.2 Experimental Part 94
3.3.2.1 General 94
3.3.2.2 General Experimental Procedure 94
3.3.2.3 Powder X-ray diffraction 94
3.3.2.4 EDX measurements 94
3.3.2.5 Conductivity measurements 95
3.3.3 Results and Discussion 96

3.3.4 Conclusion 100

References 101

4 Conclusion and Outlook 102

5 Summary 107

5.1 Investigations into the Synthesis of Ternary and Ouaternary Lithium (Oxo)nitridosilicates 107

5.2 $Ba_{32}[Li_{15}Si_9W_{16}N_{67}O_5]$ – a Ba-containing Oxonitridolitho-tungstosilicate with a Highly Condensed Network Structure 108

5.3 $LiCa_4Si_4N_8F$ and $LiSr_4Si_4N_8F$ – Nitridosilicate Fluorides with a BCT-Zeolite Type Network Structure 110

5.4 $Li_{24}Sr_{12}[Si_{24}N_{47}O]F:Eu^{2+}$ - Structure and Luminescence of an Orange Phosphor for Warm White LEDs 112

5.5 Li^+ ion Conductivity Investigations of Li_2SiN_2:Ca,Mg^{2+} 113

6 Appendix 115

6.1 Supporting Information for Chapter 2.3 115

6.2 Supporting Information for Chapter 2.4 118

6.3 Supporting Information for Chapter 3.2 121

7 Publications 123

7.1 List of Publications Included in this Thesis 123

7.2 Conference Contributions 124

7.3 CSD Numbers 124

8 Curriculum Vitae 125

1 Introduction

Almost two centuries ago, the element lithium was discovered. The Swedish scientist Johann August Arfvedson found the latter 1817 in the mineral petalite ($LiAl(Si_2O_5)_2$).[1-3] Therefore, he named it after the Greek word for stone (λίθος), lithium. One year later William Thomas Brande and Sir Humphrey Davy isolated for the first time smaller amounts of the alkali metal element lithium by electrolysis of Li_2O.[1-2] In 1855 it became possible to obtain larger amounts of elemental lithium by electrolysis of LiCl.[2] First, there were no obvious applications of lithium. Later, lithium was employed for the safe storage of heavy hydrogen in nuclear weapons as well as for the reaction to tritium. Thus, a rapidly increasing importance of lithium and its compounds started during World War II.[4-5] Due to question of energy management in our society this trend lasts until nowadays. The search for alternative energies and storage systems is indispensable. Therefore, lithium batteries moved into the focus of research as their efficiency makes them promising candidates for the solution of the problem of energy storage.[6-8] Lithium is also used for further applications as shown in Figure 1. Thus, lithium is currently one of the elements with the fastest growing demand rate.

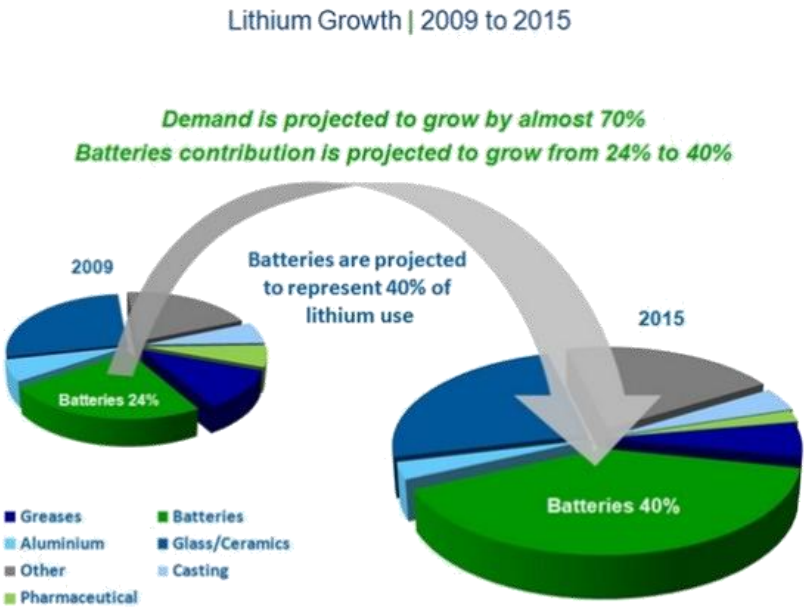

Figure 1. Growth of lithium from 2009 until 2015.[9]

With the increasing importance of lithium *Juza* et al. studied the quasi binary system Li_3N-Si_3N_4 in 1953.[10] During this research the novel compound class of nitridosilicates was discovered. Only decades later - due to the growing technological relevance of non-oxidic materials as high performance ceramics (Si_3N_4, AlN) - nitridosilicates and nitride compounds were again in the scientific focus and a systematic investigation of the latter took place.[11-13]

Usually, there is no natural occurrence of (oxo)nitridosilicates due to the ubiquitous presence of oxygen and water in our world. Sinoite (Si_2N_2O) – which however has meteoritic origin – is the only known exception.[14-15] Typically Si-N bonding is less stable than Si-O bonding. Thus, most solid nitrides are thermodynamically less stable than their corresponding oxides. Consequently, only kinetically hindered nitridosilicates – such with a high degree of condensation - are stable in air and towards hydrolysis.[13] As a general consequence, the bonding situation in oxo- and nitridosilicates is significantly different, although both compounds are consisting of building blocks formed by SiN_4 or SiO_4 tetrahedra, respectively. From a structural point of view nitridosilicates exhibit more structural opportunities, since oxosilicates are restricted to terminal and simply bridging oxygen. In comparison to Si-O distances the Si-N distances are larger and less ionic, which makes threefold and even fourfold linkage of neighboring tetrahedral centers possible. Additionally, both edge- as well as corner-sharing of SiN_4 tetrahedra exist in nitridosilicates, while SiO_4 tetrahedra exclusively share common corners.[16-17] The only known exception is fibrous SiO_2. However, its existence has not been unambiguously substantiated.[18] Due to the exceptional structural variety of nitridosilicates an extended range for the degree of condensation κ = n(Si):n(N) is given. K has a maximum value of $^3/_4$, e.g. in Si_3N_4. Corresponding to non-condensed tetrahedral anions, the values for oxosilicates reach only between $^1/_4$ and $^1/_2$ in SiO_2.[16, 19] The mentioned structural opportunities of nitridosilicates lead to non-condensed,[20] one-dimensional,[21-22] and layer-like silicate substructures[23] as well as three-dimensional silicate frameworks, which can be found in $EA_2Si_5N_8$ (*EA* = Sr, Ba) (Figure 2).[24] These examples illustrate the great structural variability of (oxo)nitridosilicates (chapter 2).

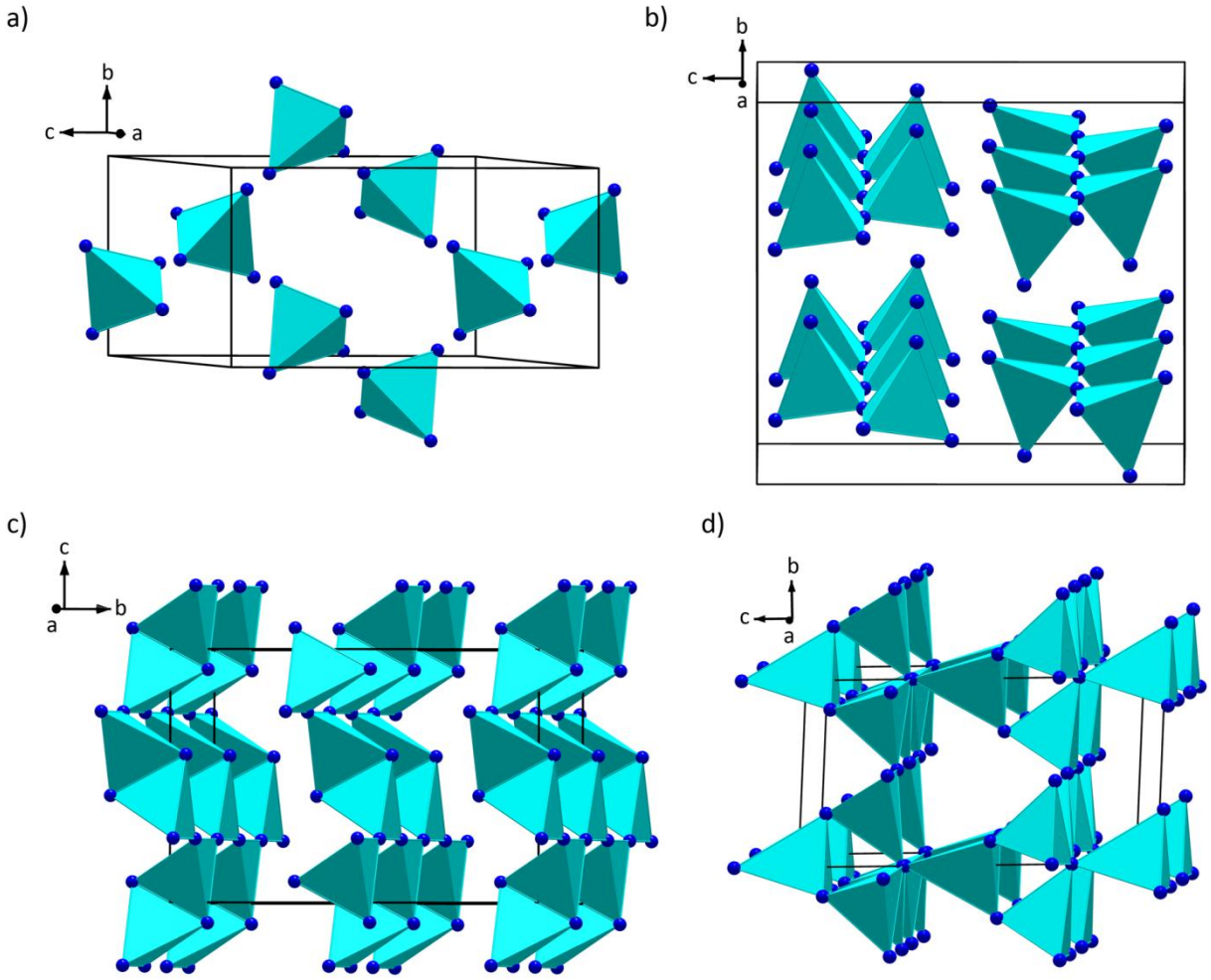

Figure 2. Silicate substructure of a) Ca_4SiN_4 (isolated SiN_4 tetrahedra);[20] b) Eu_2SiN_3 (non-branched single-chains of corner sharing SiN_4 tetrahedra);[22] c) $BaSiN_2$ (sheets of corner and edge sharing SiN_4 tetrahedra;[23] d) $MYbSi_4N_7$ (M = Eu, Sr, Ba; highly condensed network of corner sharing SiN_4 tetrahedra and $[N(SiN_3)_4]$ building blocks.[25-27] SiN_4 tetrahedra are depicted in turquoise.

Several interesting materials properties are connected with these structural possibilities. Such materials properties are of special interest since the development and use of energy-efficient technologies is essential for our future. Especially, through the automotive sector and electric lighting huge energy consumption is given. Thus, the improvement of the ecological footprint of these areas is of great potential. Therefore, materials scientists as well as solid-state chemists deal with syntheses, comprehensive structural characterizations and materials property investigations of novel compounds. Especially, solid-state materials, including innovations for electric vehicles and lighting play an important role.[28-29] Li-containing nitrides may find application as solid-state electrolytes in lithium ion-batteries

with a possible use in electric vehicles.[6-7, 30] For example, thoroughly investigated Li_2SiN_2 is a lithium nitridosilicate exhibiting Li-ion conductivity.[30-32] Regarding the lighting industry, several nitridosilicates show luminescence properties upon doping with rare earth ions like Eu^{2+} or Ce^{3+}, and are being used as luminescent materials in phosphor-converted light-emitting diodes (pc-LEDs).[33-40] The utilization as phosphor for pc-LEDs is the currently most important application of nitridosilicates, which will be discussed in chapter 3 in detail.[41-42] Next to the already mentioned applications, nitridosilicates may be used as nonlinear optic materials in computer and optical signal processing devices, optical frequency conversion, and telecommunications.[32, 43-44] Due to their high thermal conductivity nitridosilicates can also be applied as heat sink materials.[45-46] Furthermore, nitridosilicates show a great hardness due to higher covalency of bonds, e.g. $SrSi_7N_{10}$ exhibits a Vickers hardness of 16.1(5) GPa.[47] Thus, multinary lithium (oxo)nitridosilicates might be very promising from a structural point of view as well as concerning applications.

The objective of this thesis was the synthesis, identification and characterization of novel lithium (oxo)nitridosilicates in order to investigate as well as to expand the materials properties of this compound class. Therefore, different synthesis strategies were carried out. Crystal structure elucidation with single-crystal X-ray diffraction was carried out on new compounds. Moreover, investigations of physical properties like luminescence and lithium ion conductivity were performed. The first part of this thesis deals with the synthesis and characterization of novel multinary lithium (oxo)nitridosilicates with different silicate substructures. In the second part intriguing luminescence properties of a lithium (oxo)nitridosilicatefluoride plus doping of Li_2SiN_2 with Ca^{2+}/Mg^{2+} - in order to achieve an enhancement of the lithium ion conductivity – will be discussed. With the reported compounds an extension in the class of lithium (oxo)nitridosilicates was gained and observation of luminescence points out their possible applications.

References

[1] H. H. Binder, *Lexikon der chemischen Elemente: das Periodensystem in Fakten, Zahlen und Daten*, S. Hirzel, Stuttgart, **1999**.

[2] P. Enhang, *Encyclopedia of the Elements*, Wiley-VCH, Weinheim, **2004**.

[3] Q.-S. Hans-Jürgen, *Die Welt der Elemente - die Elemente der Welt*, Wiley-VCH, Weinheim, **2006**.

[4] R. Rhodes, *The Making of the Atomic Bomb*, Simon & Schuster, New York, **1986**.

[5] R. J. Pulham, P. Hubberstey, *J. Nucl. Mater.* **1983**, *115*, 239.

[6] A. D. Robertson, A. R. West, A. G. Ritchie, *Solid State Ionics* **1997**, *104*, 1.

[7] M. S. Whittingham, *Chem. Rev.* **2004**, *104*, 4271.

[8] J. F. M. Oudenhoven, L. Baggetto, P. H. L. Notten, *Adv. Energy Mater.* **2011**, *1*, 10.

[9] *http://www.miningscout.de/bilder/1206304557_blog/2453653251_ anwendung_lithium.jpg* **22.07.2017**.

[10] R. Juza, H. H. Weber, E. Meyer-Simon, *Z. Anorg. Allg. Chemie* **1953**, *273*, 48.

[11] H. Lange, G. Wötting, G. Winter, *Angew. Chem.* **1991**, *103*, 1606; *Angew. Chem. Int. Ed. Engl.* **1991**, *1630*, 1579.

[12] K. Kim, W. R. L. Lambrecht, B. Segall, *Phys. Rev. B* **1996**, *53*, 16310.

[13] W. Schnick, *Angew. Chem.* **1993**, *105*, 846; *Angew. Chem. Int. Ed. Engl.* **1993**, *32*, 806.

[14] W. H. Baur, *Nature* **1972**, *240*, 461.

[15] A. Bischoff, T. Grund, T. Jording, B. Heying, R.-D. Hoffmann, U. C. Rodewald, R. Pöttgen, *Z. Naturforsch. B* **2005**, *60b*, 1231.

[16] M. Zeuner, S. Pagano, W. Schnick, *Angew. Chem.* **2011**, *123*, 7898; *Angew. Chem. Int. Ed*. **2011**, *50*, 7754.

[17] W. Schnick, H. Huppertz, *Chem. Eur. J.* **1997**, *3*, 679.

[18] A. Weiss, *Z. Anorg. Allg. Chemie* **1954**, *276*, 95.

[19] F. Liebau, *Naturwissenschaften* **1962**, *49*, 481.

[20] H. Yamane, H. Morito, *Inorg. Chem.* **2013**, *52*, 5559.

[21] S. Lupart, M. Zeuner, S. Pagano, W. Schnick, *Eur. J. Inorg. Chem.* **2010**, 2636.

[22] M. Zeuner, S. Pagano, P. Matthes, D. Bichler, D. Johrendt, T. Harmening, R. Pöttgen, W. Schnick, *J. Am. Chem. Soc.* **2009**, *131*, 11242.

[23] Z. A. Gal, P. M. Mallinson, H. J. Orchard, S. J. Clarke, *Inorg. Chem.* **2004**, *43*, 3998.

[24] T. Schlieper, W. Milius, W. Schnick, *Z. Anorg. Allg. Chemie* **1995**, *621*, 1380.

[25] H. Huppertz, W. Schnick, *Acta Crystallogr. Sect C* **1997**, *53*, 1751.

[26] H. Huppertz, W. Schnick, *Angew. Chem.* **1996**, *108*, 2115; *Angew. Chem. Int. Ed. Engl.* **1996**, *35*, 1983.

[27] H. Huppertz, W. Schnick, *Z. Anorg. Allg. Chemie* **1997**, *623*, 212.

[28] Y. Zhu, X. He, Y. Mo, *J. Mater. Chem. A* **2016**, *4*, 3253.

[29] J. M. Phillips, M. E. Coltrin, M. H. Crawford, A. J. Fischer, M. R. Krames, R. Mueller-Mach, G. O. Mueller, Y. Ohno, L. E. S. Rohwer, J. A. Simmons, J. Y. Tsao, *Laser Photonics Rev.* **2007**, *1*, 307.

[30] H. Yamane, S. Kikkawa, M. Koizumi, *Solid State Ionics* **1987**, *25*, 183.

[31] S. Pagano, M. Zeuner, S. Hug, W. Schnick, *Eur. J. Inorg. Chem.* **2009**, 1579.

[32] M. S. Bhamra, D. J. Fray, *J. Mater. Sci.* **1995**, *30*, 5381.

[33] X.-H. He, N. Lian, J.-H. Sun, M.-Y. Guan, *J. Mater. Sci.* **2009**, *44*, 4763.

[34] K. Uheda, N. Hirosaki, H. Yamamoto, *Phys. Status Solidi A* **2006**, *203*, 2712.

[35] P. Pust, V. Weiler, C. Hecht, A. Tücks, A. S. Wochnik, A.-K. Henß, D. Wiechert, C. Scheu, P. J. Schmidt, W. Schnick, *Nat. Mater.* **2014**, *13*, 891.

[36] H. Watanabe, N. Kijima, *J. Alloys. Compd.* **2009**, *475*, 434.

[37] R.-J. Xie, N. Hirosaki, Y. Li, T. Takeda, *Materials* **2010**, *3*, 3777.

[38] H. A. Höppe, H. Lutz, P. Morys, W. Schnick, A. Seilmeier, *J. Phys. Chem. Solids* **2000**, *61*, 2001.

[39] M. Zeuner, P. J. Schmidt, W. Schnick, *Chem. Mater.* **2009**, *21*, 2467.

[40] S. Schmiechen, H. Schneider, P. Wagatha, C. Hecht, P. J. Schmidt, W. Schnick, *Chem. Mater.* **2014**, *26*, 2712.

[41] S. Schmiechen, P. Pust, P. J. Schmidt, W. Schnick, *Nachr. Chem.* **2014**, *62*, 847.

[42] R. Mueller-Mach, G. Mueller, M. R. Krames, H. A. Höppe, F. Stadler, W. Schnick, T. Juestel, P. Schmidt, *Phys. Status Solidi A* **2005**, *202*, 1727.

[43] S. R. Marder, G. D. Stucky, J. E. Sohn, *Materials for Nonlinear Optics: Chemical Perspectives,* ACS Symp. Ser.*, Vol. 455*, **1991**.

[44] H. Lutz, S. Joosten, J. Hoffmann, P. Lehmeier, A. Seilmeier, H. A. Höppe, W. Schnick, *Phys. Chem. Solids* **2004**, *65*, 1285.

[45] G. A. Slack, *J. Phys. Chem. Solids* **1973**, *34*, 321.

[46] M. Kitayama, K. Hirao, K. Watari, M. Toriyama, S. Kanzaki, *J. Am. Ceram. Soc.* **2001**, *84*, 353.

[47] G. Pilet, H. A. Höppe, W. Schnick, S. Esmaeilzadeh, *Solid State Sci.* **2005**, *7*, 391.

2 Lithium (Oxo)nitridosilicates and their Structural Diversity

2.1 Introduction

Due to their comprehensive structures as well as their outstanding materials properties (Chapter 1), (oxo)nitridosilicates are in the focus of interest. Accordingly, scientists all over the world are continuously searching for new (oxo)nitridosilicates. Since 1953 lithium nitridosilicates are well-known in the quasi-binary system Li_3N-Si_3N_4.[1] In consequence several lithium (oxo)nitridosilicates with different structures are described in literature. Table 1 gives an overview about known ternary lithium (oxo)nitridosilicates. These compounds have been studied in some depth recently due to their high mobility of lithium ions in their structures and their potential application as solid-state electrolytes (Chapter 3).

Table 1. Known lithium (oxo)nitridosilicates and their structures.

compound	structure
$LiSi_2N_3$[2]	wurtzite
Li_2SiN_2[3]	two interpenetrating cristobalite type nets which are made up from hetero-adamantane-like $[Si_4N_6]N_{4/2}$ groups
Li_5SiN_3[1]	antifluorite superstructure
Li_8SiN_4[4]	unknown
$Li_{18}Si_3N_{10}$[5]	unknown
$Li_{21}Si_3N_{11}$[6]	antifluorite superstructure
LiSiON[7]	wurtzite superstructure
$Li_5SiN_3 \cdot 2\ Li_2O$[1]	fluorite
Li_7SiN_3O[6]	antifluorite superstructure

Introduction of alkaline earth metals into lithium (oxo)nitridosilicates leads to diverse lithium alkaline earth (oxo)nitridosilicates, which can be used as efficient host lattices for phosphors

in LEDs (Chapter 3). Table 2 lists noted quaternary lithium (oxo)nitridosilicates with alkaline earth metals Ca and Sr and their structural motifs. Quaternary lithium (oxo)nitridosilicates with Mg or Ba are not known until now. Only two multinary lithium nitridosilicates with both, Mg and Ca, namely $Ca_2Mg[Li_4Si_2N_6]$ and $Li_2Ca_2[Mg_2Si_2N_6]$, were reported.[8]

Table 2. Known lithium alkaline earth (oxo)nitridosilicates and their structures.

compound	structure
$LiCa_3Si_2N_5$[9]	double chain of SiN_4 tetrahedra
$Li_2MSi_2N_4$ with *M* = Ca and Sr[10]	three-dimensional network of exclusive corner-sharing SiN_4 tetrahedra
$Li_2Sr_4Si_2N_6$[11]	2D layers of vertex-sharing SiN_4 tetrahedra
$Li_2Sr_4Si_4N_8O$[12]	BCT zeolite-type analogous network
$Li_4M_3Si_2N_6$ with *M* = Ca and Sr[13]	Non-condensed "bow-tie" $[Si_2N_6]^{10-}$ subunits

Synthesis of ternary Li-Si-N phases was typically carried out at temperatures between 700 °C and 1200 °C by solid-state reaction of Li_3N and Si_3N_4 under N_2 atmosphere (Table 3). It is clearly visible from Table 3 that the higher the synthesis temperature the less the lithium content in the ternary compounds. Compounds with high lithium content, as it would be desirable for application as solid-state electrolyte, are formed at lower temperatures (e.g. $Li_{21}Si_3N_{11}$ was synthesized at 800 °C). Also alternative synthesis routes have been reported, for example formation of crystalline Li_2SiN_2 has been achieved from the reaction of Li_3N with either amorphous "$Si(CN_2)_2$" or "$Si(NH)_2$"(Table 3). The use of these precursors in place of Si_3N_4 allows particularly reaction temperatures to be significantly reduced. Precursor approaches, which combine crystalline amide precursors and "$Si(NH)_2$", are well investigated for the synthesis of (oxo)nitridosilicates.[14] The advantage of this synthetic route is the high reactivity of the used amides, which leads to their decomposition into corresponding nitrides and imides.[15]

Table 3. Synthesis conditions of known lithium (oxo)nitridosilicates.

compound	synthesis temperature	starting materials
$LiSi_2N_3$[5]	1000 °C	Li_3N, Si_3N_4
Li_2SiN_2[3,5]	730 – 1200 °C	Li_3N, Si_3N_4;
		Li, Li_3N, "$Si(CN_2)_2$" or "$Si(NH)_2$"
		Li_3N, $SiCl_4$
Li_5SiN_3[5]	1200 °C	Li_3N, Si_3N_4
Li_8SiN_4[5]	800 °C	Li_3N, Si_3N_4
$Li_{18}Si_3N_{10}$[5]	800 °C	Si_3N_4, Li_3N
$Li_{21}Si_3N_{11}$[6]	800 °C	Si_3N_4, Li_3N
LiSiON[7]	1150 °C	Li_4SiO_4, Si_3N_4
$Li_5SiN_3 \cdot 2\ Li_2O$[16]	1100 °C	Li_3N, SiO_2
Li_7SiN_3O[6]	900 °C	Si_3N_4, Li_3N, Li_2O

Quaternary compounds were usually obtained in welded tantalum tubes under argon by heating typical starting materials for 12‑24 h. By using either Li_3N or LiN_3 as lithium‑nitrogen source the nitrogen pressure is tailored inside the tantalum ampoule. Hence, different degrees of condensation were accessible in the resulting quaternary phase structures (see Table 2 and 4). For instance, the compounds $Li_2MSi_2N_4$ (*M* = Ca, Sr), both with three-dimensional nitridosilicate substructures, were synthesized using LiN_3, which undergoes an explosive decomposition above ~ 115 °C to produce Li_3N and N_2 gas.[17] Low dimensional (oxo)nitridosilicates, however, such as $Li_4M_3Si_2N_6$ (*M* = Ca, Sr) and $LiCa_3Si_2N_5$, were synthesized using Li_3N. Also flux techniques utilizing metallic Li, like applied for example for synthesis of $Li_2MSi_2N_4$ with *M* = Ca and Sr (Table 4), are successfully synthetic approaches for (oxo)nitridosilicates. With this approach a variety of inorganic salts, complex anions and metals can be solved.[18,19] Also an enhanced solubility of nitrogen is given when alkali metals were inserting to the reaction mixture. This is a decisive aspect for the synthesis of nitrides in liquid alkali metals. Additionally, this approach enables access to several (oxo)nitridosilicates at temperatures lower than 1000 °C (Table 4).[12,20]

Table 4. Synthesis conditions of known lithium alkaline earth (oxo)nitridosilicates.

compound	synthesis temperature	starting materials
$LiCa_3Si_2N_5$[9]	900 °C	Ca, "$Si(NH)_2$", Li_3N
$Li_2MSi_2N_4$ with *M* = Ca and Sr[10]	900 °C	Li, Ca/Sr, "$Si(NH)_2$", LiN_3
$Li_2Sr_4Si_2N_6$[11]	900 °C	Sr, "$Si(NH)_2$", LiN_3
$Li_2Sr_4Si_4N_8O$[12]	900 °C	Li, Sr, "$Si(NH)_2$", LiN_3, Li_2O
$Li_4M_3Si_2N_6$ with *M* = Ca and Sr[13]	900 °C	Ca/Sr, "$Si(NH)_2$", Li_3N

In summary, it can be stated that in literature reports on ternary lithium nitridosilicates $LiSi_2N_3$, Li_2SiN_2, Li_5SiN_3, $Li_{18}Si_3N_{10}$ and $Li_{21}Si_3N_{11}$ exists. However, up to now only two of it, namely $LiSi_2N_3$ and Li_2SiN_2, have been completely characterized by single crystal data (Figure 1). For the other above mentioned Li/Si/N compounds single crystal data are still needed. To gain information about their solid state structures and thereby again about their ion conductivities these data are indispensable.

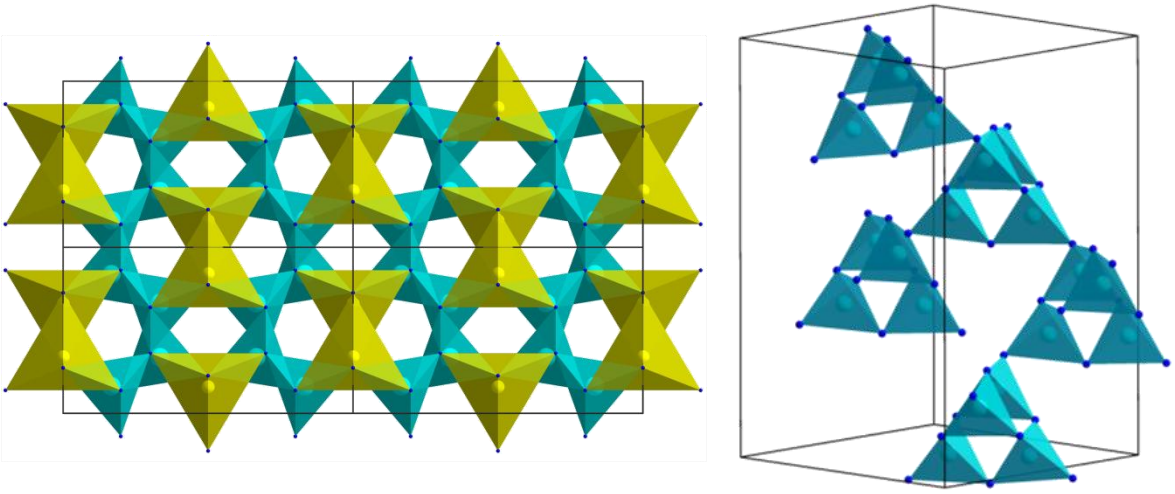

Figure 1. Crystal structure of $LiSi_2N_3$, view along [001] (left); branch of the cristobalite network in Li_2SiN_2 (right); SiN_4 tetrahedra turquoise, LiN_4 terahedra yellow.

Although quaternary lithium alkaline earth (oxo)nitridosilicates with Ca and Sr are accessible, the respective compounds as well as new compounds in the system Li/Ba/Si/N are still missing. Therefore it is the responsibility of scientists to search for new synthetic pathways that put forth crystalline products and also new compounds to obtain possibly new functional materials. In the course of this work, several synthetic pathways were investigated with the goal to synthesize and characterize hitherto unknown representatives of the mentioned compound classes. First of all, chapter 2.2 gives an overview about different efforts on the synthesis of ternary lithium (oxo)nitridosilicates as well as quaternary lithium (oxo)nitridosilicates with Ba and their general results. During this work a metathesis reaction was established in order to avoid thermodynamic sinks and the synthesis of already known compositions in the Li/Si/(O)/N system. This reaction mechanism is based on an similar synthetic approach developed by *Durach* et al. for a large number of new lanthanum (oxo)nitridosilicates.[21-24] This type of solid-state metathesis reaction was consistently performed in tungsten crucibles heated inductively with a radio-frequency furnace and based on the decomposition of an alkaline earth hydride EAH_2 with *EA* = Sr and Ba (e.g. decomposition of BaH_2 at 675 °C)[25] and its reaction with LiF to EAF_2. The latter resublimates at the cooled reactor wall of the furnace and the remaining EA^{2+} reacts with the preorganized starting materials "$Si(NH)_2$" or Si_3N_4 and $LiNH_2$ (Scheme 1).

Scheme 1:

Through this developed metathesis reaction it was possible to obtain the novel lithium (oxo)nitridosilicates $Ba_{32}[Li_{15}Si_9W_{16}N_{67}O_5]$ (chapter 2.3), $LiCa_4Si_4N_8F$ as well as $LiSr_4Si_4N_8F$ (chapter 2.4) and the new phosphor material $Li_{24}Sr_{12}Si_{24}N_{47}OF:Eu^{2+}$ (chapter 3.2).

References

[1] R. Juza, H. H. Weber, E. Meyer-Simon, *Z. Anorg. Allg. Chem.* **1953**, *273*, 48.

[2] M. Orth, W. Schnick, *Z. Anorg. Allg. Chem.* **1999**, *625*, 1426.

[3] S. Pagano, M. Zeuner, S. Hug, W. Schnick, *Eur. J. Inorg. Chem.* **2009**, 1579.

[4] J. Lang, J.-P. Charlot, *Rev. Chem. Miner.* **1970**, *7*, 121.

[5] H. Yamane, S. Kikkawa, M. Koizumi, *Solid State Ionics* **1987**, *25*, 183.

[6] M. Casas-Cabanas, H. Santner, M. R. Palacin, *J. Solid State Chem.* **2014**, *213*, 152.

[7] Y. Laurent, J. Guyader, G. Roult, *Acta Crystallogr. B* **1981**, *37*, 911.

[8] S. Schmiechen, F. Nietschke, W. Schnick, *Eur. J. Inorg. Chem.* **2015**, 1592.

[9] S. Lupart, W. Schnick, *Z. Anorg. Allg. Chemie* **2012**, *638*, 2015.

[10] M. Zeuner, S. Pagano, S. Hug, P. Pust, S. Schmiechen, C. Scheu, W. Schnick, *Eur. J. Inorg. Chem.* **2010**, 4945.

[11] S. Lupart, S. Pagano, O. Oeckler, W. Schnick, *Eur. J. Inorg. Chem.* **2011**, 2118.

[12] S. Pagano, S. Lupart, M. Zeuner, W. Schnick, *Angew. Chem.* **2009**, *121*, 6453; *Angew. Chem. Int. Ed.* **2009**, *48*, 6335.

[13] S. Pagano, S. Lupart, S. Schmiechen, W. Schnick, *Z. Anorg. Allg. Chem.* **2010**, *636*, 1907.

[14] M. Zeuner, F. Hintze, W. Schnick, *Chem. Mater.* **2009**, *21*, 336.

[15] M. Zeuner, S. Pagano, W. Schnick, *Angew. Chem.* **2011**, *123*, 7898; *Angew. Chem. Int. Ed*. **2011**, *50*, 7754.

[16] R. Juza, H. H. Weber, E. Meyer-Simon, *Z. Anorg. Allg. Chem.* **1953**, *273*, 48.

[17] H. D. Fair, R. F. Walker, *Energ. Mater.* **1977**, *1*.

[18] R. J. Pulham, P. Hubberstey, *J. Nucl. Mater.* **1983**, *115*, 239.

[19] P. Hubberstey, P. G. Roberts, *J. Chem. Soc. Dalton Trans.* **1994**, 667.

[20] Z. A. Gál, P. M. Mallinson, H. J. Orchard, S. J. Clarke, *Inorg. Chem.* **2004**, *43*, 3998.

[21] D. Durach, L. Neudert, P. J. Schmidt, O. Oeckler, W. Schnick, *Chem. Mater.* **2015**, *27*, 4832.

[22] D. Durach, W. Schnick, *Eur. J. Inorg. Chem.* **2015**, 4095.

[23] D. Durach, F. Fahrnbauer, O. Oeckler, W. Schnick, *Inorg. Chem.* **2015**, *54*, 8727.

[24] P. Schultz, D. Durach, W. Schnick, O. Oeckler, *Z. Anorg. Allg. Chemie* **2016**, *642*, 603.

[25] W. Grochala, P. Edwards, *Chem. Rev.* **2004**, *104*, 1283.

2.2 Investigations into the Synthesis of Ternary and Quaternary Lithium (Oxo)nitridosilicates

2.2.1 Introduction

Nitridosilicates represent an intriguing class of materials with various materials properties, and are typically made up of highly condensed tetrahedral network structures. Especially, lithium-containing nitridosilicates have high potential for Li^+ ion conductivity, and alkaline earth nitridosilicates emerged as promising host materials for Eu^{2+}-doped luminophores, which find broad application in phosphor-converted (pc)-LEDs (chapter 1). However, reports on lithium nitridosilicates, and also Ba-containing lithium nitridosilicates are quite rare or rather do not exist. As already stated, these compounds are of great importance regarding their materials properties and play a significant role in current research in nitride chemistry. In contrast to common strategies of preparing nitridosilicates, different synthetic approaches were performed to avoid thermodynamic sinks and to synthesize novel compounds. Therefore, both starting materials and reaction conditions were modified. In the following, syntheses strategies and their results are discussed in detail.

2.2.2 Experimental Part

2.2.2.1 General

Owing to the sensitivity to air and moisture of the starting materials, all manipulations were performed in flame-dried Schlenk-type glassware attached to a vacuum line (10^{-3} mbar) and in an argon-filled glovebox (Unilab, MBraun, Garching, O_2 <1 ppm, H_2O <1 ppm).

2.2.2.2 Ampoule reactions

For ampoule reactions, the starting materials were ground under argon atmosphere in a glovebox. The mixtures were placed in tantalum ampoules. The ampoules were arc-welded under Ar atmosphere and water cooling to prevent hydrolysis and chemical reactions during welding. The ampoules were placed in a silica tube and then heated in a tube furnace under vacuum. The reaction mixtures were heated to temperatures up to 1000 °C and the temperature was maintained for 4 - 24 h. Subsequently, the ampoule was cooled down to 350 °C at different rates, and finally quenched to room temperature by switching off the furnace.

2.2.2.3 Crucible reactions

Further high-temperature reactions were investigated by using a radio-frequency furnace (rf-furnace) (type IG 10/200, frequency 200 kHz, max electrical output 12 kW, Hüttinger, Freiburg).[1] The finely ground reaction mixtures were placed in a tungsten crucible under argon atmosphere (glove box) and then transferred into a water-cooled quartz reactor of a rf-furnace under nitrogen atmosphere. The temperature was raised to maximum 1500 °C, kept for varying times, cooled with different cooling rates and subsequently quenched to room temperature by switching off the rf-furnace.

2.2.2.4 High-pressure reactions

Different reactions of Li-N-sources (Li_3N, LiN_3, $LiNH_2$) with Si_3N_4 or "$Si(NH)_2$" under high-pressure and high-temperature were investigated by employing the multianvil technique in a Walker-type module (Voggenreiter, Mainleus) combined with a 1000 t press.[2-6] Syntheses were performed at 800 °C and 6 GPa.

2.2.2.5 Elemental Analysis

The chemical composition of some obtained products was investigated by energy dispersive X-ray (EDX) spectroscopy. For this purpose, a JSM-6500F scanning electron microscope (SEM, Jeol) containing a Si/Li EDX detector (Oxford Instruments, model 7418) was used.

2.2.2.6 Powder X-ray Diffraction

Most reaction products were obtained as bulk samples and investigated by powder X-ray diffraction (PXRD). Therefore, a STOE STADI P diffractometer (Cu-$K_{\alpha1}$ or Mo-$K_{\alpha1}$ radiation, Ge(111) monochromator, Mythen1K detector) in Debye-Scherrer geometry was used.

2.2.2 Results and Discussion

Ampoule and crucible reactions

Over the last years, several syntheses strategies for (oxo)nitridosilicates have been elaborated, such as high-temperature reactions, precursor routes and flux methods. Thereby, it was the aim to find new synthetic pathways leading to crystalline products, particularly in the field of ternary lithium (oxo)nitridosilicates, as well as novel representatives of the Li/Si/N and Li/Ba/Si/N compound classes. Thus, advanced functional materials may be obtained. In this thesis, different new approaches to novel lithium oxonitridosilicates were investigated. These include high temperature reactions in tantalum ampoules and tungsten crucibles as well as high-pressure reactions. Thereby, various starting materials in varying molecular ratios were used as well as different temperatures, reaction times and cooling rates were investigated. All products were characterized by powder X-ray diffraction. Table 1 gives an overview of most promising reaction conditions and products.

Table 1. Reaction conditions and products for the synthesis of lithium (oxo)nitridosilicates.

starting materials	reaction vessel	temperature [°C]	time [h]	products
lithium silicides	tantalum ampoule tungsten crucible	700 – 1300 °C	5h	known Li/Si or Li/Si/N compounds
Li_2SiN_2	tantalum ampoule tungsten crucible	800 °C	10 - 24h	known Li/Si/N compounds, microcrystalline products, no reaction
Si:Li_3N	tantalum ampoule	500 - 900 °C	4 – 8h	microcrystalline Li_8SiN_4
Si-precursors	tantalum ampoule tungsten crucible	700 – 1500 °C	5 - 24h	microcrystalline products, known Li/Si/N compounds, lithium tantalum/tungsten nitrides (Li_7TaN_4/Li_6WN_4)

Most ternary Li/Si/N phases are typically accessed by solid state reaction of the binary nitrides Li_3N and Si_3N_4. The investigated synthetic pathways include, among others, reactions starting from specially synthesized compounds - namely Li_2SiN_2, Li_7Si_3 and $Li_{12}Si_7$ - in order to verify their suitability as starting materials. According to *Gruber* et al. phase-pure samples of Li_7Si_3 and $Li_{12}Si_7$ were obtained by heating stoichiometric amounts of Li and Si in hermetically sealed Ta ampoules at 750 °C.[7] The respective diffraction patterns are depicted in Figure 1 and 2. A detailed description for the synthesis of phase-pure samples of Li_2SiN_2 is given in chapter 3.3.

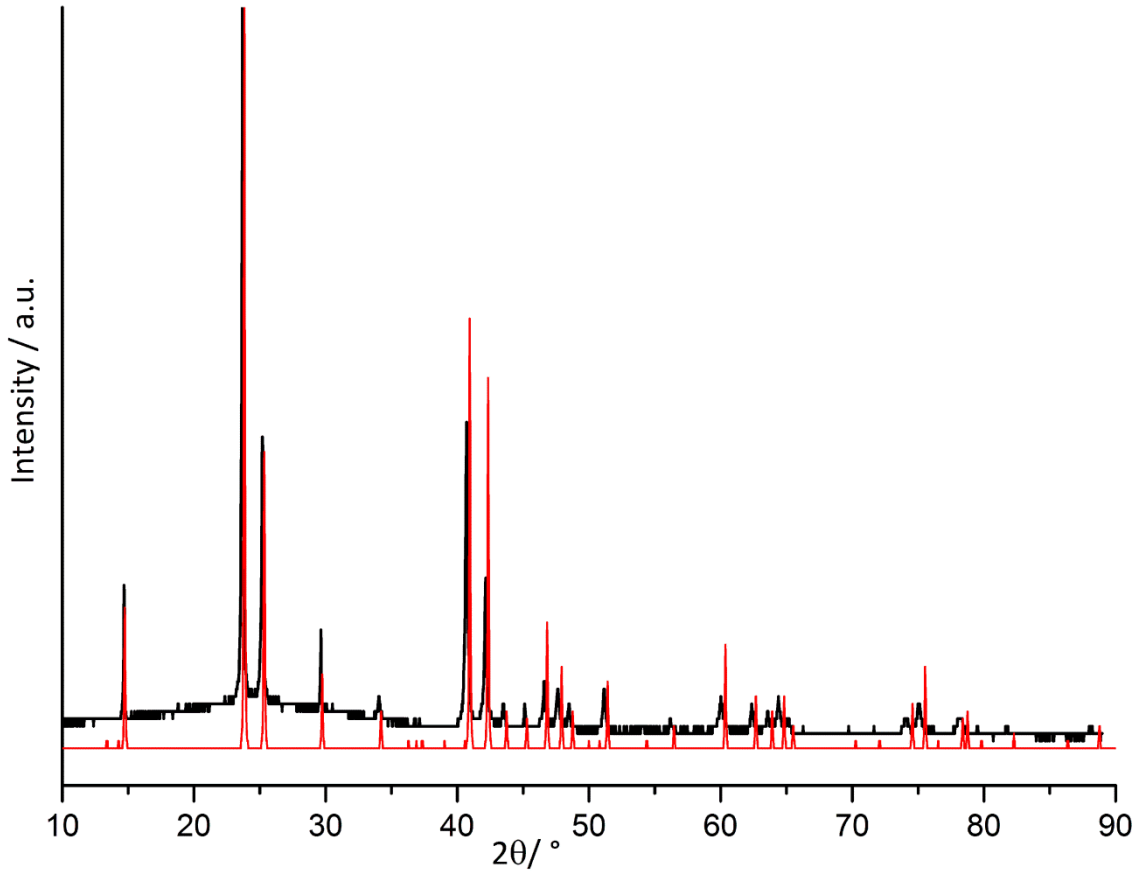

Figure 1. Characteristic section of the experimental powder diffraction pattern (Cu-$K_{\alpha1}$ radiation, black) of the sample containing Li_7Si_3. Red lines describe the simulation of the structural model obtained from single-crystal structure of Li_7Si_3.

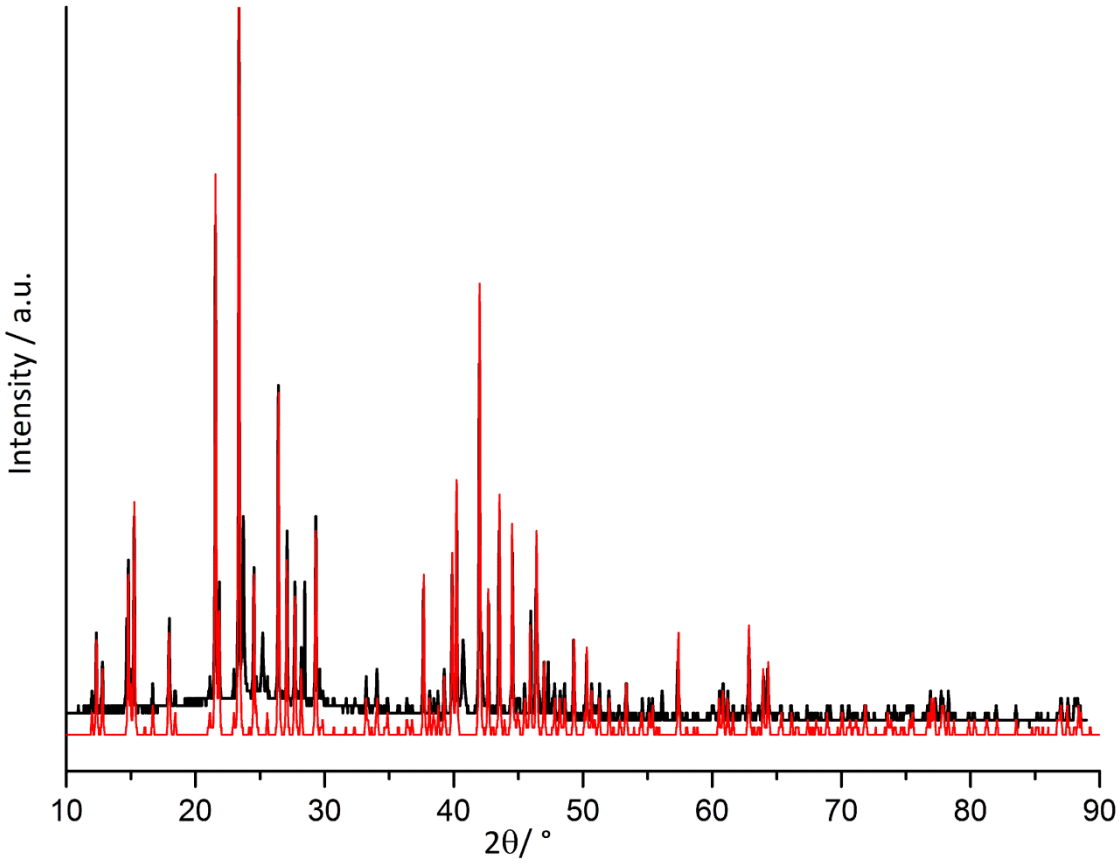

Figure 2. Characteristic section of the experimental powder diffraction pattern (Cu-$K_{\alpha1}$ radiation, black) of the sample containing $Li_{12}Si_7$. Red lines describe the simulation of the structural model obtained from single-crystal structure of $Li_{12}Si_7$.

By reaction of the synthesized lithium silicides with Li-N-sources like Li_3N, LiN_3 or $LiNH_2$, partly in combination with metallic Li as flux, formation of lithium silicides with an elevated Li-content (reaction products $Li_{12}Si_7$ and $Li_{22}Si_5$) compared to starting materials Li_7Si_3 and $Li_{12}Si_7$, and known lithium nitridosilicates ($LiSi_2N_3$, Li_2SiN_2) started at 800 °C. For reactions at 900 °C and above, complete formation to lithium nitridosilicates ($LiSi_2N_3$, Li_2SiN_2, $Li_{18}Si_3N_{10}$) was observed. All experiments starting from Li_2SiN_2 led either to microcrystalline products of known lithium nitridosilicates (Li_5SiN_3, $Li_{21}Si_3N_{11}$) or a further reaction of Li_2SiN_2 has not taken place.

In 2013, synthesis of the nitridogermanate Li_8GeN_4 was reported by *Aoyama* et al.[8] The latter was synthesized by reaction of Ge and Li_3N in a molar ratio of 1:2.5 at 700 °C in sealed Ta ampoules. An analogous solid-state reaction was performed in the system Li/Si/N. By reac-

tion of Si and Li_3N in a molar ration of 1:2.5, a microcrystalline sample containing Li_8SiN_4 was obtained. Corresponding powder X-ray diffraction pattern is shown in Figure 3. Due to small crystal sizes, structure determination by using single-crystal X-ray diffraction data is not possible yet.

Furthermore, the reactive precursors "$Si(NH)_2$", "$Si_2(NH)_3$" and "$Si(CN_2)_2$" were also investigated as starting materials. Their reaction with different Li-N-compounds (Li_3N, LiN_3, $LiNH_2$, LiH) and fluxing agents (Li, LiCl) often yielded microcrystalline or metallic reaction products containing known lithium nitridosilicates (e.g. Li_2SiN_2) or lithium tantalum and tungsten nitrides (e.g. Li_7TaN_4, Li_6WN_4) depending on the used reaction vessel.

In summary, the experiments mentioned above indicate that a synthetic access to novel compositions and structures of this compound class could not be achieved with the tried reactions.

High-pressure reactions

In order to investigate further synthetic approaches to lithium nitridosilicates, high-pressure reactions were performed. These included reactions of different Li-N-sources (Li_3N, LiN_3, $LiNH_2$) and Si_3N_4 or "$Si(NH)_2$" at 6 GPa and 800 °C in h-BN crucibles by employing the multi-anvil technique. In summary, Li_3BN_2 was the main product of nearly all reactions. For one approach the formation of Li_2SiN_2 was observed. This suggested that, despite the thermodynamically preferred formation of the stable compound Li_3BN_2, also an incorporation of Li in the target compound is possible. Additionally, through a further approach starting from 15 mg (0.11 mmol)Si_3N_4, 26.06 mg (0.75 mmol) Li_3N and 15.70 mg (0.32 mmol) LiN_3 yielded a colorless powder, which was characterized by EDX measurements and by PXRD (Fig. 3).

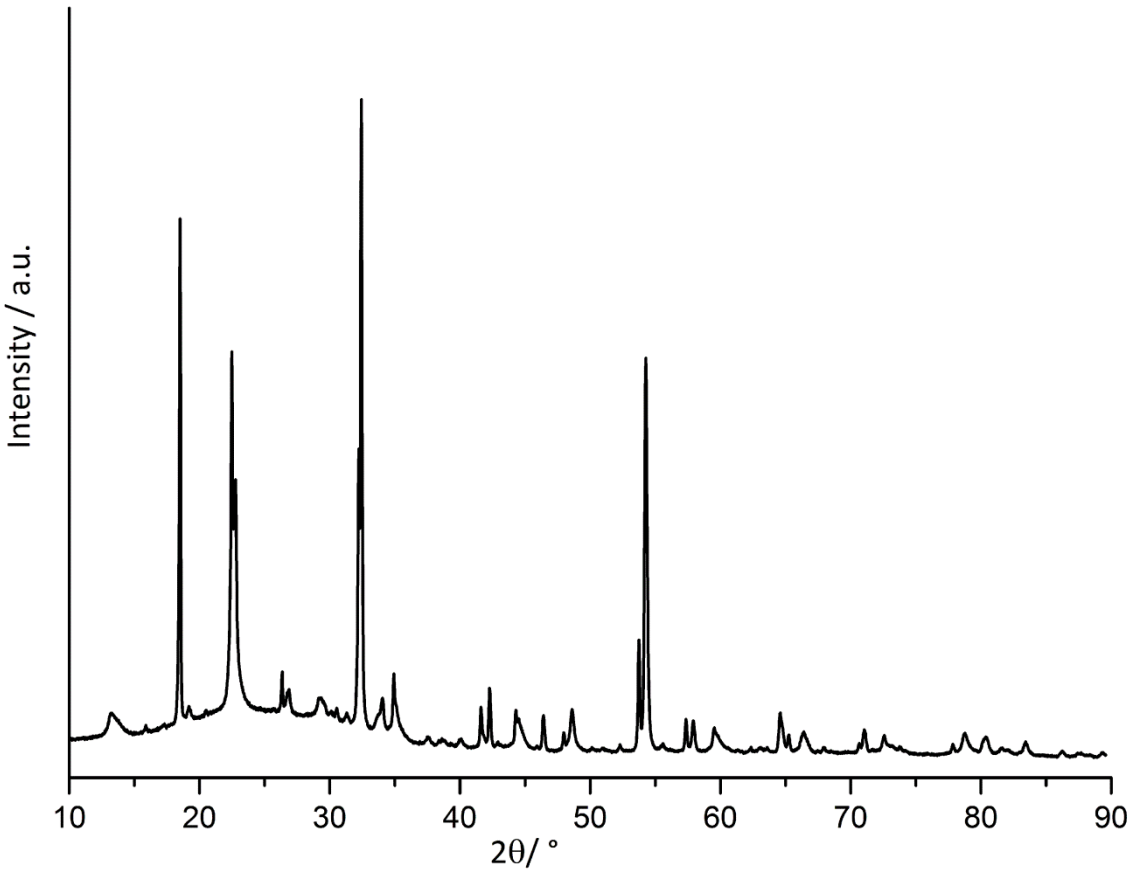

Figure 3. Experimental PXRD data (Cu-$K_{\alpha 1}$ radiation) of the high-pressure synthesis of "Li_8SiN_4". No reflections could be assigned to known phases.

Screening of numerous databases yielded no match with any known phase(s). The experimental powder pattern exhibits both sharp and broad reflections with different intensities, and less intensive reflections, which indicates the formation of more than one phase. Indexing by using the charge-flipping algorithm did not lead to unambiguous results. For further characterization of the reaction product, phase purity of the sample has to be improved, or larger single crystals for single-crystal analyses are necessary. EDX measurements also confirm a new composition of a ternary lithium nitridosilicate since no other elements than Si and N were detectable; also no Si_xN_y compound was identifiable in the powder diffraction pattern. The presence of Li cannot be determined by EDX measurements, thus, further experiments for an accurate determination of the composition is needed.

Reactions with Ba

A variety of barium nitridosilicates and lithium nitridosilicates with Mg, Ca and Sr, e.g $Li_2Ca_2[Mg_2Si_2N_6]$, $Li_4Sr_3Si_2N_6$, $Li_2MSi_2N_4$ (*M* = Ca, Sr) or $Li_4Ca_3Si_2N_6$ are existent.[9-10] Therefore, synthesis of barium lithium nitridosilicates may also exist. This assumption is confirmed by the phase diagram of Ba-Li. As can be seen in Fig. 4 solely a liquid phase is present above 727 °C. At compositions of 50 mol-% Li and more the liquid phase begins already above 300 °C.[11]

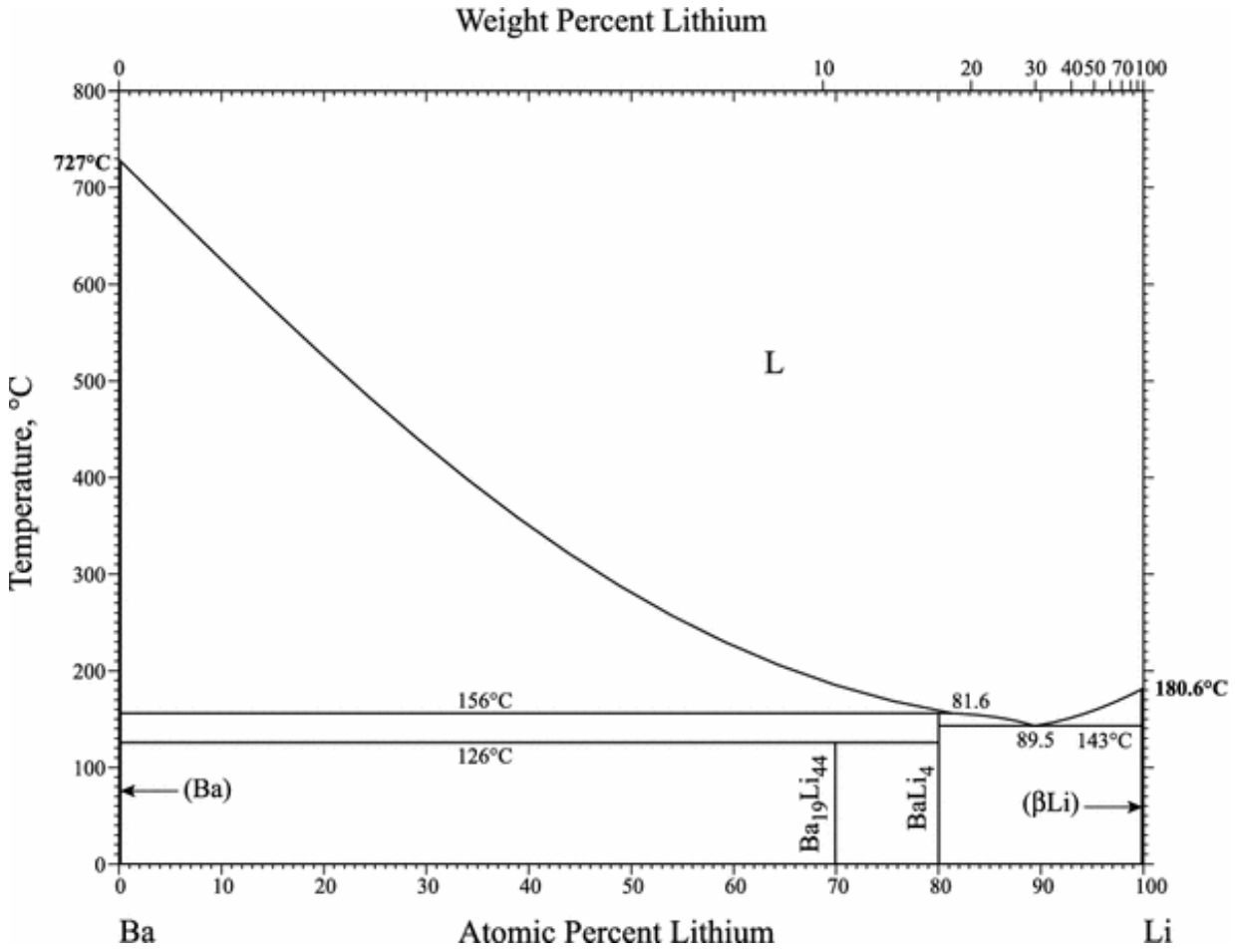

Figure 4. Ba-Li phase diagram.

For this reason, several reactions of usual Si sources (SDI, Si_3N_4 and TIDS) with different Li (Li, Li_3N and LiN_3) and Ba compounds (Ba, BaF_2, BaH_2, $BaCl_2$) were investigated. All of these reactions were performed in tantalum ampoules between 900 and 1000 °C with varying molar ratios. In general, no quaternary barium lithium nitridosilicate was obtained. The reaction samples often yielded amorphous or heterogeneous products containing microcrystalline compounds. The characterization of these compounds was not possible, as conventional single-crystal X-ray diffraction of crystals smaller than 1000 μm^3 is unfeasible. Since the powder patterns indicate the presence of different phases, also powder X-ray diffraction analyses are inadequate for structure elucidation. Next to unidentifiable reaction samples, the formation of already known compounds was observed. One example is the formation of $BaSiN_2$ and $LiSi_2N_3$ or Li_2SiN_2, resulting from reactions of SDI and Ba with LiN_3 or Li_3N. Moreover, reactions of SDI, Ba, Li and Li_3N yielded conglomerations of $BaSiN_2$, Li_7TaN_4, $LiSi_2N_3$, Li_2SiN_2, and $LiBaH_3$. The exchange of SDI against Si_3N_4 led to reaction mixtures of $BaSiN_2$, Li_7TaN_4 as well as Li_2SiN_2. With TIDS as Si precursor, only amorphous products were obtained, which, according to EDX measurements, do not include all three elements Ba, Si, and N.

In summary, the investigated reactions indicate that for a synthetic access to barium lithium nitridosilicates the used starting materials and reaction conditions had to be further optimized. Even though the formation of unknown barium lithium nitridosilicates seems reasonable by the use of lithium flux, an incorporation of Ba into the system Li/Si/N was not observed up to now. One explanation might be the larger ionic radius of Ba^{2+} (1.35 Å) compared to Ca^{2+} (1.00 Å), Sr^{2+} (1.18 Å), or also Mg^{2+} (0.57 Å). In combination with the small Si^{4+} ion (0.26 Å), structures containing Ba, Si, and N might be too unstable and interstructural voids may be too small for incorporation of Ba^{2+}.[12]

2.2.3 Conclusion

The synthesis of novel nitridosilicates by common (high-temperature) syntheses routes is more and more challenging. In this section, diverse efforts to synthesize crystalline lithium nitridosilicates or novel compositions and structures of this compound class as well as lithium nitridosilicates with Ba were reported reaching from uncommon starting materials to novel reaction conditions. In conclusion, with all of these investigations and conditions, no unknown or compounds with a good enough crystallinity were obtained. Nevertheless, high-pressure high-temperature reactions seem to be promising since reactions indicated the formation of an unknown Li/Si/N compound. Therefore, these harsh conditions should definitely be pursued in further works. They can help in avoiding thermodynamic sinks, for example, the very stable compound Li_2SiN_2. The difficulties in structural characterization of the obtained products could be circumvented by the addition of NH_4Cl as a mineralizer leading to an increase of crystallinity. Thereby, a number of novel nitridophosphate compounds, e.g. b-PN(NH)[13] or b- and g-$P_4N_6(NH)$,[14-15] have been structurally elucidated by high-pressure reactions. Thus, it can be expected that the high-pressure high-temperature method will be in the focus of interest for further researches, also for the synthesis of novel lithium nitridosilicates. Another possibility to obtain novel compounds could be alternative synthetic routes by switching, for example, from common bottom-up syntheses to top-down syntheses. Thus, for example, $Li_2Ba_xSr_{1-x}Si_2N$, may be synthesized by addition of Ba^{2+} into already known lithium nitridosilicates. Furthermore, crystallinity of ternary lithium nitridosilicates may be optimized for accurate structural elucidation.

References

[1] W. Schnick, H. Huppertz, R. Lauterbach, *J. Mater. Chem.* **1999**, *9*, 289.

[2] N. Kawai, S. Endo, *Rev. Sci. Instrum.* **1970**, *41*, 1178.

[3] D. Walker, M. A. Carpenter, C. M. Hitch, *Am. Mineral.* **1990**, *75*, 1020.

[4] D. Walker, *Am. Mineral.* **1991**, *76*, 1092.

[5] D. C. Rubie, *Phase Transitions* **1999**, *68*, 431.

[6] H. Huppertz, *Z. Kristallogr.* **2004**, *219*, 330.

[7] T. Gruber, D. Thomas, C. Röder, F. Mertens, J. Kortus, *J. Raman Spectrosc.* **2013**, *44*, 934.

[8] H. Aoyama, S. Kuwano, K. Kuriyama, K. Kushida, *J. Alloys. Compd.* **2013**, *517*, 11.

[9] S. Schmiechen, F. Nietschke, W. Schnick, *Eur. J. Inorg. Chem.* **2015**, 1592.

[10] S. Lupart, Doctoral Thesis, University of Munich (LMU), Germany, **2012**.

[11] http://link.springer.com/article/10.1007/s11669-010-9755-z (**22**.**07**.**2017**).

[12] R. D. Shannon, *Acta Crystallogr. Sect. A* **1976**, *32*, 751.

[13] A. Marchuk, F. J. Pucher, F. W. Karau, W. Schnick, *Angew. Chem.* **2014**, *126*, 2501; *Angew. Chem. Int. Ed.* **2015**, *54*, 2383.

[14] D. Baumann, W. Schnick, *Angew. Chem.* **2014**, *126*, 14718; *Angew. Chem. Int. Ed.* **2014**, *53*, 14490.

[15] D. Baumann, W. Schnick, *Inorg. Chem.* **2014**, *53*, 7977.

2.3 $Ba_{32}[Li_{15}Si_9W_{16}N_{67}O_5]$- a Ba-containing Oxonitridolithotungstosilicate with a Highly Condensed Network Structure

published in: *Eur. J. Inorg. Chem.* **2017**, 1100.

authors: Katrin Horky and Wolfgang Schnick

DOI: 10.1002/ejic.201601385

http://onlinelibrary.wiley.com/doi/10.1002/ejic.201601385/abstract

Abstract: The oxonitridolithotungstosilicate $Ba_{32}[Li_{15}Si_9W_{16}N_{67}O_5]$ was synthesized by metathesis reaction of the reactive starting compounds $Si(NH)_2$, $LiNH_2$, LiF and BaH_2 in a radio-frequency furnace at 1000 °C using tungsten crucibles. Single crystals of $Ba_{32}[Li_{15}Si_9W_{16}N_{67}O_5]$ were received as byproduct from reaction of the starting materials with the crucible. The crystal structure ($P2_1/n$ (no. 14), a = 8.3402(3), b = 8.5465(3), c = 16.6736(6) Å, β = 99.1950(10)°, Z = 1, R_1(all) = 0.0302) was solved and refined on the basis of single-crystal X-ray diffraction data. $Ba_{32}[Li_{15}Si_9W_{16}N_{67}O_5]$ is the first oxonitridolithotungstosilicate containing a three-dimensional network of vertex- (WN_4) and edge-sharing (LiN_3O, Li/SiN_3O and SiN_3O) tetrahedra with Ba^{2+} ions which fill the voids of the structure. The network is characterized by channels of *fünfer* rings running along [100] as well as of *sechser* and *achter* rings along [010]. Magnetic measurements prove the oxidation state +VI of W. X-ray spectroscopy, lattice energy calculations with MAPLE and X-ray diffraction confirm the chemical composition and the structural model of $Ba_{32}[Li_{15}Si_9W_{16}N_{67}O_5]$. IR spectra corroborate absence of N-H bonds. The optical band gap of $Ba_{32}[Li_{15}Si_9W_{16}N_{67}O_5]$ has been determined by UV-Vis spectroscopy.

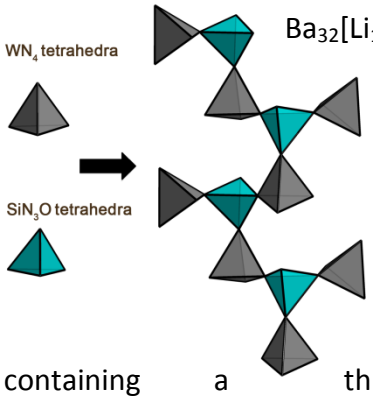

2.3.1 Introduction

Nitrides show outstanding structures and materials properties. Therefore, the search for new compounds, structures and properties has been pursued frequently in this compound class.[1-2] Formally, (oxo)nitridosilicates are structurally related with oxosilicates by exchanging all or a part of O by N. (Oxo)nitridosilicates are typically built up from $Si(O,N)_4$ tetrahedra. The presence of nitrogen leads to a wide range of additional structural possibilities as nitrogen can bridge up to four neighboring tetrahedral centers and enables corner-sharing as well as edge-sharing of $Si(O,N)_4$ tetrahedra.[3-6] So $BaSi_7N_{10}$ was the first highly condensed nitridosilicate with edge-sharing SiN_4 tetrahedra.[3] On the basis of their great structural variety, diverse and outstanding materials properties arose for (oxo)nitridosilicates e.g. luminescence of rare earth doped compounds, like $MSi_2O_2N_2$ (*M* = Ca, Sr, Ba) and $M_2Si_5N_8:Eu^{2+}$ (*M* = Ca, Sr, Ba).[7-9] These materials found industrial application in phosphor-converted (pc)-LEDs as highly efficient luminescent materials.[4] Furthermore, lithium (oxo)nitridosilicates are known for their lithium conductivity properties. For example Li_2SiN_2, Li_8SiN_4 as well as $Li_{14}Ln_5[Si_{11}N_{19}O_5]O_2F_2$ (with *Ln* = Ce and Nd) have been described as Li^+ conductors, which makes them interesting for potential applications in lithium batteries.[10-14] In the (oxo)nitridosilicate compound class several representatives with Li and Ba e.g. LiSiON,[15] $LiSi_2N_3$,[16-17] Li_2SiN_2,[10-12, 18-19] Li_8SiN_4,[11] $BaSiN_2$,[20] $BaSi_6N_8$,[21] $BaSi_7N_{10}$,[3] $Ba_2Si_5N_8$,[22] $Ba_5Si_2N_6$ and $BaSi_6N_8O$[23] have been reported.[24] Furthermore, some alkaline-earth containing lithium (oxo)nitridosilicates with Ca and Sr, e.g. $Li_2Sr_4Si_4N_8O$,[25] $Li_2CaSi_2N_4$[26] and $Li_2Ca_2[Mg_2Si_2N_6]$, have been described in literature.[27] Lithium (oxo)nitridosilicates in combination with barium have not been discovered as yet.

For tungsten, several ternary tungsten nitrides ($LiWN_2$),[28] tungstates (Li_2WO_4)[29] as well as nitridotungstate oxides ($(OLi_2Ca_4)_3[WN_4]_4$)[30] with Li and alkaline earth metals (Ba, Ca) have been described.

The first ternary nitrides of lithium with transition metals Cr, Mo and W have been synthesized by Juza *et al*. by reaction of Li_3N with the respective elements or their nitrides. The brown, moisture sensitive products had the chemical composition Li_9MN_5.[31-32] In addition, compounds like $LiWN_2$ and Li_6WN_4 are also well-known. The former is a layered nitride with

hexagonal structure and was obtained by reaction of Li_2WO_4 in flowing NH_3 gas at 745 °C.[28] Li_6WN_4 crystallizes in a fluorite type superstructure.[33] An analogous tungsten nitride with an alkaline earth metal instead of lithium is represented by the compound Ba_3WN_4. Its crystal structure can be related with the Na_3As structure type. In Ba_3WN_4 the centers of the WN_4 tetrahedra together with Ba^{2+} are building an arrangement which corresponds with the hexagonal Na_3As type.[34] The compound $((OLi_2Ca_4)_3[WN_4]_4)$[30] is the junction between the described lithium and alkaline earth tungsten nitrides and is characterized by a close structural relationship to the Th_3P_4 structure type.[30] However, no comparable structural diversity of the above mentioned tungsten compounds is known as it has been described for (oxo)nitridosilicates. Such an exceedingly diverse linking pattern for $Si(O,N)_4$ tetrahedra is not known for $W(O,N)_4$ tetrahedra in the systems Li-W-N and Ba-W-N. In general, the typical structural feature of the named compounds are isolated $[M^{VI}N_4]^{6-}$ or $[M^{VI}O_4]^{2-}$ tetrahedral anions (e.g. Li_6WN_4, TT-$Ba_3[MN_4]$, HT-$Ba_3[MN_4]$ or Li_2WO_4).[29, 33-35] As described by R. Niewa and H. Jacobs only the exchange of lithium by the larger alkali metal cations results in further condensation of the nitridometalate tetrahedra e.g. like in $Na_3[WN_3]$ or $Cs_5[Na\{W_4N_{10}\}c]$.[36]

Recently, we described a synthetic approach to lanthanum nitridosilicates by metathesis reactions in radio-frequency furnaces. In this contribution, we applied this technique successfully to obtain the first Ba-containing oxonitridolithotungstosilicate $Ba_{32}[Li_{15}Si_9W_{16}N_{67}O_5]$. The latter compound combines and expands the structural features of tungsten nitrides together with (oxo)nitridosilicates. The results could point to a further extension of the structural diversity of (oxo)nitridosilicates and thus could lead to interesting new materials properties.

2.3.2 Results and Discussion

2.3.2.1 Synthesis and Chemical Analysis

$Ba_{32}[Li_{15}Si_9W_{16}N_{67}O_5]$ was obtained as a crystalline side phase by solid-state metathesis reaction performed in a tungsten crucible heated inductively with a radio-frequency furnace. The synthesis route is based on the decomposition of an alkaline-earth hydride (decomposition of BaH_2 at 675 °C)[37] and its reaction with LiF to BaF_2. The latter resublimates at the reactor wall. The remaining Ba reacts with the pre-organized starting materials $Si(NH)_2$ and $LiNH_2$. A similar reaction path was already reported for the synthesis of lanthanum nitridosilicates.[38] The oxygen content originates assumedly from impurities of commercially acquired starting materials. According to earlier observations, the incorporation of tungsten can presumably be traced back to the oxygen contamination resulting in the formation of tungsten(VI) oxide on the surface of the crucible. Subsequently, WO_3 may react with the reaction mixture to form $Ba_{32}[Li_{15}Si_9W_{16}N_{67}O_5]$ (see Scheme 1, a)). But also a targeted incorporation of tungsten is possible. Exchange of LiF against WCl_6 in the initial reaction mixture showed that $Ba_{32}[Li_{15}Si_9W_{16}N_{67}O_5]$ is also formed. Probably, in this case the decomposition of BaH_2 in conjunction with WCl_6 leads to the formation of $BaCl_2$ (Scheme 1, b)). Subsequently, the remaining Ba and W react with the residual starting materials to the title compound as orange powder amongst other, partly unknown, phases. $Ba_{32}[Li_{15}Si_9W_{16}N_{67}O_5]$ forms light orange block-like crystals, which are rather sensitive to air and moisture (Figure 1).

a) $Si(NH)_2 + LiNH_2 + BaH_2 + LiF + WO_3 \longrightarrow Ba_{32}[Li_{15}Si_9W_{16}N_{57}O_5] + BaF_2 + H_2$

b) $Si_3N_4 + LiNH_2 + BaH_2 + WCl_6 + O_2 \longrightarrow Ba_{32}[Li_{15}Si_9W_{16}N_{57}O_5] + BaCl_2 + H_2$

Scheme 1: Mechanism of the metathesis reactions; a) tungsten from reaction with the crucible, b) tungsten from WCl6 as starting material.

Through energy-dispersive X-ray spectroscopy (EDX) the elemental composition was established. The results from the EDX analyses are, within the precision limits of this method, consistent with the composition obtained from the single-crystal structure analysis. FT-IR spectroscopy of isolated crystals of $Ba_{32}[Li_{15}Si_9W_{16}N_{67}O_5]$ (Figure S1, Supporting Information) confirms absence of N-H bonds and thus the absence of hydrogen.

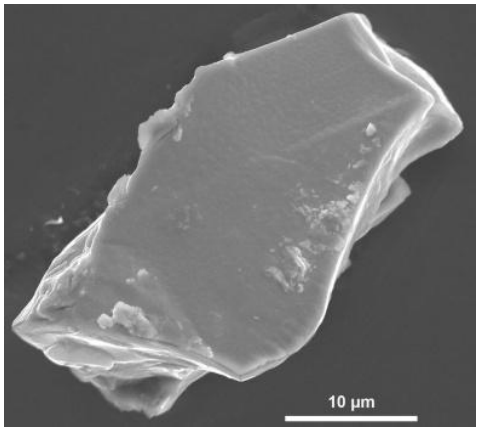

Figure 1. SEM image of a crystal of $Ba_{32}[Li_{15}Si_9W_{16}N_{67}O_5]$.

To proof the oxidation state of W in the compound, magnetic measurements were performed. The sample of separated crystals of $Ba_{32}[Li_{15}Si_9W_{16}N_{67}O_5]$ showed diamagnetic behavior (Figure S2, Supporting Information). Consequently, oxidation state +VI for W in $Ba_{32}[Li_{15}Si_9W_{16}N_{67}O_5]$ is validated.

2.3.2.2 Single-Crystal Structure Analysis

The novel Ba-containing nitridolithotungstosilicate crystallizes in the monoclinic space group $P2_1/n$ (no. 14). The heavy atoms W, Ba and Si were refined anisotropically. Reflections with badly determined intensities, due to partial shading by the beam stop, were omitted. The crystallographic data are given in Table 1, the atomic coordinates and isotropic displacement parameters are summarized in Table 2. The anisotropic displacement parameters are listed in Table S1 in the Supporting Information.

Table 1. Crystallographic data of the single-crystal structure determination of $Ba_{32}[Li_{15}Si_9W_{16}N_{67}O_5]$.

Formula	$Ba_{16}[Li_{7.5}Si_{4.5}W_8N_{33.5}O_{2.5}]$
Crystal system	monoclinic
Space group	$P2_1/n$ (no. 14)
a [Å]	8.3402(3)
b [Å]	8.5465(3)
c [Å]	16.6736(6)
β [°]	99.1950(10)
Cell volume [Å^3]	1173.21(7)
Formula units per unit cell	1
ρ [g·cm^{-3}]	6.16458
Crystal size [mm]	0.01 x 0.02 x 0.03
μ [mm^{-1}]	32.846
T [K]	293(2)
Diffractometer	Bruker D8 Venture
Radiation (λ [Å])	X-ray (λ = 0.71073 Å)
F(000)	1828
ϑ range [°]	3.436 ≤ *ϑ* ≥ 25.349
Total no. of reflections	20556
Independent reflections	2139 [R(int) = 0.0563]
Refined parameters	109
Goodness of fit	1.024
R_1 (all data)	0.0302
R_1 [$F^2 > 2\sigma(F^2)$]	0.0210
w R_2 (all data)	0.0384
w R_2 [$F^2 > 2\sigma(F^2)$]	0.0367
$\Delta\rho_{max}$, $\Delta\rho_{min}$ [e/Å^{-3}]	1.632; −1.122

Table 2. Atomic coordinates, isotropic displacement parameters and side occupancies of $Ba_{32}[Li_{15}Si_9W_{16}N_{67}O_5]$.

Atom	*x*	*y*	*z*	U_{eq}	*s.o.f.*
W1	0.21581(4)	0.96349(3)	0.63882(2)	0.00454(8)	1
W2	0.75291(4)	0.50307(3)	0.62730(2)	0.00482(8)	1
Ba1	0.00640(6)	0.76567(5)	0.77444(3)	0.01177(11)	1
Ba2	0.04085(6)	1.26424(5)	0.50989(3)	0.01155(11)	1
Ba3	0.98206(5)	1.22563(5)	0.74732(3)	0.00948(11)	1
Ba4	0.82319(5)	0.49663(5)	0.91214(3)	0.00850(11)	1
Si1A	0.0893(11)	0.8054(10)	0.9569(5)	0.01838(19)	0.125
Si2	0.3188(3)	1.0479(2)	0.85296(13)	0.0096(5)	1
Li1A	0.0893(11)	0.8054(10)	0.9569(5)	0.0183(19)	0.875
Li2	0.1139(16)	1.1364(14)	0.9514(8)	0.013(3)	1
O1	0.2018(6)	0.9378(6)	0.9023(3)	0.0074(12)	0.625
N1	0.2018(6)	0.9378(6)	0.9023(3)	0.0074(12)	0.375
N2	0.7469(7)	0.4974(7)	0.7381(4)	0.0125(14)	1
N3	0.0041(7)	1.0203(7)	0.6112(4)	0.0088(13)	1
N4	0.3404(8)	1.0823(7)	0.5785(4)	0.0138(15)	1
N5	0.2352(7)	0.7426(7)	0.6259(4)	0.0119(14)	1
N6	0.6595(8)	0.3190(7)	0.5820(4)	0.01508(15)	1
N7	0.2721(7)	1.014231(4)	0.7488(4)	0.0106(14)	1
N8	0.9769(8)	0.5073(7)	0.6135(4)	0.0114(14)	1
N9	0.6413(8)	0.6781(7)	0.5849(4)	0.0137(15)	1

2.3.2.3 Structure Description

The crystal structure of the title compound is depicted in Figure 2a. $Ba_{32}[Li_{15}Si_9W_{16}N_{67}O_5]$ is built up of vertex- and edge-sharing Q^4-type (LiN_3O, Li/SiN_3O and SiN_3O tetrahedra) and vertex-sharing Q^3-type WN_4 tetrahedra, forming a three-dimensional network with Ba^{2+} ions filling the voids of the structure. Since the network is built up of SiN_3O, LiN_3O, Li/SiN_3O and WN_4 tetrahedra, the compound can be classified as a oxonitridolithotungstosilicate.[39] Thus, the combination of the Si/N and W/N compound classes leads to a structural extension. In this compound the WN_4 tetrahedra exhibit a broader linking pattern as they are not isolated as usual in the ternary tungsten nitrides mentioned above.

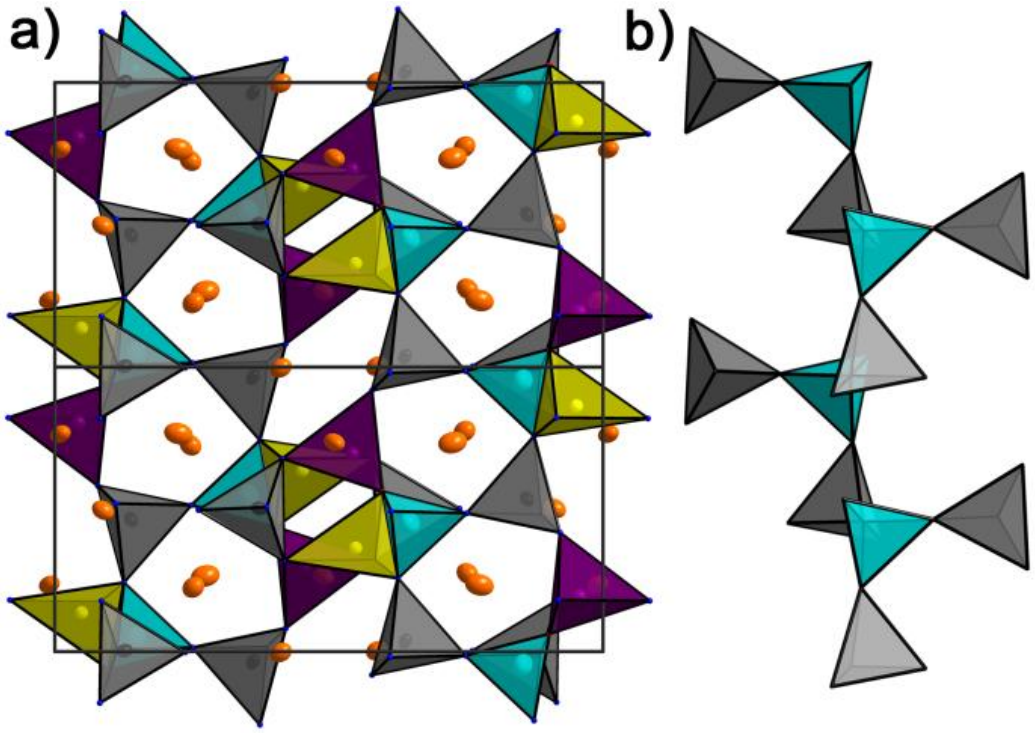

Figure 2. a) Crystal structure of $Ba_{32}[Li_{15}Si_9W_{16}N_{67}O_5]$, projection along [100] with $Si(N,O)_4$ tetrahedra (turquoise), $Li(N,O)_4$ tetrahedra (yellow), $LiSi(N,O)_4$ tetrahedra (purple), WN_4 tetrahedra (gray) and Ba positions (orange), Ba, W and Si in ellipsoidal depiction; b) connection of SiN_4 (turquoise) and WN_4 (gray) tetrahedra.

They are part of the three-dimensional network in which WN_4 tetrahedra are alternatingly connected with SiN_4 tetrahedra in chains running along [001]. Every SiN_4 tetrahedron is connected with an additional WN_4 group (Figure 2b). The degree of condensation $\kappa = n(Li,Si,W) : n(N,O)$ is 0.56, indicating that $Ba_{32}[Li_{15}Si_9W_{16}N_{67}O_5]$ can be considered as a highly condensed oxonitridolithotungstosilicate. Moreover, there are two mixed-occupied positions. One cation site (Li1ASi1A) is occupied by both Li and Si in an atomic ratio of $^7/_8$: $^1/_8$. This simultaneously occupation seems plausible because the completely exchange between tetrahedrally coordinated Si^{4+} and Mg^{2+} as well as Li^+ is possible.[27] For example the first representatives of nitridomagnesosilicates are $M[Mg_3SiN_4]$ (M = Ca, Sr, Eu) with a substitution of Mg for Si.[40] With respect to the diagonal relationship between Mg and Li in the periodic table and similiar ionic radii of Mg^{2+} (0.57 Å)[41] and Li^+ (0.59 Å)[41] consequently Si^{4+} can also partly be substituted by Li^+ as demonstrated here. This kind of a mixed position of Li and Si is observed for the first time. The other Si site was also tested for Li, a mixed occupation cannot be found for this site. The other site (N1O1) is an anion position mixed-occupied with N and O in an atomic ratio of $^3/_8$: $^5/_8$. The distribution of N1O1 was done due to the shortest Si-N distance. Besides, it is the only crystallographic site, which has no contact to W. The high charge of W is better stabilized through N than O. The Li and Si positions were initially refined freely and subsequently fixed. Free refinement of Li1ASi1A was performed to estimate the Li content in $Ba_{32}[Li_{15}Si_9W_{16}N_{67}O_5]$. In order to achieve charge neutrality, also with regard to the atomic ratio O:N, a Si:Li content of 0.125:0.875 was fixed. The network contains two terminal, three singly bridging and three N atoms interconnecting three tetrahedra. The mixed-occupied N/O position reveals a bridging-motive like it is also found for O for example in α-$Na_7[H_3SiW_9O_{34}] \cdot 9\ H_20$[42] or $Si_{6-Z}Al_zO_zN_{8-Z}$ (Z = 2.0, 2.9, 4.0).[43] The point symbol for the framework has been determined by TOPOS[44-45] and is $\{3.5^2.6^2.7\}\ \{3^2.4.5^2.6^3.7.8\}\ \{3^4.4^2.6^2.7^2\}\ \{3^5.4^4.5^2.6^2.7^2\}\ \{3^6.4^5.5^3.6\}$. To the best of our knowledge, this tetrahedra topology has not been found in any other compound so far. Aside from *dreier* and *vierer* rings the network is characterized by *fünfer*, *sechser* and *achter* rings forming channels along [100] and [010].[46-47] *Dreier* rings, themselves are linked through *sechser* rings and thus connect the *fünfer* ring channels. Along [010] *sechser* ring

channels, once again combined through *dreier* rings, alternate with *achter* ring channels (Figure 3a, b).

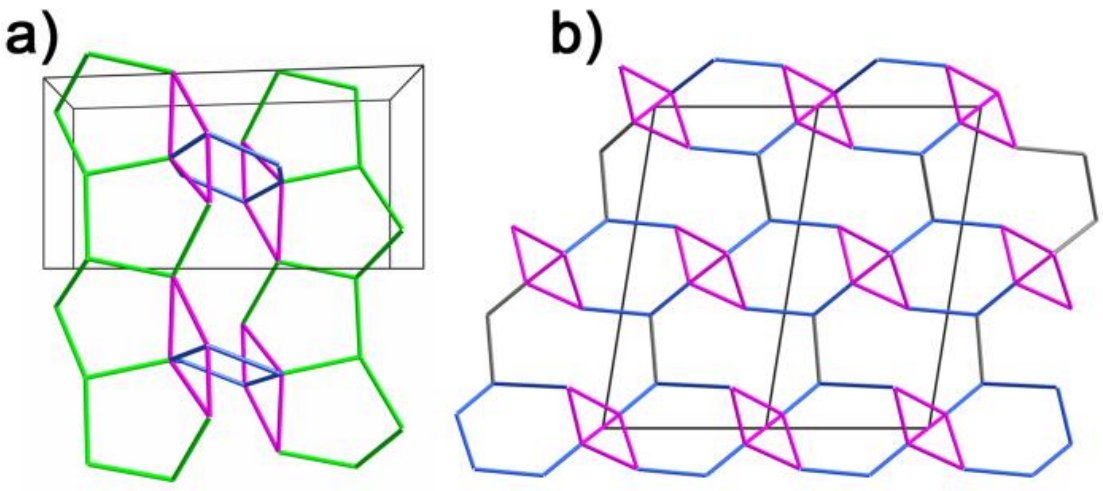

Figure 3. Topological representation of $Ba_{32}[Li_{15}Si_9W_{16}N_{67}O_5]$; (a) *fünfer* ring channels (green) connected by *dreier* (pink) and *sechser* (blue) rings along [100]; (b) *sechser* rings (blue) connected by *dreier* (pink) rings and *achter* (gray) ring channels along [010].

The distances Si-N [1.741(7)-1.774(6) Å] and Si-O [1.665(5) Å] are in accordance with comparable compounds, e.g. $LiCa_3Si_2N_5$ [1.716(6)-1.807(5) Å][48] and $Sr_2Si_5N_8$ [1.653(9)-1.7865(5) Å][22] as well as $LiLa_5Si_4N_{10}O$ [1.677(3) Å][49] and $Ce_{10}[Si_{10}O_9N_{17}]Br$ [1.664(4)-1.709(7) Å].[50] The longer Li-N [2.142(14)-2.182(15) Å] and Li-O [2.069(13) Å] distances are also in good agreement with distances found e.g. in $Li_4Sr_3Si_2N_6$ [2.018(11)-2.357(10) Å][6] and $Na_{10}(Li_2[MnO_4]_4)$ [1.91-1.956 Å][51] or Li_2O [1.981 Å].[52] The W-N distances range between 1.818(6) and 1.919(6) Å. These values are as well similar to the W-N distance in Li_6WN_4 [1.914 Å][33] or $Li_{0.84}W_{1.16}N_2$ [2.105(1) Å].[53] There are four crystallographically independent Ba^{2+} positions. These positions are surrounded by N and the mixed-occupied position N1O1 (Ba1 and Ba2) with coordination numbers ranging from 6 to 8 (Figure 4). The Ba-N and Ba-N/O [2.731(6)-3.366(6) Å] distances are also in between the reference ranges known from literature for similar compounds like $Ba_2AlSi_5N_9$[54] [2.547(7)-3.680(7) Å] or $Ba_5Si_2N_6$ [2.61(2)-3.40(2) Å].[24] Moreover, all distances are in good agreement with the sum of the ionic radii according to Shannon.[55] A comparison of the powder diffraction pattern of the sample with

the theoretical powder diffraction pattern, simulated on the basis of single-crystal structure elucidation, shows that $Ba_{32}[Li_{15}Si_9W_{16}N_{67}O_5]$ occurs as a side phase of the sample amongst other, partly unknown, phases (Figure S3 in the Supporting Information).

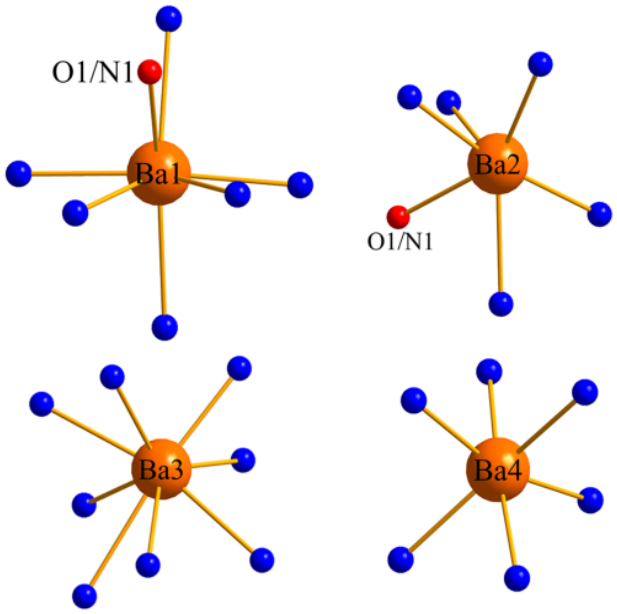

Figure 4. Coordination spheres of the barium sites in $Ba_{32}[Li_{15}Si_9W_{16}N_{67}O_5]$ (red: N1O1 mixed-occupied position/atom; blue N atoms).

2.3.2.4 Lattice-Energy Calculations (MAPLE)

To proof the electrostatic consistency of the crystal structure MAPLE (**MA**delung **P**art of **L**attice **E**nergy)[41, 56-58] calculations have been carried out. Thereby electrostatic interactions in an ionic crystal are considered, which are based on the distance, charge and coordination spheres of the concerned ions. The results are shown in Table 3. As reference for W^{VI}, the maple value of WN_2 was employed. The calculated partial MAPLE values by the MAPLE software of W, Ba, Si, Li, N and O for $Ba_{32}[Li_{15}Si_9W_{16}N_{67}O_5]$ correlate well with typical ranges of partial MAPLE values of comparable compounds in literature (Table 3). As expected, the values of the mixed N/O and Li/Si sites range between those of N and O and Li and Si, respectively. For a comparison of the total MAPLE value for $Ba_{32}[Li_{15}Si_9W_{16}N_{67}O_5]$ (397721 kJ/mol), calculated by the MAPLE software, a theoretical reaction equation, which leads to $Ba_{32}[Li_{15}Si_9W_{16}N_{67}O_5]$, is constructed of different nitrides and Li_2O (Table 3, theoretical model). The total MAPLE values of the single nitrides and Li_2O were added, appropriate to the theoretical reaction equation, to get a theoretical total MAPLE value for $Ba_{32}[Li_{15}Si_9W_{16}N_{67}O_5]$ (392393 kJ/mol). The total MAPLE value corresponds well with the sum of the MAPLE values of the different nitrides and Li_2O, which formally constitute the sum formula of $Ba_{32}[Li_{15}Si_9W_{16}N_{67}O_5]$. The values differ by 1.34 %, which is in the range of tolerance. Thus, the electrostatic consistency of the crystal structure has been confirmed.

Table 3. Partial MAPLE values and MAPLE sums [kJ/mol] for $Ba_{32}[Li_{15}Si_9W_{16}N_{67}O_5]$.

Partial MAPLE values of $Ba_{32}[Li_{15}Si_9W_{16}N_{67}O_5]$[a]		Theoretical model	
W1	17772	+ 2.5	Li_2O
W2	18128	+ 8	WN_2
Ba1	1550	+ 16	$BaSiN_2$
Ba2	1753	+ 1.25	Li_2SiN_2
Ba3	1566	− 4.25	β-Si_3N_4
Ba4	2200		
Si1	9756		
Li1ASi1A	1708		
Li2	885		
N1O1	3066		
N2	4858		
N3	4907		
N4	4634		
N5	5690		
N6	4588		
N7	5965		
N8	5733		
N9	4689		
Sum of the partial MAPLE values	∑ = 397721		∑ = 392393
			Δ = 1.34 %

[a] Typical partial MAPLE values [kJ/mol]:
Ba^{2+} 1500 - 2000; Si^{4+} 9000 - 10200; N^{3-} 4300 – 6200; O^{2-} 2000 – 2800; Li^{+} 550 - 860; W^{6+} 18979.[4, 48]

2.3.2.5 UV-VIS Spectroscopy

Determination of the optical band gap was done by means of solid-state UV-Vis spectroscopy. The reflectance spectrum shows a weak absorption band around 456 nm, corresponding to the light orange body color (Figure S4, Supporting Information). Accordingly, the band gap was estimated to be ~ 2.71 eV.

2.3.3 Conclusions

With the synthesis of $Ba_{32}[Li_{15}Si_9W_{16}N_{67}O_5]$ the first compound in the system Ba-Li-Si-W-N-O was obtained. As Li, Si and W are part of the network the compound can be classified as oxonitridolithotungstosilicate.

It is characterized by a highly condensed framework of vertex- and edge-sharing LiN_3O, Li/SiN_3O and SiN_3O tetrahedra as well as vertex-sharing WN_4 units. The tetrahedra are condensed to different kinds of rings. Whereby *fünfer*, *sechser* and *achter* rings form channels along [100] and [010]. The cavities of the structure are filled with Ba^{2+} ions which are coordinated by 6 to 8 anions.

$Ba_{32}[Li_{15}Si_9W_{16}N_{67}O_5]$ is the first example for a mixed cation position of Li and Si. In addition it is the first compound that combines the Si/N and W/N compound class which has not been known so far. This combination leads to a structural expansion of the W-N system, as the WN_4 tetrahedra show a hitherto unknown linkage with SiN_4 tetrahedra. The occurrence of linked WN_4 tetrahedra in $Ba_{32}[Li_{15}Si_9W_{16}N_{67}O_5]$ is an exceptional feature since in other tungsten nitrides with Li and Ba isolated $[M^{VI}N_4]^{6-}$ tetrahedra anions are common.

Besides, the title compound shows that the mentioned metathesis route is particularly suitable for the synthesis of new (oxo)nitridosilicates still in other systems as La-Si-N.

2.3.4 Experimental Section

2.3.4.1 General

Most reagents and products are air and moisture sensitive, accordingly all manipulations were performed under inert-gas conditions. For this purpose either flame-dried glassware attached to a vacuum line (10^{-3} mbar) or an Ar-filled glove box (Unilab, MBraun, Garching; O_2 < 1 ppm, H_2O < 1 ppm) were used.

2.3.4.2 Synthesis of $Ba_{32}[Li_{15}Si_9W_{16}N_{67}O_5]$

$Si(NH)_2$ (19.9 mg, 0.34 mmol, according to *Winter* et al.),[59] $LiNH_2$ (31.7 mg, 1.38 mmol, Aldrich, 95 %), LiF (35.9 mg, 1.38 mmol, Aldrich, > 99 %) and BaH_2 (100.1 mg, 0.72 mmol, Materion, 99.7 %) were thoroughly mixed in an agate mortar and filled into a tungsten crucible (Plansee, Bad Urach, 99.97 %). The oxygen content originates assumedly from impurities of commercially acquired starting materials, which implies the formation of WO_3 with tungsten originating from the reaction vessel. To proof if the incorporation of tungsten is also specifically feasible, WCl_6 instead of LiF has been used. Therefore Si_3N_4 (24.3 mg, 0.17 mmol, UBE, 99.9 %), $LiNH_2$ (31.6 mg, 1.38 mmol, Aldrich, 95 %), WCl_6 (68.3 mg, 0.17 mmol, Aldrich, 99.9 %) and BaH_2 (75.6 mg, 0.54 mmol, Materion, 99.7 %) were thoroughly ground in an agate mortar and filled into a tungsten crucible (Plansee, Bad Urach, 99.97 %). The crucibles were transferred into a water-cooled silica glass reactor of a radio-frequency furnace (Typ AXIO 10/450, max. electrical output 10 kW, Hüttinger Elektronik, Freiburg).[60] Within 1h both samples were heated under purified nitrogen to 1000 °C, maintained for 10 h at that temperature and finally quenched to room temperature by switching off the furnace. The product yielded a few orange, moisture and air sensitive crystals of $Ba_{32}[Li_{15}Si_9W_{16}N_{67}O_5]$ in an inhomogeneous sample. The synthesis approach with WCl_6 instead of LiF as starting compound, yielded $Ba_{32}[Li_{15}Si_9W_{16}N_{67}O_5]$ as orange powder in a heterogeneous sample.

2.3.4.3 SEM and EDX Spectroscopy

To determine the morphology and the chemical composition of the title compound, a JEOL JSM 6500F field emission scanning electron microscope (SEM), operated at 8.5 kV, provided with a Si/Li EDX detector (Oxford Instruments, model 7418), was used. The obtained orange

crystals were prepared on conductive adhesive films and coated with carbon (BAL-TEC MED 020, Bal Tec AG), to ensure electrical conductivity on the sample surface. Within the sensitivity range of the method these measurements exclude the presence of other elements than Ba, (Li), Si, W, N and O. The EDX analyses of the compound leads to an average atomic ratio Ba/Si/W = 22:3:10 (three measurements on the crystal used for single-crystal X-ray diffraction; the atomic content of N and O was excluded due to the air and moisture sensitivity of the compound; Li is not determinable). Consequently, these measurements corroborate within the required accuracy the defined empirical formula of $Ba_{32}[Li_{15}Si_9W_{16}N_{67}O_5]$.

2.3.4.4 Single-crystal X-ray diffraction

Single crystals of $Ba_{32}[Li_{15}Si_9W_{16}N_{67}O_5]$ were prepared under inert gas conditions using a microscope, which was integrated in a glove box. Isolated crystals of suitable quality were enclosed in glass capillaries and sealed under argon. Single-crystal X-ray diffraction data were collected with a D8 Venture (Bruker, Billerica MA, USA) diffractometer with Mo-K_α radiation (λ = 0.71073 Å) from a rotating anode source. Indexing of the reflections was done with SMART.[61] The reflections of the data set of $Ba_{32}[Li_{15}Si_9W_{16}N_{67}O_5]$ were integrated with SAINT.[62] A multi-scan absorption correction was applied using the program SADABS.[63] Subsequently, the structure was solved with Direct Methods (SHELXS)[64] and refined using the method of full-matrix least-squares (SHELXL).[65] The crystal structure was visualized using DIAMOND.[66]

Further details of the crystal structure investigations may be obtained from the Fachinformationszentrum Karlsruhe, 76344 Eggenstein-Leopoldshafen, Germany (Fax: +49-7247-808-666; E-Mail: crysdata@fiz-karlsruhe.de, http://www.fiz-karlsruhe.de/request for deposited data.html) on quoting the depository number (CSD – 432 182).

2.3.4.5 Powder X-ray diffraction

To verify the structural model obtained from single-crystal data, pulverized samples were enclosed in glass capillaries. Powder diffraction data were collected with a STOE STADI P diffractometer (Mo-$K_{\alpha1}$ radiation, Ge(111) monochromator, MYTHEN 1 K detector) in Debye-Scherrer geometry. Simulated powder diffraction patterns were generated by using the WinXPOW program package[67] based on the single-crystal structure data.

2.3.4.6 Magnetic Measurements

For magnetic measurements a Cryogenic Vibrating Sample Magnetometer (VSM) with a cryogenically-free cryostat was used (temperature range 1.6 – 400 K; magnetic field −5 – 5T).

2.3.4.7 UV-Vis Spectroscopy

For the reflectance spectra a JASCO V-650 UV/Vis spectrophotometer with a deuterium and a halogen lamp (Czerny-Turner monochromator with 1200 lines/mm concave grating, photomultiplier tube detector) was utilized. The measurements were carried out between 200 nm and 800 nm with 1 nm step size. By drawing two line tangents to the slope of the reflectance curve the band gap of $Ba_{32}[Li_{15}Si_9W_{16}N_{67}O_5]$ was determined. The point of intersection of the tangents was estimated as the value of the band gap.

2.3.4.8 FT-IR Spectroscopy

A Perkin-Elmer BX II spectrometer with an ATR (attenuated total reflection) setup was used for recording the FT-IR spectrum.

2.3.5 References

[1] F. J. DiSalvo, *Science* **1990**, *247*, 649.

[2] S. H. Elder, F. J. DiSalvo, L. Troper, A. Navrotsky, *Chem. Mater.* **1993**, *5*, 1545.

[3] H. Huppertz, W. Schnick, *Chem. Eur. J.* **1997**, *3*, 249.

[4] M. Zeuner, S. Pagano, W. Schnick, *Angew. Chem., 123*, **2011**, 7898; *Angew. Chem. Int. Ed*. **2011**, *50*, 7754.

[5] W. Schnick, *Int. J. Inorg. Mater.* **2001**, *3*, 1267.

[6] S. Pagano, S. Lupart, S. Schmiechen, W. Schnick, *Z. Anorg. Allg. Chem.* **2010**, *636*, 1907.

[7] H. A. Höppe, H. Lutz, P. Morys, W. Schnick, A. Seilmeier, *J. Phys. Chem. Solids* **2000**, *61*, 2001.

[8] R. Mueller-Mach, G. Mueller, M. R. Krames, H. A. Höppe, F. Stadler, W. Schnick, T. Juestel, P. Schmidt, *Phys. Status Solidi (a)* **2005**, *202*, 1727.

[9] M. Seibald, T. Rosenthal, O. Oeckler, W. Schnick, *Crit. Rev. Solid State Mater. Sci.* **2014**, *39*, 215.

[10] M. S. Bhamra, D. J. Fray, *J. Mater. Sci.* **1995**, *30*, 5381.

[11] J. Lang, J.-P. Charlot, *Rev. Chim. Miner.* **1970**, *7*, 121.

[12] H. Hillebrecht, J. Churda, L. Schröder, H. G. v. Schnering, *Z. Kristallogr. Suppl.* **1993**, *6*, 80.

[13] D. R. MacFarlane, J. Huang, M. Forsyth, *Nature* **1999**, *402*, 792.

[14] S. Lupart, G. Gregori, J. Maier, W. Schnick, *J. Am. Chem. Soc.* **2012**, *134*, 10132.

[15] Y. Laurent, J. Guyader, G. Roult, *Acta Crystallogr. B* **1981**, *37*, 911.

[16] M. Orth, W. Schnick, *Z. Anorg. Allg. Chemie* **1999**, *625*, 1426.

[17] J. David, Y. Laurent, J.-P. Charlot, J. Lang, *Bull. Soc. Fr. Mineral. Cristallogr.* **1973**, *96*, 21.

[18] B. Song, J. K. Jian, G. M. Cai, M. Lei, H. Q. Bao, H. Li, Y. P. Xu, W. Y. Wang, J. C. Han, X. L. Chen, *Solid State Ionics* **2009**, *180*, 29.

[19] J. Grins, Z. Shen, S. Esmaeilzadeh, *Silic. Ind.* **2004**, *69*, 9.

[20] Z. A. Gál, P. M. Mallinson, H. J. Orchard, S. J. Clarke, *Inorg. Chem.* **2004**, *43*, 3998.

[21] F. Stadler, W. Schnick, *Z. Anorg. Allg. Chem.* **2007**, *633*, 589.

[22] T. Schlieper, W. Milius, W. Schnick, *Z. Anorg. Allg. Chem.* **1995**, *621*, 1380.

[23] F. Stadler, R. Kraut, O. Oeckler, S. Schmid, W. Schnick, *Z. Anorg. Allg. Chem.* **2005**, *631*, 1773.

[24] H. Yamane, F. J. DiSalvo, *J. Alloys Compd.* **1996**, *240*, 33.

[25] S. Pagano, S. Lupart, M. Zeuner, W. Schnick, *Angew. Chem., 121*, **2009**, 6453; *Angew. Chem. Int. Ed.* **2009**, *48*, 6335.

[26] M. Zeuner, S. Pagano, S. Hug, P. Pust, S. Schmiechen, C. Scheu, W. Schnick, *Eur. J. Inorg. Chem.* **2010**, 4945.

[27] S. Schmiechen, F. Nietschke, W. Schnick, *Eur. J. Inorg. Chem.* **2015**, 1592.

[28] P. S. Herle, M. S. Hegde, N. Y. Vasanthacharya, J. Gopalakrishnan, G. N. Subbanna, *J. Solid State Chem.* **1994**, *112*, 208.

[29] W. H. Zachariasen, H. A. Plettinger, *Acta Crystallogr.* **1961**, *14*, 229.

[30] C. Wachsmann, P. Höhn, R. Kniep, H. Jacobs, *J. Alloys Compd.* **1997**, *248*, 1.

[31] R. Juza, K. Langer, K. v. Benda, *Angew. Chem.* **1968**, *80*, 373; *Angew. Chem. Int. Ed. Engl*. **1968**, *7*, 360.

[32] R. Juza, J. Haug, *Z. Anorg. Allg. Chemie* **1961**, *309*, 276.

[33] A. Gudat, S. Haag, R. Kniep, A. Rabenau, *Z. Naturforsch.* **1990**, *45b*, 111.

[34] A. Gudat, P. Höhn, R. Kniep, A. Rabenau, *Z. Naturforsch.* **1991**, *46b*, 566.

[35] P. Höhn, R. Kniep, *Z. Kristallogr.* **2000**, 329.

[36] R. Niewa, H. Jacobs, *Chem. Rev.* **1996**, *96*, 2053.

[37] W. Grochala, P. Edwards, *Chem. Rev.* **2004**, *104*, 1283.

[38] D. Durach, L. Neudert, P. J. Schmidt, O. Oeckler, W. Schnick, *Chem. Mater.* **2015**, *27*, 4832.

[39] R. Hofmann, R. Hoppe, *Z. Anorg. Allg. Chemie* **1988**, *560*, 35.

[40] S. Schmiechen, H. Schneider, P. Wagatha, C. Hecht, P. J. Schmidt, W. Schnick, *Chem. Mater.* **2014**, *26*, 2712.

[41] W. H. Baur, *Crystallogr. Rev.* **1987**, *1*, 59.

[42] V. Hubert, H. Hartl, *Z. Naturforsch. 51 b* **1996**, 969.

[43] L. Gillott, N. Cowlam, G. E. Bacon, *J. Mater. Sci.* **1981**, *16*, 2263.

[44] V. A. Blatov, M. O`Keeffe, D. M. Proserpio, *CrystEngComm* **2010**, *12*, 44.

[45] V. A. Blatov, A. P. Shevchenko, D. M. Proserpio, *Cryst. Growth Des.* **2014**, *14*, 3576.

[46] F. Liebau, *Structural Chemistry of Silicates*, Springer, Berlin, **1985**.

[47] The terms *zweier*, *dreier*, *vierer*, *fünfer*, *sechser* and *achter* rings were coined by Liebau and are derived from the German words "drei" (three) and "sechs" (six), etc. through addition of suffix "er"; however, for example a *dreier* ring is not a three-membered ring, but a six-membered ring comprising *three* tetrahedra centers.

[48] S. Lupart, W. Schnick, *Z. Anorg. Allg. Chemie* **2012**, *638*, 2015.

[49] S. Lupart, W. Schnick, *Z. Anorg. Allg. Chem.* **2011**, *638*, 94.

[50] A. Lieb, W. Schnick, *J. Solid State Chem.* **2005**, *178*, 3323.

[51] D. Fischer, R. Hoppe, *Angew. Chem., 102*, **1990**, 835; *Angew. Chem. Int. Ed. Engl.* **1990**, *29*, 800.

[52] A. Lazicki, C. S. Yoo, W. J. Evans, W. E. Pickett, *Phys. Rev. B: Condens. Matter* **2006**, *73*, 184120.

[53] S. Kaskel, D. Hohlwein, J. Strähle, *J. Solid State Chem.* **1998**, *138*, 154.

[54] J. Kechele, Doctoral Thesis thesis, University of Munich (LMU) (Germany), **2009**.

[55] R. D. Shannon, *Acta Crystallogr., Sect. A: Cryst. Found. Crystallogr.* **1976**, *32*, 751.

[56] R. Hübenthal, *Programm zur Berechnung des Madelunganteils der Gitterenergie*, **1993**.

[57] R. Hoppe, *Angew. Chem* **1966***, 78*, 52; *Angew. Chem. Int. Ed. Engl.* **1966**, *5*, 95.

[58] R. Hoppe, *Angew. Chem.* **1970***, 82*, 7; *Angew. Chem. Int. Ed. Engl.* **1970**, *9*, 25.

[59] H. Lange, G. Wötting, G. Winter, *Angew. Chem* **1991***, 103*, 1606; *Angew. Chem. Int. Ed. Engl.* **1991**, *30*, 1579.

[60] W. Schnick, H. Huppertz, R. Lauterbach, *J. Mater. Chem.* **1999**, *9*, 289.

[61] J. L. Chambers, K. L. Smith, M. R. Pressprich, Z. Jin, *SMART, v.5.059, Bruker AXS, Madison, W1, USA*, **1997-2002**.

[62] *SAINT*, *v. 6.36, Bruker AXS*, Madison, W1, USA, **1997-2002**.

[63] G. M. Sheldrick, *Multi-Scan Absorption Correction, Bruker AXS*, Madison, W1, USA, **2012**.

[64] G. M. Sheldrick, *SHELXS-97: A program for crystal structure solution*, Universitiy of Göttingen, Germany, **1997**.

[65] G. M. Sheldrick, *SHELXL-97: A programm for crystal structure refinement*, University of Göttingen, Germany, **1997**.

[66] Brandenburg, *K. Crystal Impact GbR*, Bonn, **2005**.

[67] WinXPOW, *Vers. 2.12, Stoe & Cie GmbH WinXPOW*, Darmstadt, **2007**.

2.4 $LiCa_4Si_4N_8F$ and $LiSr_4Si_4N_8F$ – Nitridosilicate Fluorides with a BCT-Zeolite Type Network Structure

published in: *Eur. J. Inorg. Chem.* **2017**, 1107.

authors: Katrin Horky and Wolfgang Schnick

DOI: 10.1002/ejic.201601386

http://onlinelibrary.wiley.com/doi/10.1002/ejic.201601386/abstract

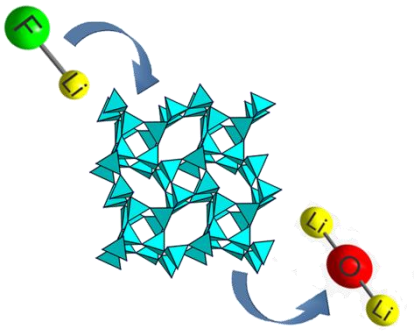

Abstract: $LiCa_4Si_4N_8F$ and $LiSr_4Si_4N_8F$ were synthesized from Si_3N_4, $LiNH_2$, CaH_2/SrH_2 and LiF through a metathesis reaction in a radio-frequency furnace. The crystal structures of both compounds were solved and refined on the basis of single-crystal X-ray diffraction data ($LiCa_4Si_4N_8F$: $P2_1/c$ (no. 14), a = 10.5108(3), b = 9.0217(3), c = 10.3574(3) Å, β = 117.0152(10)°, R_1 = 0.0422, wR_2 = 0.0724, Z = 4; $LiSr_4Si_4N_8F$: $P4nc$ (no. 104), a = 9.3118(4), b = 9.3118(4), c = 5.5216(2) Å, R_1 = 0.0160, wR_2 = 0.0388, Z = 2). The silicate substructure of both compounds is built up of vertex sharing SiN_4 tetrahedra, forming a BCT-zeolite analogous structure with Ca^{2+}/Sr^{2+}, Li^+ and F^- ions filling the voids. The crystal structure of $LiSr_4Si_4N_8F$ is homeotypic to that of $Li_2Sr_4Si_4N_8O$ as it exhibits the same zeolite-analogous $[SiN_2]^{2-}$ framework but incorporating LiF instead of Li_2O. In contrast to the respective Sr compound $LiCa_4Si_4N_8F$ shows a distortion of the BCT-zeolite analogous network as well as an additional site for F. Both F sites in $LiCa_4Si_4N_8F$ exhibit different coordination spheres compared with $LiSr_4Si_4N_8F$. The title compounds are the first lithium alkaline earth nitridosilicates containing fluorine. The crystal structures were confirmed by lattice-energy calculations (MAPLE), EDX measurements and powder X-ray diffraction. IR spectra prove absence of N-H bonds.

2.4.1 Introduction

In view of their wide abundance in the earth's crust, silicates are amongst the most important classes of minerals. Nearly all naturally occuring silicates are oxosilicates. A partial or complete exchange of O by N leads to the (oxo)nitridosilicate compound class. In the last decade an increasing number of (oxo)nitridosilicates has been synthesized. Due to strong Si-N and Si-O bonds, (oxo)nitridosilicates combine high chemical and thermal stability.[1-5] Consequently, a variety of industrial applications has been pursued. For example highly condensed networks built up from [SiN_4] tetrahedra are used as high-temperature stable materials,[6-7] while alkaline-earth (oxo)nitridosilicates function as host lattices for rare-earth doped luminescent materials in phosphor-converted LEDs (pc-LEDs).[8-12] Also systematic investigations of lithium nitridosilicates attained a number of ternary lithium nitridosilicates with interesting materials properties, for example, lithium ion conductivity.[13-17] In comparison with oxosilicates, the exchange of O by N in the anionic substructure leads to a large variety of structures for (oxo)nitridosilicates, as in $SiO_{4-x}N_x$ with x = 1 - 4 nitrogen atoms can interconnect up to four neighboring tetrahedral centers. Nevertheless, nitridozeolites are rare and the benefit of nitrogen in zeolite-like framework structures has been demonstrated only for a few examples. Besides zeolite-like Si-N frameworks in $Li_2Sr_4Si_4N_8O$ (BCT type)[5] or $Ba_2Nd_7Si_{11}N_{23}$,[3] a few examples with carbodiimide or chloride ions located in the channels of those structures, e.g. $Ba_6Si_6N_{10}O_2(CN_2)$, $Ba_3T_3N_5OCl$ (T = Si, Ta) (both NPO type)[18-20] and $Ba_{1.63}La_{7.39}Si_{11}N_{23}Cl_{0.42}:Ce^{3+}$[21] have been reported. Additionally, $M_7Si_6N_{15}$ (M = La, Ce, Pr) with its interrupted network exhibits a structure resembling those of zeolites.[22] But especially nitridozeolites are expected to have outstanding physical and chemical properties, like higher thermal stability or differing acidity/basicity. The potential of inorganic open-framework materials for possible applications reaches e. g. from sensors to electronic or optical systems.[23-24] Nevertheless, the thermal and chemical stability of such microporous nitride compounds is not often adequately enough to make their way towards applications.

Accordingly, it is of great interest to synthesize novel materials with three-dimensional framework structures built up of vertex-sharing tetrahedra. The challenge is the synthetic access for the formation of porous materials based on nitridosilicates. For instance flux methods were established to avoid problems appearing from required high reaction tem-

peratures. As nitrogen shows a considerable solubility in liquid alkali metals (Na or Li), thus the reaction temperatures could be lowered significantly. Furthermore, different reactive starting materials like "$Si(CN_2)_2$" and "$Si(NH)_2$" were employed. They turned out to be promising precursors because of their high reactivity and their decomposition at elevated temperatures to metal nitrides and imides. In case of $Ba_6Si_6N_{10}O(CN_2)$ the use of "$Si(CN_2)_2$" leads to the formation of an open network as the carbodiimide ions might even serve as temperature-resistant templates.[5, 20]

In this contribution, synthesis and structural characterization of the two first F-containing lithium alkaline-earth nitridosilicates Li*EA*$_4$Si$_4$N$_8$F (*EA* = Ca, Sr) are discussed. The title compounds show that the formation of zeolite-type nitride frameworks can also be achieved through straightforward metathesis reaction.

2.4.2 Results and Discussion

2.4.2.1 Synthesis and Sample Characterization

$LiCa_4Si_4N_8F$ as well as $LiSr_4Si_4N_8F$ have been synthesized in a solid-state metathesis reaction in tungsten crucibles. The presence of sufficient amounts of LiF in the reaction mixture of Si_3N_4, CaH_2 (in case of $LiCa_4Si_4N_8F$), SrH_2 (in case of $LiSr_4Si_4N_8F$) and $LiNH_2$ resulted in the formation of the two new F-containing phases. The driving force behind these metathesis reactions seems to be the decomposition of CaH_2 and SrH_2 and its reaction with LiF to reactive lithium and alkaline earth halides CaF_2 and SrF_2 (fluorine comes from LiF), respectively (Scheme 1). Li reacts hereinafter with remaining Ca/Sr, F and Si_3N_4 inter alia to colorless rods of $LiCa_4Si_4N_8F$ and $LiSr_4Si_4N_8F$, which are stable against air and moisture.

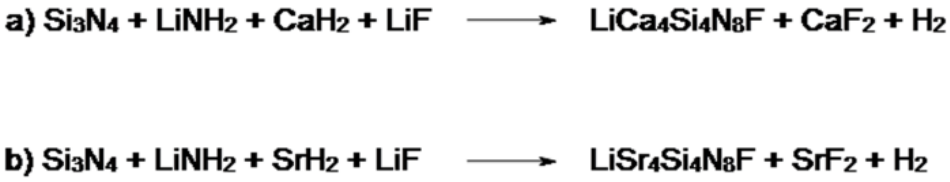

Scheme 1. Stoichiometric metathesis reactions; a) $LiCa_4Si_4N_8F$, b) $LiSr_4Si_4N_8F$.

PXRD data support the suspected reaction equations (Figure S1 and S2, Supporting Information) as both title compounds were obtained as side phases in heterogeneous reaction mixtures. CaF_2 and $Li_2SrSi_2N_4$ have been identified as side phases of the metathesis reactions. Due to further unknown phases in both reaction samples a structure solution from PXRD data was not possible.

To define the morphology and the elemental composition of the title compounds Energy-dispersive X-ray spectroscopy (EDX) was used (Figure 1). The results from the EDX analyses are consistent with the composition obtained from the single-crystal structure analysis. An atomic ratio of Ca,Sr/Si/N/F 4:4:8:1 agrees well with the formula $LiEA_4Si_4N_8F$ (*EA* = Ca, Sr), whereas Li is not determinable by EDX.

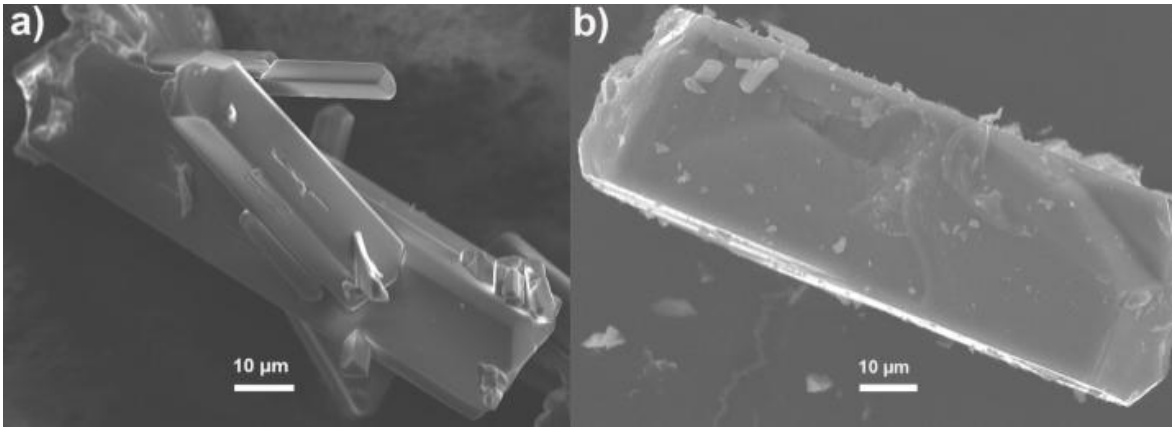

Figure 1. SEM images of crystals of $LiCa_4Si_4N_8F$ (a) and $LiSr_4Si_4N_8F$ (b).

Because of the usage of N/H containing starting materials FT-IR spectra (Figure S3 and S4, Supporting Information) of both compounds were recorded to prove the absence of N-H bonds and thus the absence of hydrogen.

2.4.2.2 Single-Crystal Structure Analyses and Structure Description

The novel F-containing nitridosilicates crystallize in the monoclinic space group $P2_1/c$ ($LiCa_4Si_4N_8F$) and the tetragonal space group $P4nc$ ($LiSr_4Si_4N_8F$), respectively. The heavy atoms were refined anisotropically. Details of the structure determination and crystallographic data are given in Table 1. Atomic coordinates as well as isotropic displacement parameters are shown in Table 2. Table S1 in the Supporting Information lists the anisotropic displacement parameters.

Table 1. Crystallographic data of the single-crystal structure determination of $LiCa_4Si_4N_8F$ and $LiSr_4Si_4N_8F$.

Formula	$LiCa_4Si_4N_8F$	$LiSr_4Si_4N_8F$
Crystal system	monoclinic	tetragonal
Space group	$P2_1/c$ (no. 14)	$P4nc$ (no. 104)
a [Å]	10.5108(3)	9.3118(4)
b [Å]	9.0217(3)	9.3118(4)
c [Å]	10.3574(3)	5.5216(2)
β [°]	117.0150(10)	
Cell volume [$Å^3$]	874.98(5)	478.78(4)
Formula units per unit cell	4	2
ρ [$g \cdot cm^{-3}$]	3.118	4.168
Crystal size [mm^3]	0.01 x 0.01 x 0.04	0.03 x 0.04 x 0.13
μ [mm^{-1}]	3.022	22.662
T [K]	293(2)	293(2)
Diffractometer	Bruker D8 Venture	Bruker D8 Venture
Radiation (λ [Å])	X-ray (λ = 0.71073)	X-ray (λ = 0.71073)
F(000)	816	552
ϑ range [°]	$8.835 \leq 2\vartheta \leq 66.33$	$8.582 \leq 2\vartheta \leq 54.81$
Total no. of reflections	9791	9041
Independent reflections	2554 [R(int) = 0.0367]	512 [R(int) = 0.0329]
Refined parameters	166	34
Goodness of fit	1.209	1.075
R_1 (all data)	0.0422	0.0169
R_1 [$F^2 > 2\sigma(F^2)$]	0.0354	0.0160
wR_2 (all data)	0.0743	0.0392
wR_2 [$F^2 > 2\sigma(F^2)$]	0.0724	0.0388
$\Delta\rho_{max}$, $\Delta\rho_{min}$ [$e/Å^{-3}$]	0.664, −0.546	1.543, −0.493

Table 2. Atomic coordinates, isotropic displacement parameters and site occupancies of $LiCa_4Si_4N_8F$ and $LiSr_4Si_4N_8F$ with standard deviations in parentheses.

Atom	Wyckoff symbol	*x*	*y*	*z*	U_{eq}	s.o.f.
$LiCa_4Si_4N_8F$						
Ca1	4e	0.36741(6)	0.93978(7)	0.14072(6)	0.00759(13)	1
Ca2	4e	0.48213(6)	1.28982(7)	0.04237(7)	0.00880(13)	1
Ca3	4e	0.05026(6)	0.74069(7)	0.98904(6)	0.00758(13)	1
Ca4	4e	0.11468(7)	1.06114(7)	0.31605(8)	0.01335(14)	1
Si1	4e	0.36263(8)	0.59964(9)	0.13105(8)	0.00364(15)	1
Si2	4e	0.14203(8)	1.11804(9)	0.09865(9)	0.00382(15)	1
Si3	4e	0.18953(8)	0.76547(9)	0.90135(8)	0.00381(15)	1
Si4	4e	0.30972(8)	1.25362(9)	0.21892(8)	0.00374(15)	1
F1	2b	1/2	1	0	0.0132(5)	1/2
F2	2c	0	1/2	0	0.0265(8)	1/2
N1	4e	0.2561(3)	1.2115(3)	0.8526(3)	0.0067(5)	1
N2	4e	0.0263(3)	0.6881(3)	0.7028(3)	0.0072(5)	1
N3	4e	0.1567(3)	0.9280(3)	0.8823(3)	0.0062(5)	1
N4	4e	0.3622(3)	0.4147(3)	0.1672(3)	0.0076(5)	1
N5	4e	0.1835(3)	1.1461(3)	0.0833(3)	0.0062(5)	1
N6	4e	0.2915(3)	0.7909(3)	0.7244(3)	0.0055(4)	1
N7	4e	0.2757(3)	0.6414(3)	0.9496(3)	0.0068(5)	1
N8	4e	0.5388(3)	0.6461(3)	0.1961(3)	0.0076(5)	1
Li1	4e	0.6837(6)	0.9949(6)	0.1731(6)	0.0117(11)	1
$LiSr_4Si_4N_8F$						
Sr1	8c	0.44336(3)	0.23358(3)	0.8985(4)	0.00600(17)	1
Si1	8c	0.11931(10)	0.23038(10)	0.9031(9)	0.0025(2)	1
F1	2a	1/2	1/2	0.907(6)	0.0171(13)	1/4
N1	8c	0.1747(19)	0.3272(19)	0.647(4)	0.0054(6)	1
N2	8c	0.936(3)	0.2077(3)	0.901(4)	0.0062(6)	1
Li1	2a	1/2	1/2	1.264(4)	0.020(4)	1/4

Both compounds represent nitridosilicates with the same BCT-zeolite analogous network, which is exclusively built up of vertex-sharing SiN_4 tetrahedra with a degree of condensation $\kappa = n(Si):n(N) = 0.50$. As calculated by TOPOS[25] the point symbol for the framework is 4.6(5). The characteristic feature of the network are *vierer*[26] and *achter*[26] rings along [001] together with *sechser*[26] rings along [100] and [010]. $LiCa_4Si_4N_8F$ and $LiSr_4Si_4N_8F$ are homeotypic to $Li_2Sr_4Si_4N_8O$.[5] In the sense of a group-subgroup relation there is no direct correlation between the structure of the title compounds. In $LiCa_4Si_4N_8F$ the network is distorted compared to the $[SiN_2]^{2-}$ network of $Li_2Sr_4Si_4N_8O$ and $LiSr_4Si_4N_8F$ (see Figure 2 and Figure 3), because both Sr-containing compounds crystallize in higher symmetric tetragonal space groups. Ca^{2+} ions or Sr^{2+} ions as well as Li^+ ions together with F^- ions are incorporated into the voids of the structure.

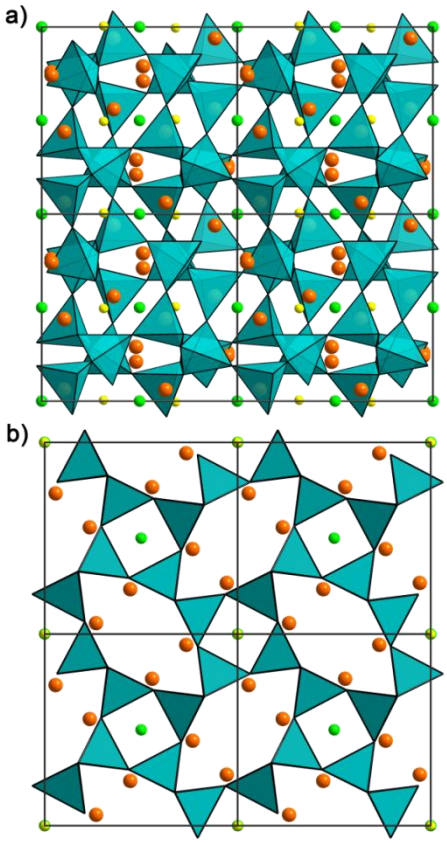

Figure 2. Crystal structure of $LiCa_4Si_4N_8F$ (a) and $LiSr_4Si_4N_8F$ (b) view along [001]; SiN_4 tetrahedra turquoise, Ca and Sr orange, F green, Li yellow.

The respective lithium position is for both compounds identical and in analogy with $Li_2Sr_4Si_4N_8O$ surrounded by four N and one F atom, which replaces in the case of $LiSr_4Si_4N_8F$ the O atom of $Li_2Sr_4Si_4N_8O$. The striking difference of $LiCa_4Si_4N_8F$ and $LiSr_4Si_4N_8F$ are the differing F sites. For $LiSr_4Si_4N_8F$ one F position is found. The fluorine atoms are located in channels together with one Li atom forming linear LiF units (see Figure 3) aligned in the *vierer*[26] ring channels along [001]. Therefore, the compound can also be formulated as $LiF@[SrSiN_2]_4$.

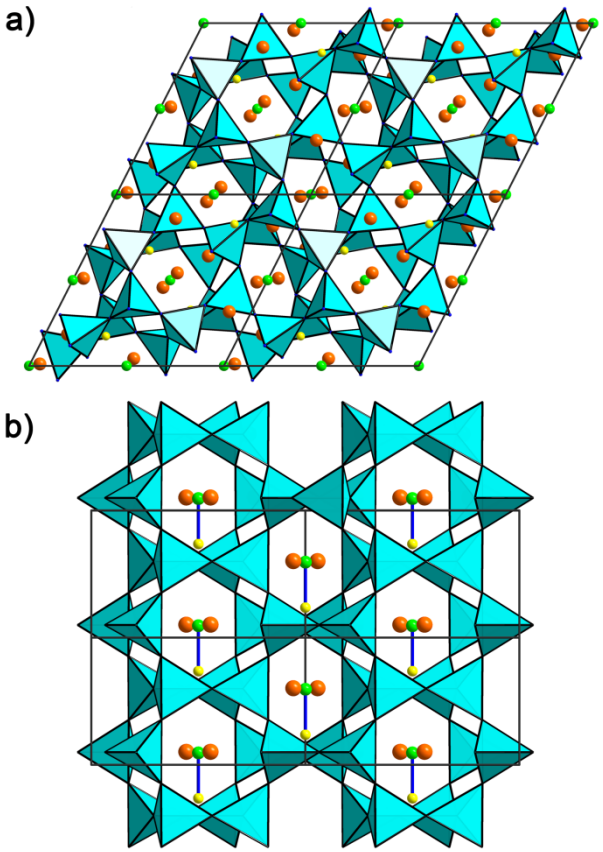

Figure 3. Crystal structure of $LiCa_4Si_4N_8F$ (a) and $LiSr_4Si_4N_8F$ (b) view along [010]; SiN_4 tetrahedra turquoise, Ca and Sr orange, F green, Li yellow, LiF units (b) highlighted with blue bonds.

Thus, the Li_2O units in $Li_2O@[SrSiN_2]_4$ are substituted through LiF units (see Figure 4). Whereas for $LiCa_4Si_4N_8F$ two fluorine sites, each half occupied, are present. Moreover, both fluorine sites are coordinated differently as compared with the F site in $LiSr_4Si_4N_8F$ (see Figure 4). In the latter compound the single F site is coordinated by one Li^+ and Sr^{2+} while in $LiCa_4Si_4N_8F$ the one F site is coordinated by two Li^+ as well as Ca^{2+}. The second F site is exclusively coordinated by Ca^{2+}. Ca^{2+} and Sr^{2+} atoms are located for both phases in the *sechser*[26]

ring channels. The observation that Ca phases are structurally different to their analogous alkaline earth phases of the heavier homologues Sr and Ba atoms is already made for $EASiN_2$ (*EA* = Ca, Sr, Ba) and $EA_2Si_5N_8$ (*EA* = Ca, Sr, Ba). Accordingly, $LiEA_4Si_4N_8F$ (*EA* = Ca, Sr) shows also the diverse coordination behavior of EA^{2+} ions. The Si-N distances range from 1.68 and 1.76 Å and correspond well with the sum of the ionic radii[27-28] as well as with typical distances (e.g. $Li_2Sr_4Si_4N_8O$,[29] Si-N: 1.71-1.76 Å and $Ba_{1.63}La_{7.39}Si_{11}N_{23}Cl_{0.42}:Ce^{3+}$,[21] Si-N: 1.68-1.77 Å). The bonding distances Ca-N and Sr-N reach from 2.40 to 2.62 Å and 2.59 to 2.98 Å, which is in the typical range. Similar values were also observed in $Ca_2Si_5N_8$[30] (Ca-N: 2.32 to 2.84 Å). The Li-N (2.02 Å to 2.17 Å) and Li-F bond lengths (1.94 Å to 1.98 Å) are also in good agreement with the interatomic distances in Li_3N, LiCaN or Li_3SrTaN_4[31-33] and LiF.[34] Especially, the bonding distances of Li-O and Li-F also corroborate the structural interpretation with incorporated F instead of O atoms in the nitridosilicate framework, as the Li-F distances are longer than typical Li-O distances (e.g. 1.84 Å in $Li_2Sr_2Al_2Ta_2N_8O$[35] or 1.78 Å in $Li_2Sr_4Si_4N_8O$[29]).

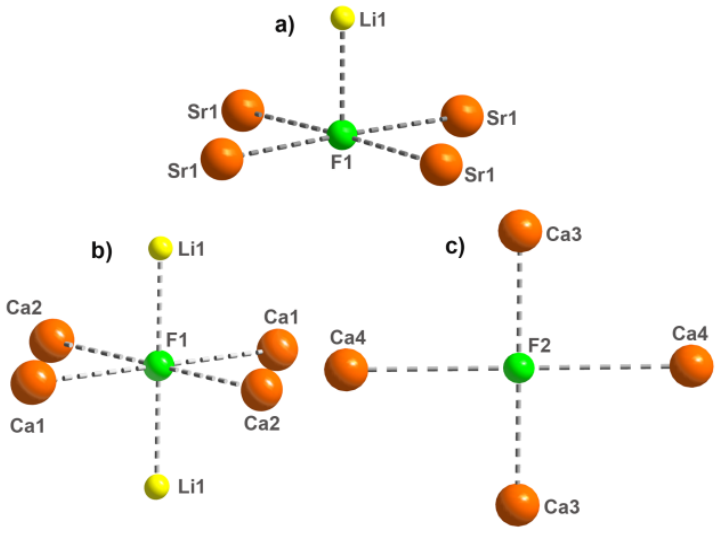

Figure 4. Coordination spheres of the fluorine sites in $LiCa_4Si_4N_8F$ (b,c) and $LiSr_4Si_4N_8F$ (a).

The addition of EuF_3 (2 mol %) to the reaction mixtures leads to a red body color of the crystals of $LiCa_4Si_4N_8F:Eu^{2+}$ and $LiSr_4Si_4N_8F:Eu^{2+}$. However, luminescence under UV irradiation at room temperature was not observed. Also lithium ion conductivity would be a conceivable

material property of the title compounds. But for this investigation a larger quantity of phase-pure samples would be necessary.

2.4.2.3 Lattice-Energy Calculations (MAPLE)

MAPLE (**MA**delung **P**art of **L**attice **E**nergy)[27, 36-38] calculations of the lattice energy have been performed to proof the electrostatic consistency of both crystal structures (see Table 3). Therefore, electrostatic interactions, which depend on the charge, distance as well as the coordination spheres of the particular ions, were considered. These calculations are particularly helpful to differentiate F^-, N^{3-} and O^{2-} as these atoms could not be distinguished solely by X-ray diffraction owing to their nearly identical scattering factors. The partial MAPLE values of all individual atoms are in good agreement with reference values and confirm once again the incorporated F atoms. By comparing MAPLE sums of different nitrides and LiF with the MAPLE values of Li*EA*$_4$Si$_4$N$_8$F (*EA* = Ca, Sr) the electrostatic consistency of the refined crystal structures has been verified. The values differ by 2.05 and 1.95 %, which is unusual for nitride compounds but has been yet observed in $Li_2Sr_4Si_4N_8O$ (2.08 %)[29] or other zeolite-type structures like $Ba_3Si_3N_5OCl$ (2 %)[39] and $Zn_8P_{12}N_{24}O_2$ (3.05 %).[40] Thus, it is likely that inorganic substructures as zeolite-like frameworks lead to larger MAPLE deviations.

Table 3. Partial MAPLE values and MAPLE sums [kJ/mol] for $LiCa_4Si_4N_8F$ and $LiSr_4Si_4N_8F$.

	$LiCa_4Si_4N_8F$	$LiSr_4Si_4N_8F$
Li^+	632	628
Ca^{2+}	1888-1964	-
Sr^{2+}	-	1782
Si^{4+}	9994-10145	10217
N^{3-}	5334-5518	5321-5345
F^-	578-632	607
Total	92597	91727
Δ	2.05 %	1.95 %

Total MAPLE; $LiCa_4Si_4N_8F$: $4/3$ x Ca_3N_2 + $4/3$ x Si_3N_4 + LiF = 90738 kJ/mol;

$LiSr_4Si_4N_8F$: 4 x $SrSiN_2$ + LiF = 89942 kJ/mol

[a] Typical MAPLE values [kJ/mol], for Ca^{2+}: 1700-2200; Sr^{2+}: 1500-2100; Si^{4+}: 9000-10200; N^{3-}: 4300-6200; F^-: 465-599; Li^+: 550-860.[5, 41-42]

2.4.3 Conclusions

We have synthesized $LiCa_4Si_4N_8F$ and $LiSr_4Si_4N_8F$, which are not only the first F-containing lithium alkaline earth nitridosilicates but also the first multinary nitride-fluorides consisting of a zeolite-related framework (BTC-type) as well. In correlation to the Sr-compound $LiCa_4Si_4N_8F$ shows a distortion of this framework along with different crystallographic sites and coordinations for fluorine. This demonstrates one more time the diverse coordination behavior and thereby the formation of slightly modified structures for Ca compared to the analogous Sr and Ba compounds. $LiSr_4Si_4N_8F$, however, is structurally almost identical to $Li_2Sr_4Si_4N_8O$. The only distinction is found in different molecular entities (LiF instead of Li_2O) hosted in the cavities of these structures. This shows the broad flexibility of this nitride network to embed diverse sorts of atoms or units. Furthermore, the title compounds are additional examples for the benefits of the engaged metathesis route, which was initially established for a variety of lanthanum (oxo)nitridosilicates.[41, 43-44] This reaction mechanism leads on the one hand to the first compounds in the system Li-*EA*-Si-N-F (*EA* = Ca, Sr). On the other hand it enabled the synthesis of new porous nitridosilicates also without any particular precursors ("$Si(CN_2)_2$", "$Si(NH)_2$" or "$Si_2(NH)_3 \cdot 6NH_4Cl$")[21, 45] and in addition the formation of a zeolite-type nitride framework at moderate temperatures. These circumstances underline the versatility of the applied reaction mechanism. Thus, it appears to be a promising route which might lead to the discovery of further new (oxo)nitridosilicates with further structural features. The title compounds are stable against air and moisture at ambient temperature and include cavities, so substitution and ion exchange are conceivable. Particularly, lithium ion conductivity experiments seem to be promising for these compounds. Consequently, the presented combination of nitridosilicates and zeolite-like frameworks could possibly lead to intriguing materials properties.

2.4.4 Experimental Section

2.4.4.1 General

Because of the air and moisture sensitivity of most starting materials all manipulations were performed under rigorous exclusion of oxygen and moisture. Therefore, either flame-dried glassware attached to a vacuum line (10^{-3} mbar) or an argon-filled glove box (Unilab, MBraun, Garching; O_2 < 1 ppm, H_2O < 1 ppm) were used.

2.4.4.2 Synthesis of $LiCa_4Si_4N_8F$

By the reaction of Si_3N_4 (20.0 mg, 0.14 mmol, UBE, 99.9 %), $LiNH_2$ (20.0 mg, 0.87 mmol, Aldrich, 95 %), CaH_2 (105.0 mg, 2.49 mmol, Aldrich, 99.99 %) and LiF (104.0 mg, 4.01 mmol, Aldrich, > 99 %) single crystals of $LiCa_4Si_4N_8F$ were obtained. The starting materials were mixed and filled into a tungsten crucible under argon atmosphere in a glove box. The sample was heated in a radio-frequency furnace (Typ AXIO 10/450, max. electrical output 10 kW, Hüttinger Elektronik, Freiburg)[46] under purified nitrogen within 1h to 1000 °C, maintained for 10 h at that temperature and finally quenched to room temperature by switching off the furnace. The reaction yielded an inhomogeneous powder with colorless rods of $LiCa_4Si_4N_8F$.

2.4.4.3 Synthesis of $LiSr_4Si_4N_8F$

For the synthesis of $LiSr_4Si_4N_8F$ Si_3N_4 (48.4 mg, 0.35 mmol, UBE, 99.9 %), $LiNH_2$ (31.7 mg, 1.38 mmol, Aldrich, 95 %), SrH_2 (67.1 mg, 0.75 mmol, Cerac, 99.5 %) and LiF (35.8 mg, 1.38 mmol, Aldrich, > 99 %) were weighed, ground and filled into a tungsten crucible. The latter was heated in a radio-frequency furnace (Typ AXIO 10/450, max. electrical output 10 kW, Hüttinger Elektronik, Freiburg)[46] under purified nitrogen to 1000 °C within 1h, maintained for 10 h at that temperature and finally quenched to room temperature by switching off the furnace. The reaction yielded an inhomogeneous sample of a yellow powder with colorless rods of $LiSr_4Si_4N_8F$.

2.4.4.4 SEM and EDX Spectroscopy

A JEOL JSM 6500F field emission scanning electron microscope (SEM), operated at 8.5 kV, provided with a Si/Li EDX detector (Oxford Instruments, model 7418) was used to analyze the chemical composition and the morphology of the title compounds. To guarantee electri-

cal conductivity on the sample surface the obtained crystals were prepared on conductive adhesive films and coated with carbon (BAL-TEC MED 020, Bal Tec AG). Within the sensitivity range of the method these measurements exclude the presence of other elements than Ca/Sr, (Li), Si, N and F. An atomic ratio of Ca,Sr/Si/N/F 4:4:8:1 results from the EDX analysis and agrees with the composition $LiCa_4Si_4N_8F$ and $LiSr_4Si_4N_8F$, whereas Li is not determinable by EDX.

2.4.4.5 Single-crystal X-ray diffraction

Single-crystal X-ray diffraction data were collected on a D8 Venture diffractometer (Bruker, Billerica MA, USA) with Mo-K_α radiation (λ = 0.71073 Å) from a rotating anode source. Indexing of the reflections and integration of the data set of $LiCa_4Si_4N_8F$ and $LiSr_4Si_4N_8F$ was done with SMART[47] and SAINT.[48] A multi-scan absorption correction using the program SADABS[49] was applied. Both crystal structures were solved by direct methods with the help of SHELXS.[50] Refinement of the structures was made with the least-squares method using SHELXL.[51] Visualization of the crystal structures was done with DIAMOND.[52]

Further details of the crystal structure investigations may be obtained from the Fachinformationszentrum Karlsruhe, 76344 Eggenstein-Leopoldshafen, Germany (Fax: +49-7247-808-666; E-Mail: crysdata@fiz-karlsruhe.de, http://www.fiz-karlsruhe.de/request for deposited data.html), on quoting the depository numbers CSD-432268 and -432269.

2.4.4.6 Powder X-ray diffraction

Pulverized samples of $LiCa_4Si_4N_8F$ and $LiSr_4Si_4N_8F$ were enclosed in glass capillaries to collect powder diffraction data with a STOE STADI P diffractometer (Mo-$K_{\alpha 1}$ radiation, Ge(111) monochromator, MYTHEN 1 K detector) in Debye-Scherrer geometry. To verify the structural model simulated powder diffraction patterns, based on the single-crystal structure data, were generated by using the WinXPOW program package and compared with the obtained powder diffraction data.

2.4.4.7 FT-IR Spectroscopy

For recording the FT-IR spectrum a Perkin-Elmer BXII spectrometer with an ATR (attenuated total reflection) setup was used.

2.4.5 References

[1] F. Stadler, O. Oeckler, J. Senker, H. A. Höppe, P. Kroll, W. Schnick, *Angew. Chem.* **2005***, 117*, 573; *Angew. Chem. Int. Ed.* **2005**, *44*, 567.

[2] Z. A. Gál, P. M. Mallinson, H. J. Orchard, S. J. Clarke, *Inorg. Chem.* **2004**, *43*, 3998.

[3] H. Huppertz, W. Schnick, *Angew. Chem.* **1997***,109*, 2765; *Angew. Chem. Int. Ed.* **1997**, *36*, 2651.

[4] H. Yamane, F. J. DiSalvo, *J. Alloys Compd.* **1996**, *240*, 33.

[5] M. Zeuner, S. Pagano, W. Schnick, *Angew. Chem.* **2011***, 123*, 7898; *Angew. Chem. Int. Ed*. **2011**, *50*, 7754.

[6] W. Schnick, *Angew. Chem.* **1993***, 105*, 846; *Angew. Chem. Int. Ed. Engl.* **1993**, *33*, 806.

[7] H. Lange, G. Wötting, G. Winter, *Angew. Chem.* **1991***, 103*, 1606; *Angew. Chem. Int. Ed. Engl.* **1991**, *30*, 1579.

[8] Y. Q. Li, G. deWith, H. T. Hintzen, *J. Solid State Chem.* **2008**, *181*, 515.

[9] R.-J. Xie, N. Hirosaki, N. Kimura, K. Sakuma, M. Mitomo, *Appl. Phys. Lett.* **2006**, *90*, 191101/191101.

[10] R.-J. Xie, N. Hirosaki, *Sci. Technol. Adv. Mater.* **2007**, *8*, 588.

[11] X. Piao, T. Horikawa, H. Hanzawa, K. Machida, *Appl. Phys. Lett.* **2006**, *88*, 161908/161901.

[12] R. Mueller-Mach, G. Mueller, M. R. Krames, H. A. Höppe, F. Stadler, W. Schnick, T. Juestel, P. Schmidt, *Phys. Status Solidi (a)* **2005**, *202*, 1727.

[13] J. Lang, J.-P. Charlot, *Rev. Chim. Miner.* **1970**, *7*, 121.

[14] H. Hillebrecht, J. Churda, L. Schröder, H. G. v. Schnering, *Z. Kristallogr. Suppl.* **1993**, *6*, 80.

[15] D. R. MacFarlane, J. Huang, M. Forsyth, *Nature* **1999**, *402*, 792.

[16] M. S. Bhamra, D. J. Fray, *J. Mater. Sci.* **1995**, *30*, 5381.

[17] S. Lupart, G. Gregori, J. Maier, W. Schnick, *J. Am. Chem. Soc.* **2012**, *134*, 10132.

[18] S. J. Sedlmaier, M. Döblinger, O. Oeckler, J. Weber, J. S. a. d. Günne, W. Schnick, *J. Am. Chem. Soc.* **2001**, *133*, 12069.

[19] S. Correll, O. Oeckler, N. Stock, W. Schnick, *Angew. Chem.* **2003***, 115*, 3674; *Angew. Chem. Int. Ed.* **2003**, *42*, 3549.

[20] S. Pagano, O. Oeckler, T. Schröder, W. Schnick, *Eur. J. Inorg. Chem.* **2009**, 2678.

[21] P. Schultz, D. Durach, W. Schnick, O. Oeckler, *Z. Anorg. Allg. Chemie* **2016**, *642*, 603.

[22] C. Schmolke, O. Oeckler, D. Bichler, D. Johrendt, W. Schnick, *Chem. Eur. J.* **2009**, *15*, 9215.

[23] A. K. Cheetham, G. Ferey, T. Loiseau, *Angew. Chem* **1999***., 111*, 3466; *Angew. Chem. Int. Ed.* **1999**, *38*, 3268.

[24] S. Natarajan, S. Mandal, *Angew. Chem.* **2008***, 120*, 4876; *Angew. Chem. Int. Ed. Engl.* **2008**, *47*, 4798.

[25] V. A. Blatov, A. P. Shevchenko, D. M. Proserpio, *Cryst. Growth Des.* **2014**, *14*, 3576.

[26] The terms *zweier*, *dreier*, *vierer*, *fünfer*, *sechser* and *achter* rings were coined by Liebau and are derived from the German words "drei" (three) and "sechs" (six), etc. through addition of suffix "er"; however, for example a *dreier* ring is not a three-membered ring, but a six-membered ring comprising *three* tetrahedra centers.

[27] W. H. Baur, *Crystallogr. Rev.* **1987**, *1*, 59.

[28] R. D. Shannon, *Acta Crystallogr., Sect. A: Cryst. Found. Crystallogr.* **1976**, *32*, 751.

[29] S. Pagano, S. Lupart, M. Zeuner, W. Schnick, *Angew. Chem.* **2009***, 121*, 6453; *Angew. Chem. Int. Ed.* **2009**, *48*, 6335.

[30] T. Schlieper, W. Schnick, *Z. Anorg. Allg. Chem.* **1995**, *621*, 1037.

[31] G. Cordier, A. Gudat, R. Kniep, A. Rabenau, *Angew. Chem.* **1989***, 101*, 1689; *Angew. Chem. Int. Ed. Engl.* **1989**, *28*, 1702.

[32] X. Z. Chen, H. A. Eick, *J. Solid State Chem.* **1997**, *130*, 1.

[33] A. Rabenau, H. Schulz, *J. Less-Common Met.* **1976**, *50*, 155.

[34] P. Cortona, *Phys. Rev. B: Condens. Matter* **1992**, *46*, 2008.

[35] P. Pust, W. Schnick, *Z. Anorg. Allg. Chemie* **2012**, *638*, 352.

[36] R. Hübenthal, *Programm zur Berechnung des Madelunganteils der Gitterenergie*, **1993**.

[37] R. Hoppe, *Angew. Chem.* **1966***, 78*, 52; *Angew. Chem. Int. Ed. Engl.* **1966**, *5*, 95.

[38] R. Hoppe, *Angew. Chem.* **1970***, 82*, 7; *Angew. Chem. Int. Ed. Engl.* **1970**, *9*, 25.

[39] A. J. D. Barnes, T. J. Prior, M. G. Francesconi, *Chem. Commun.* **2008**, 4638.

[40] F. Karau, O. Oeckler, F. Schaefers, R. Niewa, W. Schnick, *Z. Anorg. Allg. Chemie* **2007**, *633*, 1333.

[41] D. Durach, W. Schnick, *Eur. J. Inorg. Chem.* **2015**, 4095.

[42] S. Lupart, W. Schnick, *Z. Anorg. Allg. Chemie* **2012**, *638*, 2015.

[43] D. Durach, L. Neudert, P. J. Schmidt, O. Oeckler, W. Schnick, *Chem. Mater.* **2015**, *27*, 4832.

[44] D. Durach, F. Fahrnbauer, O. Oeckler, W. Schnick, *Inorg. Chem.* **2015**, *54*, 8727.

[45] S. Pagano, M. Zeuner, S. Hug, W. Schnick, *Eur. J. Inorg. Chem.* **2009**, 1579.

[46] W. Schnick, H. Huppertz, R. Lauterbach, *J. Mater. Chem.* **1999**, *9*, 289.

[47] J. L. Chambers, K. L. Smith, M. R. Pressprich, Z. Jin, *SMART, v.5.059, Bruker AXS, Madison, W1, USA*, **1997-2002**.

[48] *SAINT*, *v. 6.36, Bruker AXS*, Madison, W1, USA, **1997-2002**.

[49] G. M. Sheldrick, *Multi-Scan Absorption Correction, Bruker AXS*, Madison, W1, USA, **2012**.

[50] G. M. Sheldrick, *SHELXS-97: A program for crystal structure solution*, Universitiy of Göttingen, Germany, **1997**.

[51] G. M. Sheldrick, *SHELXL-97: A programm for crystal structure refinement*, University of Göttingen, Germany, **1997**.

[52] Brandenburg, *K. Crystal Impact GbR*, Bonn, **2005**.

3 Lithium (Oxo)nitridosilicates and their Material Properties

3.1 Introduction

Light – more than just brightness. It influences our psyche and health; we can feel insecure or even frightened by darkness, whereas light makes us feel comfortable and calms us down. Due to these feelings and with special regard to reduced energy consumption, the development of efficient light-emitting diodes (LEDs) with tunable emission colors and intensities plays a significant role. Meanwhile, inefficient light sources like incandescent light bulbs and compact fluorescent lamps are more and more replaced by the so-called phosphor-converted (pc)-LEDs.[1-3] They find broad application in diverse areas. These include medical applications, lifestyle products, general indoor and outdoor lighting, as well as use in the field of aviation and automotive lighting. The major advantages of LEDs are their long lifetimes, which decrease the maintenance costs on the one hand and, on the other hand their reduced energy consumptions. In 2030, energy consumption in the lighting sector is expected to be reduced by 40 % with this technology.[4] Therefore, pc-LEDs are the light sources of the future. Also the Nobel Prize, which was awarded to Akasaki, Amano, and Nakamura in 2014, "*for the invention of efficient blue light emitting diodes which has enabled bright and energy-saving white light sources*" clearly emphasizes the fundamental importance of (pc)-LEDs.[5]

The development of efficient LEDs for general lighting was a long journey. The technical origin dates back to 1993, as Shuji Nakamura developed the first efficient blue LED, based on GaN.[6] Currently, pc-LEDs are mainly used for general illumination. They consist of a blue-emitting (In,Al)GaN chip, which is combined with luminescent materials that are excited by the blue LED and emit light in the visible range. Usually, a broadband green to yellow (e.g. YAG:Ce^{3+}) and an orange to red emitting phosphor (e.g. Eu^{2+}-doped (oxo)nitridosilicates) are used as luminescent materials. Additive mixing of blue, green to yellow, and orange to red

phosphors, results in white light, color temperature thereby depending on the ratio of phosphors.[4, 7]

In general, the functional principle of pc-LEDs is based on the stimulation of the emission of a down-conversion phosphor material by a primary light source. Luminescence can be observed when energy transfer between a host lattice and an activator, for example, rare earth metal ions (e.g. Eu^{2+}, Eu^{3+}, Ce^{3+}), is given.[8] The excited states of the activator ions have thereby to be located in the band gap of the host lattice material. The energetic level and therefore the emission wavelength can be influenced by the chemical bonding between the activator ion and its surrounding (see Fig. 3.1.1). With increasing covalency, the energetic level decreases and emission occurs at longer wavelengths, and vice versa (nephelauxetic effect). Equally, the stronger the crystal field splitting, the longer the emission wavelengths. The conversion of light in a luminescent material is based on excitation and emission processes of activator ions, which are incorporated in the crystal structures of the host compounds. During the excitation process (irradiation with UV to blue light) of Eu^{2+}-doped compounds, one electron is transferred from the 4f state to the 5d (excited) state.[9] Subsequently, non-radiative relaxation to the lowest energy level of the excited state occurs, followed by 5d → 4f transitions under emission of photons. Due to strong interactions between 5d levels of Eu^{2+} and surrounding ligands, Eu^{2+} typically shows broad band emission. The stronger the interactions, the larger the Stokes shift, which is defined as the energetic difference between the centers of excitation and emission bands ($\lambda_{em} > \lambda_{exc}$). In general, due to short decay times and spin and parity allowed 4*f-5d* transitions, Eu^{2+} is widely used as activator ion in commercially available pc-LED phosphor materials.[10]

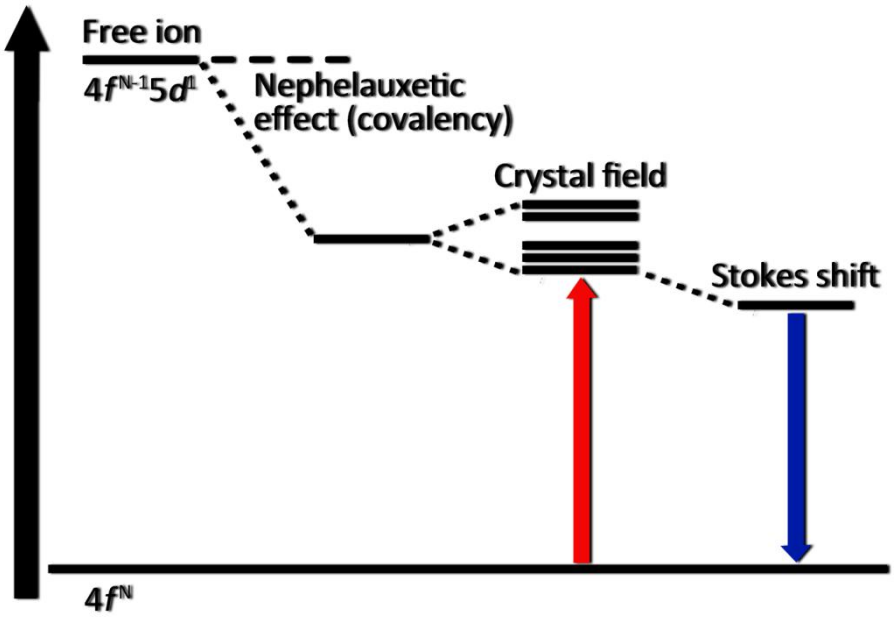

Figure 3.1.1. Scheme of excitation and emission processes in Eu^{2+}; influencing effects like the crystal field around the activator site and the nephelauxetic effect as well as the Stokes shift are considered.

In the past years, nitridosilicates and oxonitridosilicates turned out to be promising candidates for host lattices for Eu^{2+}-doping. A large number of them show highly condensed structures, which is beneficial for thermal and chemical resistance. Thus, nitridosilicates are one subject of current research. As (oxo)nitridosilicate phosphors $MSi_2O_2N_2:Eu^{2+}$ and $M_2Si_5N_8:Eu^{2+}$ (M = Ca, Sr, Ba), the latter with industrial application, have to be mentioned.[3, 7, 11] Due to the fact that emission characteristics hardly depend on the crystal structure of the host lattice, more precisely on the direct surroundings of the activator ions, modifications in crystal structures may lead to different emission wavelengths. In the following chapters, the novel compound $Li_{24}Sr_{12}[Si_{24}N_{47}O]F:Eu^{2+}$ and its outstanding luminescence properties are presented. Thereby, the influence of the incorporation of F into the crystal structure of $Li_2SrSi_2N_4:Eu^{2+}$ is discussed in detail.

Moreover, there a further material properties and applications of (oxo)nitridosilicates. Additionally, lithium ion conductivity has been researched for a number of lithium (oxo)nitridosilicates. The ternary phases $LiSi_2N_3$,[12-13] Li_2SiN_2,[13-14] Li_5SiN_3,[15-16] Li_8SiN_4[13-14] and $Li_{18}Si_3N_{10}$,[14] reported in the quasi-binary system Li_3N-Si_3N_4, all show lithium ion conduc-

tion (for example Li_2SiN_2: σ(400 K) = 1 x 10^{-3} S cm^{-1}; Li_8SiN_4: σ(400 K) = 5 x 10^{-2} S cm^{-1}) and have been discussed as candidates for Li battery applications.[13, 17-18] In order to obtain even better ionic conductivity values, which might be interesting for battery applications, further adjustments of the defect chemistry of Li_2SiN_2 through cation doping with Ca^{2+} and Mg^{2+} are also presented in the following chapter in detail.

References

[1] M. Born, T. Juestel, *Chem. Unserer Zeit* **2006**, *40*, 294.

[2] C. Feldmann, *Z. Anorg. Allg. Chemie* **2012**, *638*, 2169.

[3] R. Mueller-Mach, G. Mueller, M. R. Krames, H. A. Höppe, F. Stadler, W. Schnick, T. Juestel, P. Schmidt, *Phys. Status Solidi A* **2005**, *202*, 1727.

[4] P. Pust, P. J. Schmidt, W. Schnick, *Nature Mater.* **2015**, *14*, 454.

[5] J. Heber, *Nat. Phys.* **2014**, *10*, 791.

[6] S. Nakamura, M. Senoh, T. Mukai, *Appl. Phys. Lett.* **1993**, 62.

[7] M. Zeuner, S. Pagano, W. Schnick, *Angew. Chem.* **2011**, *123*, 7898; *Angew. Chem. Int. Ed.* **2011**, *50*, 7754.

[8] C. Ronda, *Luminescence*, Wiley-VCH Verlag, Weinheim, Germany, **2008**.

[9] H. A. Höppe, *Angew. Chem. Int. Ed.* **2009**, *48*, 3572.

[10] G. Blasse, A. Bril, *Appl. Phys. Lett.* **1967**, *11*, 53.

[11] H. A. Höppe, H. Lutz, P. Morys, W. Schnick, A. Seilmeier, *J. Phys. Chem. Solids* **2000**, *61*, 2001.

[12] M. Orth, W. Schnick, *Z. Anorg. Allg. Chemie* **1999**, *625*, 1426.

[13] J. Lang, J.-P. Charlot, *Rev. Chim. Miner.* **1970**, *7*, 121.

[14] H. Yamane, S. Kikkawa, M. Koizumi, *Solid State Ionics* **1987**, *25*, 183.

[15] R. Juza, H. H. Weber, E. Meyer-Simon, *Z. Anorg. Allg. Chemie* **1953**, *273*, 48.

[16] A. T. Dadd, P. Hubberstey, *J. Chem. Soc. Dalton Trans* **1982**, 2175.

[17] H. Hillebrecht, J. Cruda, L. Schröder, H. G. v. Schnering, *Z. Kristallogr. Suppl.* **1993**, *6*, 80.

[18] M. S. Bhamra, D. J. Fray, *J. Mater. Sci.* **1995**, *30*, 5381.

3.2 $Li_{24}Sr_{12}[Si_{24}N_{47}O]F:Eu^{2+}$ - Structure and Luminescence of an Orange Phosphor

published in: *Chem. Mater.* **2017**, *29*, 4590.

authors: Katrin Horky and Wolfgang Schnick

DOI: 10.1021/acs.chemmater.7b01363

http://pubs.acs.org/doi/abs/10.1021/acs.chemmater.7b01363

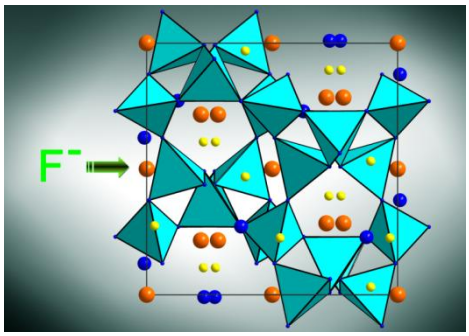

Abstract: The oxonitridosilicate fluoride phosphor $Li_{24}Sr_{12}[Si_{24}N_{47}O]F:Eu^{2+}$ was synthesized from Si_3N_4, SrH_2, $LiNH_2$, LiF and EuF_3 as dopant in a radio-frequency furnace. The crystal structure (space group $Pa\overline{3}$ (no. 205), a = 10.72830(10) Å, R_1 = 0.0401, wR_2 = 0.0885, Z = 1) of the host compound $Li_{24}Sr_{12}[Si_{24}N_{47}O]F$ was solved and refined on the basis of single-crystal X-ray diffraction data. $Li_{24}Sr_{12}[Si_{24}N_{47}O]F$ is homeotypic with the nitridosilicate $Li_2SrSi_2N_4$ as both compounds are characterized by the same tetrahedra network topology but $Li_{24}Sr_{12}[Si_{24}N_{47}O]F$ is an oxonitridosilicate and contains an additional F site. The implemented F is verified by EDX measurements as well as through calculations with PLATON. Besides, the electrostatic consistency of the refined crystal structure is proven by lattice energy calculations. The Eu^{2+}-doped compound $Li_{24}Sr_{12}[Si_{24}N_{47}O]F:Eu^{2+}$ shows an orange to red luminescence (λ_{max} = 598 nm; FWHM = 81 nm) under excitation with blue light, which differs from that of $Li_2SrSi_2N_4:Eu^{2+}$ (λ_{em} = 613 nm; FWHM = 86 nm) due to the additional F site. According to the blue-shifted emission, application in LEDs for sectors with low CRI is conceivable.

3.2.1 Introduction

With regard to their manifold structural chemistry as well as their materials properties and applications (oxo)nitridosilicates represent an intriguing compound class for development of new functional materials.[1] Due to their highly condensed network structures (oxo)nitridosilicates can be thermally and chemically rather inert and may be good candidates as rigid host lattices for Eu^{2+}-doping. Additionally, covalent character of the bonds between activator (dopant) and N causes a nephelauxetic effect, which is responsible for a red-shifted photoluminescence. Hence, Eu^{2+}-doped (oxo)nitridosilicates are well suitable as red emitting component in warm-white pc-LEDs. As examples the (oxo)nitridosilicate phosphors $Li_2SrSi_2N_4:Eu^{2+}$ or $MSi_2O_2N_2:Eu^{2+}$ and $M_2Si_5N_8:Eu^{2+}$ (M = Ca, Sr, Ba), the latter one with industrial application, can be mentioned.[1-5]

LED lighting is an essential key factor that can help to reduce electricity consumption and simultaneously solve environmental issues. Due to the continuous request of improved performance of pc-LEDs in more and more application fields the search for new phosphor materials based on (oxo)nitridosilicates is of great importance. Incorporation of further elements in (oxo)nitridosilicates has shown that again and again new structures and thus new phosphor materials became accessible. For instance, partial or formal substitution of Si by Al leads to nitridoalumosilicates. The luminophor $Sr[LiAl_3N_4]:Eu^{2+}$ as representative of the nitridoaluminate compound class combines e.g. an outstanding FWHM (~ 1180 cm^{-1}) with excellently high QE values up to 500 K.[6-7] Considering further optimization and adjustment of luminescence properties, different investigations on the solid solution series $Sr_{2-x}Ca_xSi_5N_8:Eu^{2+}$[8] or $Sr_{1-x}Ba_xSi_2O_2N_2:Eu^{2+}$ were undertaken, whereby the latter shows an unexpected red-shifted luminescence for increasing Ba^{2+} content.[9-10] Thus, these phases nicely illustrate how subtle substitution can affect luminescence properties markedly.

Several synthetic approaches to (oxo)nitridosilicates have been developed including high-temperature reactions, precursor routes, ammonothermal syntheses and flux methods with liquid sodium.[1, 11-17] Furthermore, solid-state metathesis reactions play an important role since a number of ternary or higher nitrides have been synthesized recently by this ap-

proach.[18-20] The decisive factor thereby is the application of reactive sources by coproducing a metathesis salt, whose formation acts as thermodynamic driving force of the reaction and which simultaneously acts as reactive flux. Recently, we also described a solid-state metathesis reaction, which enables incorporation of F in existing lithium nitridosilicate structures.[21] Besides the mentioned cation substitutions, we wondered whether and how incorporation of fluoride can influence luminescence properties. This purpose has now been tested in an exemplary study on the known phosphor $Li_2SrSi_2N_4:Eu^{2+}$.[4] In this contribution, we describe incorporation of F in $Li_2SrSi_2N_4:Eu^{2+}$ leading to the formation of $Li_{24}Sr_{12}[Si_{24}N_{47}O]F:Eu^{2+}$. More importantly, the modified emission characteristics and therefore possible luminescence tuning owing to the additional F site are discussed. The intriguing luminescence properties of the title compound make an application in pc-LEDs for more specialized applications, e.g. for street lighting, conceivable.

3.2.2 Experimental Section

3.2.2.1 Synthesis

For the synthesis of $Li_{24}Sr_{12}[Si_{24}N_{47}O]F:Eu^{2+}$ (with 2 mol % Eu), 20.3 mg (0.14 mmol) Si_3N_4 (UBE, 99.9 %), 16.4 mg (0.71 mmol) $LiNH_2$ (Aldrich, 95 %), 44.6 mg (1.72 mmol) LiF (Aldrich, > 99 %), 78.8 mg (0.88 mmol) SrH_2 (Cerac, 99.5 %) and 3.5 mg (0.02 mmol) EuF_3 (Aldrich, 99.99 %) as dopant were mixed in an agate mortar and filled into a tungsten crucible. All handlings were done under argon atmosphere in a glove box (Unilab, MBraun, Garching; O_2 < 1 ppm; H_2O < 1 ppm). Subsequently, the reaction vessel was transferred into a water-cooled silica glass reactor of a radio-frequency furnace (type AXIO 10/450, maximal electrical output 10 kW, Hüttinger Elektronik, Freiburg),[22] heated under N_2-atmosphere to 1000 °C within 1 h, maintained at that temperature for 10 h and then finally quenched to room temperature by switching off the furnace. The product was obtained as a heterogeneous powder with small aggregates of orange crystals showing orange luminescence after excitation with blue light. The crystals of $Li_{24}Sr_{12}[Si_{24}N_{47}O]F:Eu^{2+}$ are stable against air and water. Contact with air and water over several days does not lead to any marked decomposition.

3.2.2.2 SEM and EDX Spectroscopy

To determine the elemental composition and the morphology of the obtained crystals, a JEOL JSM 6500F field emission scanning electron microscope (SEM), operated at 8.6 kV and equipped with a Si/Li EDX detector (Oxford Instruments, model 7418), was used. In order to ensure electrical conductivity on the sample surface the obtained crystals were prepared on conductive adhesive films and were coated with carbon (BAL-TEC MED 020, Bal Tec AG). Within the sensitivity range of the method these measurements exclude the presence of other elements than Sr, Si, N F and Eu. The EDX analyses of the title compound resulted in an average atomic ratio of Sr:Si:N:O:F:Eu = 17:28:47:5:3:0.31 (normalized according to the Sr content, three measurements on different crystals; Li was not determinable by EDX).

3.2.2.3 Single-Crystal X-ray Diffraction

The X-ray diffraction data of $Li_{24}Sr_{12}[Si_{24}N_{47}O]F$ were collected with a D8 Venture (Bruker, Billerica MA, USA) diffractometer with Mo-K_α radiation (λ = 0.71073 Å) from a rotating anode source. Diffraction Data were indexed with SMART[23] and integrated with SAINT.[24] A multi-scan absorption correction was applied using the program SADABS.[25] The structure was solved with Direct Methods (SHELXS)[26] and refined using the method of full-matrix least-squares (SHELXL).[27] Visualization of the crystal structure was done with the help of DIAMOND.[28]

Further details of the crystal structure investigations may be obtained from the Fachinformationszentrum Karlsruhe, 76344 Eggenstein-Leopoldshafen, Germany (Fax: +49-7247-808-666; E-Mail: crysdata@fiz-karlsruhe.de, http://www.fiz-karlsruhe.de/request for deposited data.html) on quoting the depository number CSD-432550).

3.2.2.4 Powder X-ray Diffraction

Powder diffraction data were collected with a STOE STADI P diffractometer (Mo-$K_{\alpha 1}$ radiation, Ge(111) monochromator, MYTHEN 1 K detector) in Debye-Scherrer geometry. To verify the structural model simulated powder diffraction patterns, based on the single-crystal structure data, were generated by using the WinXPOW[29] program package and were compared with the measured powder diffraction data of the sample.

3.2.2.5 Luminescence

Luminescence of $Li_{24}Sr_{12}[Si_{24}N_{47}O]F:Eu^{2+}$ was analyzed with a luminescence microscope, consisting of a HORIBA Fluoromax4 spectrofluorimeter system attached to an Olympus BX51 microscope via fiber optics. Excitation wavelength was chosen to 440 nm. The emission spectra were measured between 440 and 800 nm with 2 nm step size. Excitation spectra were measured between 380 and 600 nm with 2 nm step size.

3.2.2.6 FTIR Spectroscopy

A Perkin Elmer BXII spectrometer with an ATR (attenuated total reflection) setup was used for recording the FTIR spectrum.

3.2.3 Results and Discussion

3.2.3.1 Synthesis and Chemical Analysis

The synthesis is based on a metathesis reaction. The driving force of this reaction is the decomposition of SrH_2 and its reaction with LiF to form SrF_2, which resublimates at the cool reactor wall. The remaining Sr reacts with excessive LiF, Si_3N_4, $LiNH_2$ and the dopant to $Li_{24}Sr_{12}[Si_{24}N_{47}O]F:Eu^{2+}$. The implemented O seemingly originates from contamination of commercially acquired reactants.

$$\mathbf{Si_3N_4 + LiNH_2 + LiF + SrH_2 + O_2 + EuF_3 \rightarrow Li_{24}Sr_{12}[Si_{24}N_{47}O]F:Eu^{2+} + SrF_2\uparrow + H_2\uparrow}$$

PXRD data support the suspected reaction mechanism (Figure S1, Supporting Information) as $Li_{24}Sr_{12}[Si_{24}N_{47}O]F:Eu^{2+}$ is only one compound among other, partly unknown, phases in the sample. $Li_{24}Sr_{12}[Si_{24}N_{47}O]F:Eu^{2+}$ forms block-like orange crystals. Through EDX analyses the morphology and the sum formula obtained from single-crystal structure refinement was validated (Fig. 1). Thus, the incorporation of F and Eu was confirmed. The presence of Eu is also proven by luminescence measurements. The cubic symmetry is also obvious from the SEM image as the crystal of $Li_{24}Sr_{12}[Si_{24}N_{47}O]F:Eu^{2+}$ exhibits a cuboctahedral habitus. With respect to the usage of N-H containing reagents a FT-IR spectrum (Figure S2, Supporting Information) of the title compound was recorded to confirm the absence of N-H bonds and thus the absence of hydrogen. Thus, the combination of EDX measurements and FTIR spectroscopy prove the absence of any other elements than Li, Sr, Si, N, O and F.

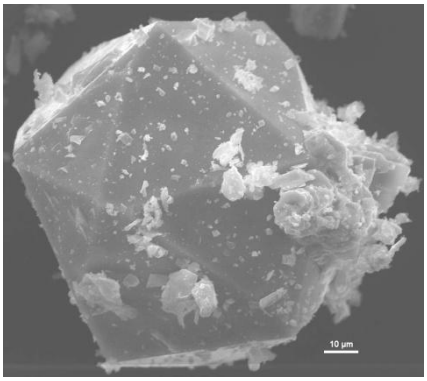

Figure 1. SEM image of a crystal of $Li_{24}Sr_{12}[Si_{24}N_{47}O]F$.

3.2.3.2 Single-Crystal Structure Analysis

The crystal structure of $Li_{24}Sr_{12}[Si_{24}N_{47}O]F$ was solved by using single-crystal X-ray diffraction data. The solution and refinement was performed in the cubic space group $Pa\overline{3}$ (no. 205) with a = 10.72830(10) Å. The heavy atoms were refined anisotropically. Table 1 contains the crystallographic data. The atomic coordinates and isotropic displacement parameters are listed in Table 2. Anisotropic displacement parameters are summarized in the Supporting Information (Table S1). The small amount of Eu^{2+} was neglected in the refinement of the crystal structure as well as for lattice energy calculations (MAPLE) because of its insignificant contribution to the scattering density.

Table 5. Crystallographic data of the single–crystal structure determination of $Li_{24}Sr_{12}[Si_{24}N_{47}O]F$.

parameter	**comment**
formula	$Li_{24}Sr_{12}[Si_{24}N_{47}O]F$
crystal system	cubic
space group	$Pa\overline{3}$ (no. 205)
lattice parameters / Å	a = 10.72830(10)
cell volume / Å^3	1234.79(3)
formula units per unit cell	1
crystal size / mm^3	0.020 x 0.020 x 0.020
density / g·cm^{-3}	3.477
μ / mm^{-1}	13.516
T / K	293(2)
radiation / Å	Mo K_α (λ = 0.71073)
F(000)	1210
ϑ range / °	$3.289 \leq \vartheta \leq 36.338$
independent reflections	1000 [R_{int} = 0.0718]
refined parameters	38
goodness of fit	1.286
R_1	0.0444 / 0.0401
(all data / for $F^2 > 2\sigma(F^2)$)	
wR_2	0.0899 / 0.0885
(all data / for $F^2 > 2\sigma(F^2)$)	
$\Delta\rho_{max}$, $\Delta\rho_{min}$ (e·Å^{-3})	1.379, –1.347

Table 6. Atomic coordinates and equivalent isotropic displacement parameters (in Å^3) of $Li_{24}Sr_{12}[Si_{24}N_{47}O]F$.

atom	site	*x*	*y*	*z*	U_{eq}
Sr1	8c	0.28398(3)	0.28398(3)	0.28398(3)	0.00818(12)
Sr2	4a	0	0	0	0.01494(17)
Si1	24d	0.02135(8)	0.13099(8)	0.25591(8)	0.00291(15)
N1O1	24d	0.0092(3)	0.2283(3)	0.1243(2)	0.0058(4)
N2O2	24d	0.0621(3)	0.2309(3)	0.3755(3)	0.0090(5)
F1	4b	1/2	1/2	1/2	0.069(14)
Li1	24d	0.0293(8)	0.3938(8)	0.2250(8)	0.0199(15)

3.2.3.3 Crystal Structure Description

The title compound is homeotypic to $Li_2SrSi_2N_4$ (Z = 12).[30] $Li_{24}Sr_{12}[Si_{24}N_{47}O]F$ (Z = 1) consists of Sr^{2+}, Li^+, F^- and a framework structure of vertex-sharing Q^4 type $Si(N/O)_4$ tetrahedra. As already reported the network of the compound contains exclusively N/O atoms bound covalently to two Si atoms and crystallizes according to *O'Keeffe* in *Net 39*. This leads to a degree of condensation $\kappa = n(Si):n(N/O) = 0.5$ comparable with SiO_2 or $MSiN_2$ (M = Be, Mg, Ca, Sr, Ba, Mn, Zn).[30-34] The structural motif of the Si(N/O) framework are *siebener*[35] rings annulated by four *dreier*[35] rings. Per unit cell there are twenty-four tetrahedra which are forming *dreier*[35] rings and *siebener*[35] rings. One part of the Li^+ and Sr^{2+} ions is located in the channels running parallel to the crystallographic axes of the Si(N/O) network (Fig. 2), whereas the remaining part is distributed amongst the voids of the structure.[30] In comparison to $Li_2SrSi_2N_4$ (Fig. 2a) an additional atom position in $Li_{24}Sr_{12}[Si_{24}N_{47}O]F$ exists (Fig. 2c) which is located at the middle of the cell edges as well as the center of the unit cell and is occupied to one quarter with F (Fig. 2b). Another distinction between $Li_2SrSi_2N_4$ and $Li_{24}Sr_{12}[Si_{24}N_{47}O]F$ are the mixed positions N/O in $Li_{24}Sr_{12}[Si_{24}N_{47}O]F$. These sites are occupied with N and O (2 %) in an atomic ratio of $^{47}/_{48} : {}^{1}/_{48}$, whereas in $Li_2SrSi_2N_4$ the corresponding positions are fully occupied with N. In view of the SiN_3O tetrahedra network and the isolated F site, the

compound can be classified as an oxonitridosilicate fluoride. In addition the crystal structure contains two crystallographically independent heavy-atom sites, each coordinated by N/O. The coordination sphere of Sr1 is a regular trigonal prism (Fig. 3a, orange) and is located in the middle between three *siebener*[35] rings (Fig. 3c). Sr2 is coordinating two *dreier*[35] rings in the form of a distorted octahedron (Fig. 3b). In his further coordination sphere the F site is surrounded by six Li atoms also in a distorted octahedral way. The observed Sr-N/O [2.637(3)-2.791(3) Å] distances are in good agreement with those in comparable compounds, such as $Li_2SrSi_2N_4$ [2.631(4) – 2.791(3) Å][30] as well as with the sum of the ionic radii.[36]

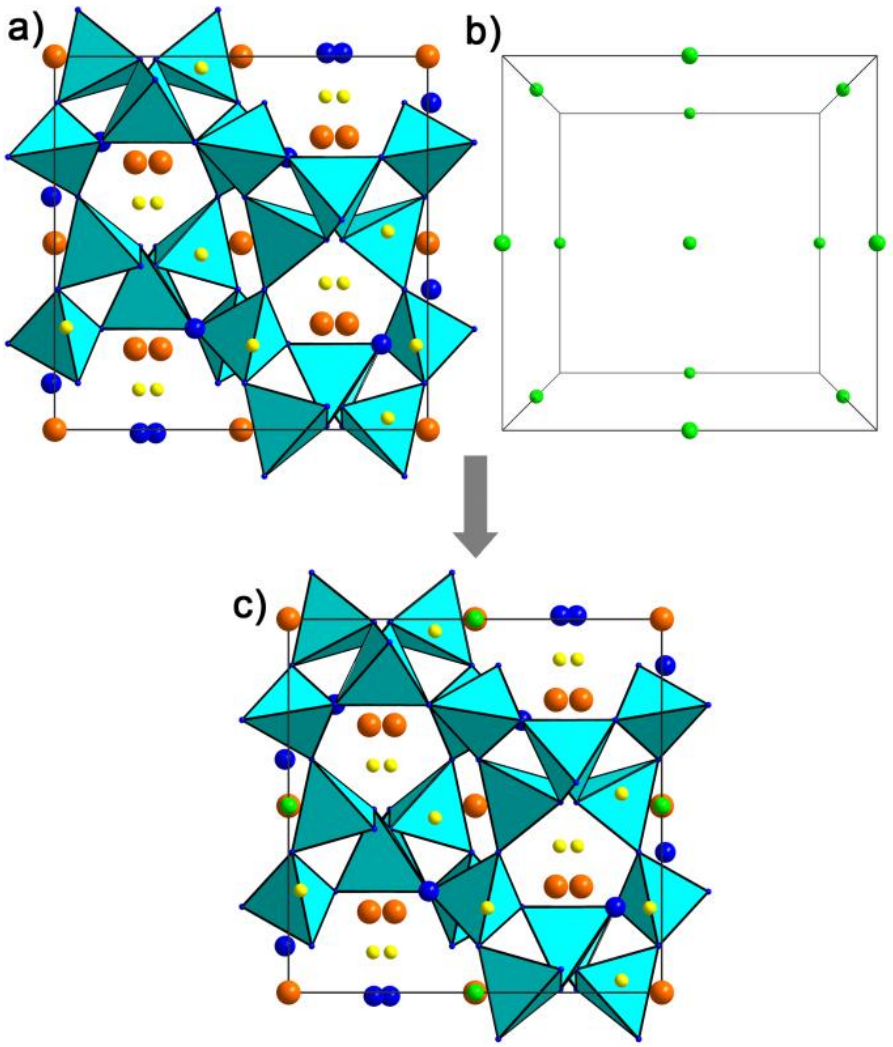

Figure 2. Crystal structure of $Li_2SrSi_2N_4$ (a) and F position at cell edges and the middle of the cell (b) leads to crystal structure of $Li_{24}Sr_{12}[Si_{24}N_{47}O]F$ (c); viewing direction along [100], Sr^{2+} orange, N/O dark blue, Si^{4+} inside the turquoise tetrahedra, Li^+ yellow, F^- green.

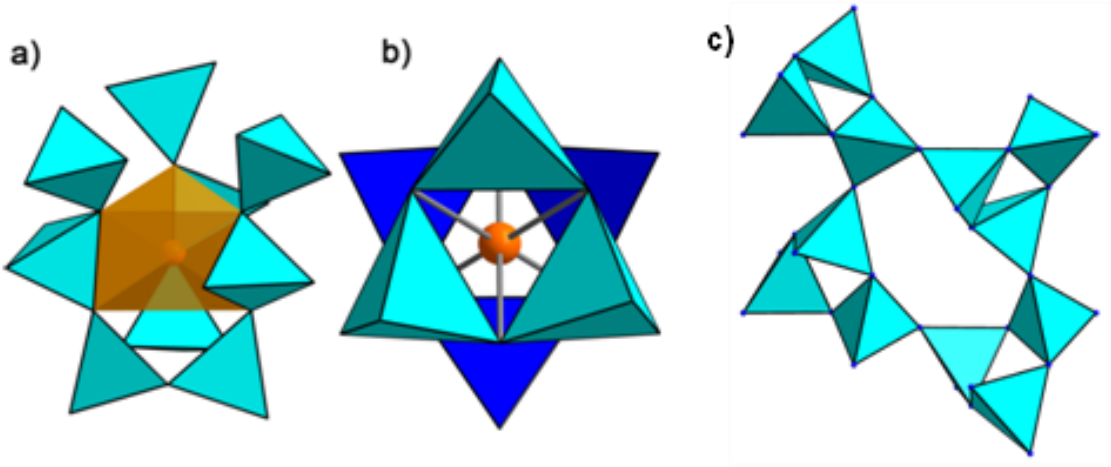

Figure 3. Coordination spheres of Sr1 (a) and Sr2 (b); $Si(N/O)_4$ tetrahedra form *dreier* rings, four of them build up *siebener* rings (c).

The distances Si-N,O in $Li_{24}Sr_{12}[Si_{24}N_{47}O]F$ range between 1.728(3) and 1.760(3) Å and are typical for (oxo)nitridosilicates.[16] With values from 2.076(9) to 2.405(9) Å the Li-N/O distances are in the typical range. Similar values were observed in comparable compounds, e.g. $LiCa_3Si_2N_5$ [1.998(8) – 3.044(16) Å][37] or Li_2O [1.981 Å].[38]

3.2.3.4 Investigations with PLATON

F^- represents a large ion and exhibits an ionic radius of 1.33 Å.[36] PLATON was used to confirm the incorporation of F into the crystal structure of $Li_2SrSi_2N_4$. Both size and positions of the voids in the crystal structure of $Li_2SrSi_2N_4$ were identified and calculated with CALC VOID.[39] Thereby, van der Waals radii of all atoms within the structural model (symmetry expanded to *P*1) were taken into account. Resulting voids are sufficiently large for F^- and are located at the middle of cell edges and the center of the cell. Analysis of the electron density of $Li_{24}Sr_{12}[Si_{24}N_{47}O]F$ in PLATON, plotted in *P*1, additionally verifies the localization of F on these positions (Fig. 4).

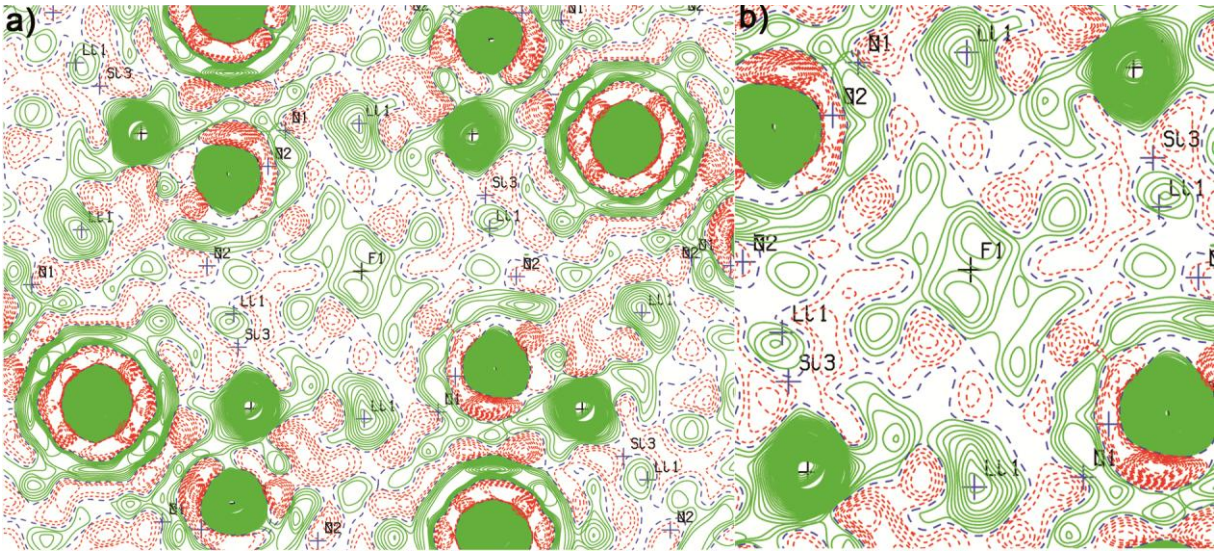

Figure 4. Electron density of $Li_{24}Sr_{12}[Si_{24}N_{47}O]F$ (a), F site (1, 0, ½) enlarged (b); contour level −6.00 e·Å^{-3} (green = positive electron density, red = negative electron density).

3.2.3.5 Lattice Energy Calculations

To prove the electrostatic consistency of the crystal structure, MAPLE calculations (MAPLE, Madelung part of lattice energy) were performed.[40-43] These calculations are especially useful to determine the site occupancies of F, N and O, as these ions can hardly be distinguished by conventional X-ray diffraction owing to their similar X-ray scattering factors. The calculated partial MAPLE values of Sr, Si, Li and N/O are consistent with reference values (Table 3). Since both N sites in $Li_{24}Sr_{12}[Si_{24}N_{47}O]F$ are singly bridging atoms, the O content was equally distributed to both sites. Other distributions resulting in MAPLE values with larger deviation, thus an occupation of only one N site with O is unlikely. Consideration of partly occupied sites is not possible with the MAPLE software, thus the value of the under-occupied F site is smaller than the characteristic range. But yet, by comparing the MAPLE sums of different nitrides, LiF and Li_2O with the MAPLE values of $Li_{24}Sr_{12}[Si_{24}N_{47}O]F$, the electrostatic balance of the refined crystal structure has been verified. The values differ only by 0.70 %, which is in the range of tolerance.

Table 7. Partial MAPLE values and MAPLE sums [kJ/mol] for $Li_{24}Sr_{12}[Si_{24}N_{47}O]F$.

	$Li_{24}Sr_{12}[Si_{24}N_{47}O]F$
Li^+	716
Sr^{2+}	1616-1729
Si^{4+}	9785
N^{3-}/O^{2-}	5384-5401
F^-	13
Total	531089
Δ	0.70 %

Total MAPLE; $Li_{24}Sr_{12}[Si_{24}N_{47}O]F$: 1 x LiF + 1 x Li_2O + 4 x Si_3N_4 + 12 x $SrSiN_2$ + 7 x Li_3N = 527395 kJ/mol.

[a] Typical MAPLE values [kJ/mol] for Sr^{2+}: 1500-2100; Si^{4+}: 9000-10200; N^{3-}: 4300-6200; O^{2-} 2000–2800; F^-: 465-599; Li^+: 550-860.[1, 17, 37]

3.2.3.6 Luminescence

Doping with Eu^{2+} yielded orange body colored samples of $Li_{24}Sr_{12}[Si_{24}N_{47}O]F:Eu^{2+}$ (2 mol % Eu^{2+}, nominal composition), which show intense luminescence in the orange to red spectral region under irradiation with blue light (Fig. 5). Luminescence investigations were performed for aggregates of the title compound sealed in silica glass capillaries. All particles show comparable orange to orange-red emission under irradiation with blue light.

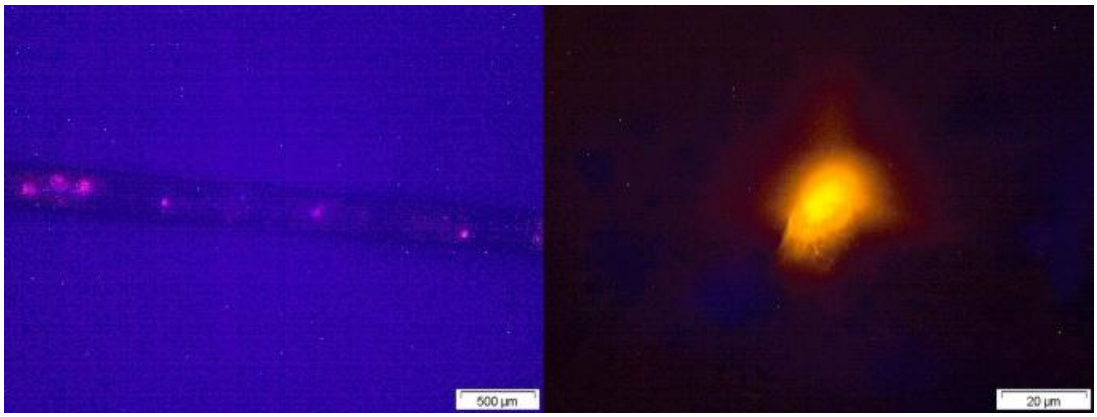

Figure 5. Orange luminescence of $Li_{24}Sr_{12}[Si_{24}N_{47}O]F:Eu^{2+}$ under blue light.

Emission and excitation spectra are displayed in Figure 6. As the excitation spectrum shows a broad band with a maximum at ~ 470 nm, $Li_{24}Sr_{12}[Si_{24}N_{47}O]F:Eu^{2+}$ can be excited very well by blue light originating from a (Ga,In)N-LED. Excitation of the title compound at ~ 470 nm yields a typical broadband emission, which can be traced back to the parity allowed $4f^6 5d^1$-$4f^7$-transition of Eu^{2+}. The emission band is in the red spectral region centered at 598 nm with a full width at half-maximum (FWHM) of 81 nm.

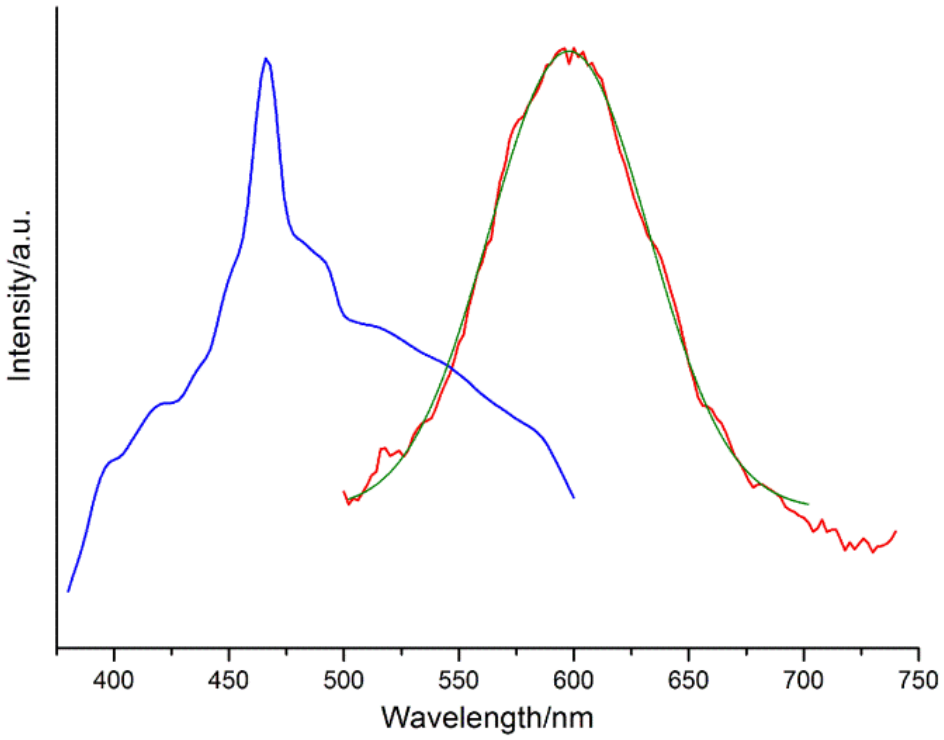

Figure 6. Smoothed excitation (blue) and emission (red) spectra of $Li_{24}Sr_{12}[Si_{24}N_{47}O]F:Eu^{2+}$ with Gauss fit (green) for determination of fwhm.

However, the Eu^{2+} doped compounds $BaGa_2S_4$ and $BaAl_2S_4$ also crystallizing in *Net 39* show blue to green or blue emissions.[44-45] Due to more covalent Eu-N instead of Eu-S bonds the emission maximum of the compound $Li_{24}Sr_{12}[Si_{24}N_{47}O]F:Eu^{2+}$ is strongly red shifted compared to the mentioned sulfides. Accordingly, the title compound is a further example illustrating the nephelauxetic effect. Emissions similar to $Li_{24}Sr_{12}[Si_{24}N_{47}O]F:Eu^{2+}$ are observed in comparable compounds like $Li_2SrSi_2N_4:Eu^{2+}$ (λ_{em} = 613 nm; FWHM = 86 nm),[4] $(Ca,Sr)AlSiN_3:Eu^{2+}$ (λ_{em} = 610-660 nm; FWHM = 90 nm)[46] or $Sr_2Si_5N_8:Eu^{2+}$ (λ_{em} = 609 nm; FWHM = 88 nm).[47-48] The latter compounds are industrially applied LED phosphor materials and show quite narrow emissions just as $Li_{24}Sr_{12}[Si_{24}N_{47}O]F:Eu^{2+}$, caused by a small number of heavy atom sites and the highly symmetrical environments of this sites. These specific structural features such as highly symmetrical surrounding of the activator ion, an ordered and rigid host lattice and a small number of heavy atom sites, are beneficial for narrow band red emission. This has been particularly shown for various compounds crystallizing in the

UCr_4C_4-structure type, like $M[Mg_2Al_2N_4]$ (M = Ca, Sr, Ba, Eu)[49] or $Sr[Mg_3SiN_4]:Eu^{2+}$.[50] In comparison to $Li_2SrSi_2N_4:Eu^{2+}$ $Li_{24}Sr_{12}[Si_{24}N_{47}O]F:Eu^{2+}$ exhibits a blue-shifted and a slightly narrower emission. We assume that the starting material LiF serves not only as F source, but acts as fluxing agent as well, thus the synthetic process leads to an improved homogeneity of $Li_{24}Sr_{12}[Si_{24}N_{47}O]F:Eu^{2+}$. This implicates a smaller phase width of the sample and thereby a narrower emission of $Li_{24}Sr_{12}[Si_{24}N_{47}O]F:Eu^{2+}$ compared to that of $Li_2SrSi_2N_4:Eu^{2+}$. This is a benefit of the reaction mechanism since with a narrower emission of the red-emitting component, the large portion of the emission in the infrared outside the sensitivity of the human eye can be reduced. The observed blue-shift can be traced back to the partially occupation with O of all N sites, induced to the F content, in $Li_{24}Sr_{12}[Si_{24}N_{47}O]F:Eu^{2+}$. The additional O content results in a decrease of the nephelauxetic effect, which leads to the blue-shifting of the emission of $Li_{24}Sr_{12}[Si_{24}N_{47}O]F:Eu^{2+}$ in comparison to $Li_2SrSi_2N_4:Eu^{2+}$. In relation to $Li_2CaSi_2N_4:Eu^{2+}$ (λ_{em} = 585 nm; FWHM = 79 nm)[51] the small red-shift of $Li_{24}Sr_{12}[Si_{24}N_{47}O]F:Eu^{2+}$ is probably due to the larger Sr^{2+} ions in the crystal structure. A similar effect was already described in the solid solution series $Sr_xBa_{1-x}Si_2O_2N_2$.[52] Therefore, the emission behavior of the title compound is located in the middle of the end members of the solid solution series $Li_2Ca_xSr_{1-x}Si_2N_4:Eu^{2+}$ (2 %) (λ_{em} = 585-613 nm; FWHM = 79-120 nm)[51] caused by the influence of the incorporated F, which leads for reason of charge neutrality to partial substitution of all N sites with O.

Summarizing the title compound shows a narrow emission at a shorter wavelength than $Li_2SrSi_2N_4:Eu^{2+}$. The blue-shift results in a lower CRI. Narrowing of the FWHM should enhance the efficiency of $Li_{24}Sr_{12}[Si_{24}N_{47}O]F:Eu^{2+}$. Due to inaccessibility of bulk samples of $Li_{24}Sr_{12}[Si_{24}N_{47}O]F:Eu^{2+}$ quantum efficiency measurements were not possible so far. The luminescence properties of $Li_{24}Sr_{12}[Si_{24}N_{47}O]F:Eu^{2+}$ lead in combination with a yellow to green phosphor to a more efficient white LED for applications with lower CRI.

3.2.4 Conclusion

In this contribution, the crystal structure and luminescence properties of a new oxonitridosilicate fluoride phosphor are reported. $Li_{24}Sr_{12}[Si_{24}N_{47}O]F:Eu^{2+}$ represents the third F-containing lithium alkaline earth nitridosilicate known so far.[21] The new orange to orange-red emitting nitride phosphor $Li_{24}Sr_{12}[Si_{24}N_{47}O]F:Eu^{2+}$ was prepared by a metathesis reaction. The title compound is homeotypic with $Li_2SrSi_2N_4:Eu^{2+}$ and exhibits the same type of tetrahedra network (*Net 39*) but contains an additional F site. The applied metathesis reaction leads to an incorporation of F in the crystal structure of $Li_2SrSi_2N_4:Eu^{2+}$. Consequently, through the synthesis route a further structural expansion of (oxo)nitridosilicates was possible. The herein presented compound shows an interesting change of luminescence properties induced by the incorporation of F. The emission is narrower and blue-shifted (λ_{em} = 598 nm; FWHM = 81 nm) when compared to that of $Li_2SrSi_2N_4:Eu^{2+}$ (λ_{em} = 613 nm; FWHM = 86 nm). Bulk samples of $Li_{24}Sr_{12}[Si_{24}N_{47}O]F:Eu^{2+}$ for quantum efficiency measurements were not yet obtained. The title compound is a further example for determinability of luminescence properties also on heterogeneous samples as already described by Xie et al. for the single particle diagnosis approach.[53] The results of this investigation illustrate the potential of (oxo)nitridosilicates as host lattices for Eu^{2+}-doped luminescent materials. By virtue of its stability towards air and moisture as well as its luminescence properties a possible application of cubic $Li_{24}Sr_{12}[Si_{24}N_{47}O]F:Eu^{2+}$ as phosphor in LEDs for more specialized applications appears conceivable. Besides, by further variation of the ratio F/O luminescence properties of the title compound may be further modified. Hence, $Li_{24}Sr_{12}[Si_{24}N_{47}O]F:Eu^{2+}$ is an example of a flexible system, which enables tuning of luminescence properties and widens the group of novel orange to red-emitting systems. By incorporation of F into other host lattices it is possible to achieve materials of specific properties, precisely tunable pursuant to respective application. This purpose could be feasible with the presented metathesis reaction

3.2.5 References

[1] M. Zeuner, S. Pagano, W. Schnick, *Angew. Chem.* **2011***, 123*, 7898; *Angew. Chem. Int. Ed*. **2011**, *50*, 7754.

[2] R. Mueller-Mach, G. Mueller, M. R. Krames, H. A. Höppe, F. Stadler, W. Schnick, T. Juestel, P. Schmidt, *Phys. Status Solidi A* **2005**, *202*, 1727.

[3] H. A. Höppe, H. Lutz, P. Morys, W. Schnick, A. Seilmeier, *J. Phys. Chem. Solids* **2000**, *61*, 2001.

[4] S. Pagano, Doctoral Thesis thesis, University of Munich (LMU) (Germany), **2009**.

[5] M. Zeuner, P. J. Schmidt, W. Schnick, *Chem. Mater.* **2009**, *21*, 2467.

[6] P. Pust, P. J. Schmidt, W. Schnick, *Nat. Mater.* **2015**, *14*, 454.

[7] P. Pust, V. Weiler, C. Hecht, A. Tucks, A. S. Wochnik, A.-K. Henß, D. Wiechert, C. Scheu, P. J. Schmidt, W. Schnick, *Nat. Mater.* **2014**, *13*, 891.

[8] Y. Q. Li, G. deWith, H. T. Hintzen, *J. Solid State Chem.* **2008**, *181*, 515.

[9] B.-G. Yun, Y. Miyamoto, H. Yamamoto, *J. Electrochem. Soc.* **2007**, *154*, J320.

[10] M. Seibald, T. Rosenthal, O. Oeckler, F. Fahrnbauer, A. Tücks, P. J. Schmidt, W. Schnick, *Chem. Eur. J.* **2012**, *18*, 13446.

[11] Z. A. Gál, P. M. Mallinson, H. J. Orchard, S. J. Clarke, *Inorg. Chem.* **2004**, *43*, 3998.

[12] H. Yamane, F. J. DiSalvo, *J. Alloys Compd.* **1996**, *240*, 33.

[13] T. Watanabe, K. Nonaka, J. Li, K. Kishida, M. Yoshimura, *J. Ceram. Soc. Jpn.* **2012**, *120*, 500.

[14] T. M. Richter, R. Niewa, *Inorganics* **2014**, *2*, 29.

[15] T. Schlieper, W. Schnick, *Z. Anorg. Allg. Chem.* **1995**, *621*, 1037.

[16] W. Schnick, H. Huppertz, *Chem. Eur. J.* **1997**, *3*, 679.

[17] D. Durach, W. Schnick, *Eur. J. Inorg. Chem.* **2015**, 4095.

[18] S. Schmiechen, F. Nietschke, W. Schnick, *Eur. J. Inorg. Chem.* **2015**, 1592.

[19] P. Strobel, S. Schmiechen, M. Siegert, A. Tucks, P. J. Schmidt, W. Schnick, *Chem. Mater.* **2015**, *27*, 6109.

[20] H.-J. Meyer, *Dalton Trans.* **2010**, *39*, 5973.

[21] K. Horky, W. Schnick, *Eur. J. Inorg. Chem.* **2016**, doi: 10.1002/ejic.201601386.

[22] W. Schnick, H. Huppertz, R. Lauterbach, *J. Mater. Chem.* **1999**, *9*, 289.

[23] J. L. Chambers, K. L. Smith, M. R. Pressprich, Z. Jin, **1997-2002**.

[24] *SAINT v. 6.36, Bruker AXS*, Madison, W1, USA, 1997-2002.

[25] Sheldrick, G. M. *Multi-Scan Absorption Correction, Bruker AXS*, Madison, W1, USA, 2012.

[26] Sheldrick, G. M. *SHELXS-97: A program for crystal structure solution*, Universitiy of Göttingen, Germany, 1997.

[27] Sheldrick, G. M. *SHELXL-97: A programm for crystal structure refinement*, University of Göttingen, Germany, 1997.

[28] Brandenburg, K. *Crystal Impact GbR*, Bonn, 2005.

[29] WinXPOW, *Vers. 2.12, Stoe & Cie GmbH WinXPOW*. Darmstadt, 2007.

[30] M. Zeuner, S. Pagano, S. Hug, P. Pust, S. Schmiechen, C. Scheu, W. Schnick, *Eur. J. Inorg. Chem.* **2010**, 4945.

[31] Z. A. Gál, P. M. Mallinson, H. J. Orchard, S. J. Clarke, *Inorg. Chem.* **2004**, *43*, 3998.

[32] P. Eckerlin, A. Rabenau, H. Nortmann, *Z. Anorg. Allg. Chem.* **1967**, *353*, 113.

[33] T. Endo, Y. Sato, H. Takizawa, M. Shimada, *J. Mater. Sci. Lett.* **1992**, *11*, 424.

[34] M. Winterberger, R. Marchand, M. Maunaye, *Solid State Commun.* **1977**, *21*, 733.

[35] Liebau, F. Structural Chemistry of Silicates, Springer, Berlin, **1986** (The terms *dreier* rings and *siebener* rings were coined by Liebau and are derived from the German words "drei" (three) and "sieben" (seven), etc. through addition of suffix "er"; however, for example a *dreier* ring is not a three-membered ring, but a six-membered ring comprising *three* tetrahedra centers).

[36] R. D. Shannon, *Acta Crystallogr., Sect. A: Cryst. Found. Crystallogr.* **1976**, *32*, 751.

[37] S. Lupart, W. Schnick, *Z. Anorg. Allg. Chemie* **2012**, *638*, 2015.

[38] A. Lazicki, C. S. Yoo, W. J. Evans, W. E. Pickett, *Phys. Rev. B: Condens. Matter* **2006**, *73*, 184120.

[39] P. v. d. Sluis, A. L. Spek, *Acta Crystallogr.* **1990**, *A46*, 194.

[40] W. H. Baur, *Crystallogr. Rev.* **1987**, *1*, 59.

[41] Hübenthal, R. A p*rogram for calculation of Madelung part of lattice energy*, Vers. 4; Universität Gießen: 1993.

[42] R. Hoppe, *Angew. Chem.* **1966**, *78*, 52; *Angew. Chem. Int. Ed. Engl.* **1966**, *5*, 95.

[43] R. Hoppe, *Angew. Chem.* **1970**, *82*, 7; *Angew. Chem. Int. Ed. Engl.* **1970**, *9*, 25.

[44] M. O'Keeffe, *Acta Crystallogr., Sect A: Found. Crystallogr.* **1992**, *48*, 670.

[45] R. B. Jabbarov, C. Chartier, B. G. Tagiev, O. B. Tagiev, N. N. Musayeva, C. Barthou, P. Benalloul, *J. Phys. Chem. Solids* **2005**, *66*, 1049.

[46] K. Uheda, N. Hirosaki, H. Yamamoto, *Phys. Status Solidi A* **2006**, *203*, 2712.

[47] F. Stadler, Doctoral Thesis, University of Munich (LMU) (Germany), **2006**.

[48] Y. Q. Li, J. E. J. v. Steen, J. W. H. v. Krevel, G. Botty, A. C. A. Delsing, F. J. DiSalvo, G. d. With, H. T. Hintzen, *J. Alloys Compd.* **2006**, *417*, 273.

[49] P. Pust, F. Hintze, C. Hecht, V. Weiler, A. Locher, D. Zitnanska, S. Harm, D. Wiechert, P. J. Schmidt, W. Schnick, *Chem. Mater.* **2014**, *26*, 6113.

[50] S. Schmiechen, H. Schneider, P. Wagatha, C. Hecht, P. J. Schmidt, W. Schnick, *Chem. Mater.* **2014**, *26*, 2712.

[51] M. Zeuner, Doctoral Thesis thesis, University of Munich (LMU) (Germany), **2009**.

[52] V. Bachmann, C. Ronda, O. Oeckler, W. Schnick, A. Meijerink, *Chem. Mater.* **2009**, *21*, 316.

[53] T. Takeda, N. Hirosaki, S. Funahashi, R. Xie, *Materials Discovery* **2015**, *1*, 29.

3.3 Li^+ ion Conductivity Investigations of Li_2SiN_2:Ca,Mg^{2+}

3.3.1 Introduction

In the last decades, the need for mobile power supply and efficient energy storage has continuously increased. As a consequence, rechargeable batteries have become a key technology in modern society.[1-4] By avoiding the use of liquid electrolytes, the reliability as well as the safety of batteries has remarkably been improved. Thus, solid lithium ion conductors gain in importance and current energy storage devices comprise all-solid-state lithium batteries. For their improvement, solid electrolytes with high lithium ion conductivity are essential. The variety of materials with the basic requirements for all-solid-state batteries, i.e. high ionic conductivity at the operating temperature and a high chemical, electrochemical, and thermal stability, is still very low.[5-6] Therefore, great effort has been put into the search for new solid electrolytes and a variety of crystalline, glassy, or composite materials have been considered.[1-3, 7] Especially, lithium nitridosilicates have recently been studied regarding their lithium ion mobility. Table 1 gives an overview of lithium ion conductivities of reported ternary lithium nitridosilicates.

Table 1. Comparison of conductivities at 400 K and activation energies of selected lithium nitridosilicates.

	$\sigma_{400\,K}$ (S m^{-1})	E_a (kJ mol^{-1})
$LiSi_2N_3$	1.9×10^{-5}	64
Li_2SiN_2	1.1×10^{-3}	53
Li_5SiN_3	4.7×10^{-3}	57
Li_8SiN_4	5.0×10^{-2}	46
$Li_{18}Si_3N_{10}$	2.9×10^{-3}	55
$Li_{21}Si_3N_{11}$	8.6×10^{-4}	54

Furthermore, nitridosilicates show a high chemical stability combined with high decomposition temperatures as well as high mechanical strength, and are often inert to oxidation and corrosive environments.[8-9] Thus, ternary lithium nitridosilicates are interesting materials for

novel solid electrolytes. Li_2SiN_2, for example, shows an ion conductivity of 1.1 x 10^{-3} S m^{-1}.[10-11] But for commercial application in lithium ion batteries, an ion conductivity of 0.1 S cm^{-1} is needed.[12] Therefore, Li^+ ion conductivity has to be improved, for example, by doping lithium ion-conductive solid electrolytes with ions of higher charges. For instance, $LiSi_2N_3$ has been chemically doped with Ca_3N_2 by forming $Li_{1-2x}Ca_xSi_2N_3$ (x = 0‑0.2), which leads to an increase in the ion conductivity of almost four orders of magnitude higher.[13] Equally, it was the aim to incorporate Ca^{2+} or Mg^{2+} into the Li_2SiN_2 host lattice. The radii of Li^+ and Ca^{2+} ions as well as Mg^{2+} are 0.73, 0.96 and 0.70 Å.[13] Upon doping of Li_2SiN_2, Li^+ may be substituted by the dopants Ca^{2+} or Mg^{2+}. Due to modification of the Li_2SiN_2 framework, which is caused by doping with $Ca^{2+}$and Mg^{2+}, interactions between the ions should decrease and, simultaneously, the number of defects in the structure is expected to increase, which leads to higher Li^+ mobility. Additionally, the number of mobile Li^+ ions should also be increased as the incorporation of aliovalent substitutional Ca^{2+}or Mg^{2+} ions is expected to be accompanied by Li^+ vacancies for reasons of charge compensation. In the following section, chemical doping in Li_2SiN_2 with the aim to further improve and optimize the Li^+ ion conductivity in Li_2SiN_2 solid electrolyte is described.

3.3.2 Experimental Part

3.3.2.1 General

With respect to air and moisture sensitivity of the starting materials and products, all manipulations were performed in flame-dried Schlenk-type glassware, which was attached to a vacuum line (10^{-3} mbar), or were performed in an argon-filled glovebox (Unilab, MBraun, Garching, O_2 <1 ppm, H_2O <1 ppm) with rigorous exclusion of oxygen and moisture.

3.3.2.2 General Experimental Procedure

Phase-pure samples of Li_2SiN_2 and $Li_{2-2x}Ca/Mg_xSiN_2$ (with x = 0.1) were prepared under high-temperature conditions under N_2 atmosphere. Si_3N_4 (50 mg, 0.36 mmol) and Li_3N (50 mg, 1.44 mmol) or Si_3N_4 (46.76 mg, 0.33 mmol), Li_3N (41.80 mg, 1.20 mmol) and Ca (4.00 mg, 0.01 mmol) or MgH_2 (2.63 mg, 0.08 mmol), respectively, were mixed and ground under an argon atmosphere, and transferred into a tungsten crucible (Plansee, Bad Urach, 99.97 %). Subsequently, the crucible was placed in a radio-frequency furnace (Typ AXIO 10/450, max. electrical output 10 kW, Hüttinger Elektronik, Freiburg)[14] and heated to 1000 °C within 1 h, maintained for 10 h and finally quenched to room temperature by switching off the furnace. The synthesis yielded colorless powders, which were sensitive to air and moisture.

3.3.2.3 Powder X-ray diffraction

Powder X-ray diffraction was performed to investigate the phase purity of the products. Diffraction data were collected with a STOE Stadi P diffractometer (Stoe & Cie, Darmstadt, Germany, Ge(111) monochromator, Mythen 1K detector). The samples were enclosed in glass capillaries with diameters of 0.3 mm under argon atmosphere for measurement. Rietveld refinement was carried out using the TOPAS package.[15]

3.3.2.4 EDX measurements

To investigate the atomic ratio Si/N and the incorporation of Mg^{2+}/Ca^{2+}, the samples were analyzed by energy-dispersive X-ray spectroscopy. Carbon-coated samples were examined with a scanning electron microscope (SEM) JSM-6500F (Jeol) equipped with a Si/Li EDX detector 7418 (Oxford Instruments). The determined compositions are within the typical error ranges and with regard to the fact that lithium cannot be detected by this method.

3.3.2.5 Conductivity measurements

For the electrical conductivity measurements, a series of pellets with a diameter of 5 mm and thickness of ~1 mm was obtained by uniaxially cold pressing (22 kN) the Li_2SiN_2 and Li_2SiN_2:Ca^{2+}/Mg^{2+} powders. The pellets were coated with gold thin films blocking electrodes (150 nm) by thermal evaporation. Impedance measurements were done by C. Dietrich (Group of Prof Dr. J. Janek, Institute of Physical Chemistry, Justus-Liebig-Universität Gießen, Germany) in the frequency range of 1 MHz to 100 mHz.

3.3.3 Results and Discussion

Phase-pure samples are indispensible for impedance measurements. To perform these measurements, samples have to be pressed to form pellets of specific diameter and thickness and even surfaces. The first step was to synthesize phase-pure samples of Li_2SiN_2 as a reference. Therefore, different starting materials in varying molar ratios, and syntheses temperatures were investigated. Phase-pure samples have exclusively been obtained by using "$Si(NH)_2$" and a double excess of Li_3N as starting materials, and a synthesis temperature of 1000 °C. A second synthesis optimization including the variation of different doping agents (CaH_2, Ca_3N_2 and Ca) yielded phase-pure samples of Li_2SiN_2:Ca^{2+}. First experiments were performed under ambient conditions. But thorough investigations indicated moisture-sensitivity of obtained products, which is why following experiments were handled under strict exclusion of air and moisture.

The experiments resulted in different qualities of the products, depending on applied starting materials. Therefore, stable pellets have only been obtained after reaction of Si_3N_4 and Li_3N instead of SDI as Si-source. We expect that due to the higher density of Si_3N_4 compared to that of "$Si(NH)_2$", Si_3N_4 shows better compressibility. Last but not least, a further synthesis optimization for preparation of phase-pure samples of Li_2SiN_2 with Mg^{2+} was also performed (variation of doping agents Mg, Mg_3N_2, MgH_2). In summary, phase-pure samples of Li_2SiN_2, Li_2SiN_2:$Ca^{2+}$and Li_2SiN_2:Mg^{2+} were synthesized with Si_3N_4 and were only accessible with double excess of Li_3N and pure Ca and MgH_2. For pressing pellets under inert conditions, also the starting material "$Si(NH)_2$" had to be exchanged by Si_3N_4.

EDX measurements were used to determine the elemental composition of the product and to confirm the incorporation of Ca^{2+}/Mg^{2+} (see Table 2). Small amounts of oxygen were detected, which can be ascribed to partial hydrolysis of the compound when exposed to air. The determined atomic ratio agrees well with the sum formula. Li cannot be detected by EDX; no further elements except Si, N, Ca, Mg (and O) were detected.

Table 2. EDX measurements of doped Li_2SiN_2 with Ca^{2+} and Mg^{2+}.

element	Ø atom-%	calculated atom-%
Li	-	37
Ca/Mg	2	2
Si	26	20
O	7	-
N	65	41

To exclude possible side phases, powder diffraction patterns were collected. Rietveld refinements of the diffraction patterns showed phase purity (see Fig. 1, Li_2SiN_2:Mg^{2+}as representative example).

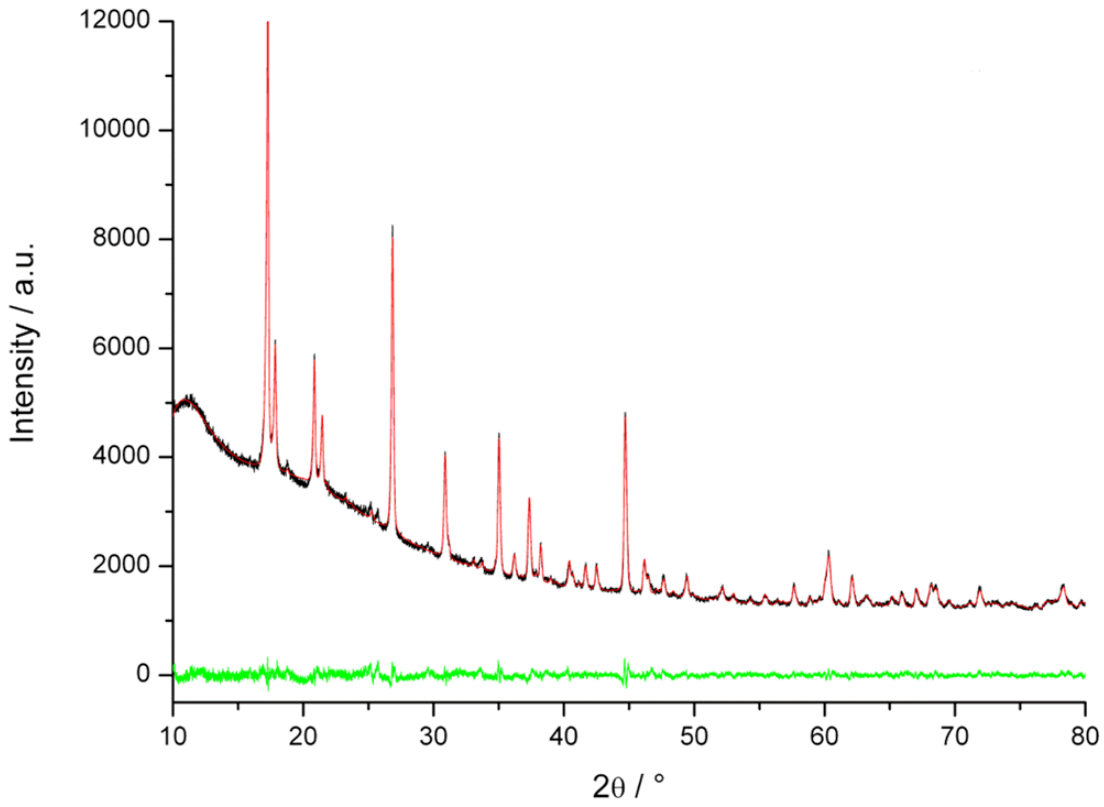

Figure 1. Characteristic section of the Rietveld profile fit for a sample of Li_2SiN_2:Mg^{2+}: observed (black line) and calculated (red line) powder diffraction patterns of the sample as well as difference profile (green line).

TOPOS analyses were employed to investigate structural voids and channels, in which Li^+ ions are expected to be located. The voids in the crystal structure were calculated by employing Voronoi-Dirichet polyhedra. Each void smaller than 1.45 Å (Slater radius of Li^+)[16] was omitted. The analysis of Li_2SiN_2 on the basis of the crystal structure refinement yielded possible 1D migration pathways along the crystallographic *c*-axis, as shown in Figure 2. *Anurova* et al. calculated the voids of more than 2000 known compounds containing Li^+ ions with the TOPOS program.[17] All of the analyzed compounds exhibit infinite lithium pathways: Li^+ ion conductivity was experimentally proven. According to these calculations, anisotropic lithium ion conductivity is plausible with respect to the structural chemistry of Li_2SiN_2.

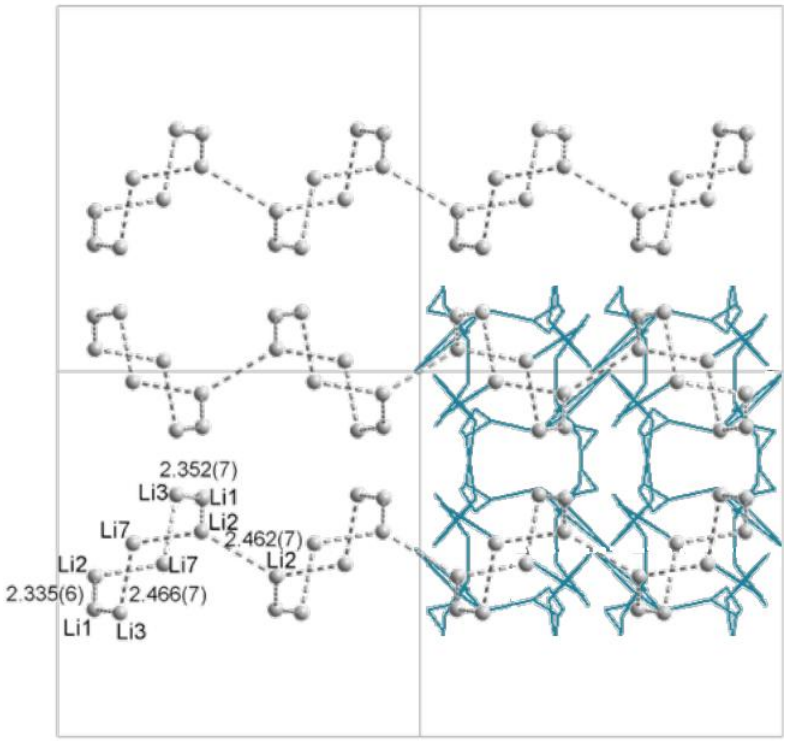

Figure 2. Calculated possible Li^+ pathways (blue) according to the voids in the structure and unit cell of Li_2SiN_2 viewing along [001].

To determine Li^+ ion conductivity of Li_2SiN_2, Li_2SiN_2:$Ca^{2+}$and Li_2SiN_2:Mg^{2+}, impedance measurements should have been performed. As described above, pressing pellets turned out to be a challenging task. During the conductivity measurements the pellets broke, presumably the samples were not stable enough for impedance measurements. Thus, it was not possible to receive values for the conductivity of Li_2SiN_2, Li_2SiN_2:Ca^{2+} and Li_2SiN_2:Mg^{2+}. In addition, an alternative measurement setup was tested. Therefore, powder samples instead of pellets were used. However, this novel method was still in the maturing phase and does not yet provide incontestable results. Obtained values for Li^+ ion conductivity of Li_2SiN_2 widely vary from the values known from literature. A reason may be that the thickness of measured samples cannot be determined unequivocally, which is an important value for determination of Li^+ ion conductivity.

3.3.4 Conclusion

In the previous chapter, synthesis of phase-pure samples of Li_2SiN_2 doped with Ca^{2+} and Mg^{2+} was described. The prepared pellets of phase-pure samples of Li_2SiN_2, Li_2SiN_2:Ca^{2+}as well as Li_2SiN_2:Mg^{2+} were not stable during the conductivity measurements. Therefore, it has not been possible to determine conductivity values so far. Given that doping of Li_2SiN_2 with Ca^{2+} and Mg^{2+} was successful, only the pellets stability needs to be optimized in future researches to determine the lithium ion conductivity. Perhaps sintering of the samples may be helpful to increase their density and their hardness. In this context, it is important to recall that doping of $LiSi_2N_3$ with Ca^{2+} resulted in an ionic conductivity enhancement up to 4 orders of magnitude while the activation energy decreased from 0.69 eV (undoped) down to 0.22 eV. Thus, the doped samples of Li_2SiN_2 with Mg^{2+} and Ca^{2+} should also show remarkably improved lithium ion conductivity.

References

[1] M. S. Whittingham, *Chem. Rev.* **2004**, *104*, 4271.

[2] J. F. M. Oudenhoven, L. Baggetto, P. H. L. Notten, *Adv. Energy Mater.* **2011**, *1*, 10.

[3] M. Park, X. Zhang, M. Chung, G. B. Less, A. M. Sastry, *J. Power Sources* **2010**, *195*, 7904.

[4] M. Armand, J.-M. Tarascon, *Nature* **2008**, *451*, 652.

[5] N. Kamaya, K. Homma, Y. Yamakawa, M. Hirayama, R. Kanno, M. Yonemura, T. Kamiyama, Y. Kato, S. Hama, K. Kawamoto, A. Mtsui, *Nat. Mater.* **2011**, *10*, 682.

[6] C. Masquelier, *Nat. Mater.* **2011**, *10*, 649.

[7] A. D. Robertson, A. R. West, *J. Solid State Chem.* **1982**, *44*, 354.

[8] M. Zeuner, S. Pagano, W. Schnick, *Angew. Chem.* **2011**, *123*, 7898; *Angew. Chem. Int. Ed*. **2011**, *50*, 7754.

[9] W. Schnick, *Angew. Chem.* **1993**, *105*, 846; *Angew. Chem.Int. Ed.* **1993**, *32*, 806.

[10] J. Lang, J.-P. Charlot, *Rev. Chim. Miner.* **1970**, *7*, 121.

[11] H. Hillebrecht, J. Cruda, L. Schröder, H. G. v. Schnering, *Z. Kristallogr. Suppl.* **1993**, *6*, 80.

[12] A. D. Robertson, A. R. West, A. G. Ritchie, *Solid State Ionics* **1997**, *104*, 1.

[13] E. Narimatsu, Y. Yamamoto, T. Takeda, T. Nishimura, N. Hirosaki, *J. Mater. Res.* **2011**, *26*, 1133.

[14] W. Schnick, H. Huppertz, R. Lauterbach, *J. Mater. Chem.* **1999**, *9*, 289.

[15] A. Coelho, *TOPAS Academic*, Brisbane, Australia, **2007**.

[16] J. C. Slater, *J. Chem. Phys.* **1964**, *41*, 3199.

[17] N. A. Anurova, V. A. Blatov, G. D. Ilyushin, O. A. Blatova, A. K. Ivanov-Schitz, *Solid State Ionics* **2008**, *179*, 2248.

4 Conclusion and Outlook

Lithium (oxo)nitridosilicates are interesting compounds, not only from a structural point of view but also as they show intriguing materials properties. In the course of this work various synthetic approaches were used in order to obtain new members of this compound class. Thus, the focus of this thesis was set on the finding of a synthesis route enabling access to novel lithium (oxo)nitridosilicates. Finally, a metathesis route was successful for the synthesis of so far unknown multinary lithium (oxo)nitridosilicates.

In general ternary lithium (oxo)nitridosilicates were synthesized between 700 °C and 1200 °C by solid-state reaction of Li_3N and Si_3N_4 under N_2 atmosphere. Known quaternary compounds with Ca and Sr were usually obtained in welded tantalum tubes under argon by heating typical starting materials for 12‑24 h at 900 °C (chapter 2). Thus, uncommon starting materials and novel reaction conditions were tested with the aim of preparing unknown ternary lithium (oxo)nitridosilicates as well as unknown quaternary lithium (oxo)nitridosilicates with Ba. In conclusion, with all of these investigations – reaching from synthesized starting materials, high-temperature synthesis in open as well as closed systems to high-pressure reactions - no unknown or crystalline compounds were obtained (chapter 2.2). However, high-pressure reactions hold a lot of promise as they indicated the formation of an unknown Li/Si/N compound and therefore should be favored in future works.

A metathesis approach combing the precursors "$Si(NH)_2$" and $La(NH_2)_3$ with lanthanum halides (LaX_3, X = F, Cl, Br) plus earth alkali hydrides (EAH_2, EA = Ca, Sr, Ba) already yielded several unknown lanthanum (oxo)nitridosilicates.[1] Consequently, this route served as a further starting point and was transferred to lithium (oxo)nitridosilicates. In this work, the corresponding lithium compounds instead of the lanthanum compounds were used as starting materials and the mentioned approach was successfully applied to the system Li/Si/(O)/N. Furthermore, it was also possible to exchange "$Si(NH)_2$" and "$Si_2(NH)_3 \cdot 6NH_4Cl$" against Si_3N_4 within this approach, which is of great advantage as Si_3N_4 is commercially available. All novel compounds of this work were exclusively obtained with this type of reaction. Thermodynam-

ic sinks and the synthesis of already known compounds were avoid with this route as the decomposition of the *EA*H_2 around 600 °C (CaH_2: 600 °C, BaH_2/SrH_2: 675 °C)[2] and its reaction to *EA*X_2 - with the halide originating from LiX - acts as driving force for the reaction. Next to further intermediates, presumably finely dispersed and reactive Li metal is formed, which reacts with the remaining *EA*, LiX, $LiNH_2$ and Si_3N_4. Oxygen contents originating assumedly from impurities of commercially acquired starting materials. EuF_3 was added to all reactions as doping agent. Furthermore, it has to be mentioned that this approach leads to a good crystallinity of the reaction products, which was not observed for the other routes but is necessary for a structure elucidation by single–crystal X-ray diffraction.

With this synthesis route four so far unknown multinary lithium (oxo)nitridosilicates – namely $Ba_{32}[Li_{15}Si_9W_{16}N_{67}O_5]$ (chapter 2.3), $LiCa_4Si_4N_8F$ as well as $LiSr_4Si_4N_8F$ (chapter 2.4) plus $Li_{24}Sr_{12}Si_{24}N_{47}OF:Eu^{2+}$ (chapter 3.1) - with intriguing structures have been obtained. Presumably, the composition of the starting materials is decisive whether the X ion is incorporated in the lithium (oxo)nitridosilicate or not. Thus, syntheses are possible in which the halide is incorporated or not, as shown with the synthesis of $Ba_{32}[Li_{15}Si_9W_{16}N_{67}O_5]$ and Li*EA*$_4Si_4N_8F$ (EA = Ca,Sr). In contrast to the lanthanum (oxo)nitridosilicates, the formation of ternary lithium (oxo)nitridosilicates was not observed with this route until now. For example, the compound $La_3[SiN_3O]$ represents a lanthanum oxonitridosilicate consisting only of La, Si, N and O, whereas for the synthesis of the obtained lithium (oxo)nitridosilicates either the F ions of LiF as well as the EA ions of *EA*H_2 (EA = Ca, Sr) are necessary. Additionally, the incorporation of W was novel for this route leading to the first oxonitridolithotungstosilicate $Ba_{32}[Li_{15}Si_9W_{16}N_{67}O_5]$. All in all, further structural variations were achieved with this type of reaction by the incorporation of F and W into the Li/Si/(O)/N compound class. With $Ba_{32}[Li_{15}Si_9W_{16}N_{67}O_5]$ a mixed cation position of Li and Si plus the combination of the Si/N and W/N compound was observed for the first time. The mentioned combination leads to a structural expansion, since the WN_4 tetrahedra show a hitherto unknown linkage with SiN_4 tetrahedra. The occurrence of linked WN_4 tetrahedra in $Ba_{32}[Li_{15}Si_9W_{16}N_{67}O_5]$ is an exceptional feature since in other tungsten nitrides with Li and Ba isolated $[M^{VI}N_4]^{6-}$ tetrahedra anions are common. Furthermore, this combination led to an incorporation of Ba into lithi-

um (oxo)nitridosilicates, which was not observed before. Moreover, the compounds $LiCa_4Si_4N_8F$ and $LiSr_4Si_4N_8F$ are not only the first F-containing lithium alkaline earth nitridosilicates, they are the first multinary nitride-fluorides consisting of a zeolite-related framework (BTC-type) as well, which is exclusively built up of vertex-sharing SiN_4 tetrahedra with a degree of condensation κ = n(Si):n(N) = 0.50. This shows the broad structural variability of nitridosilicates. In addition, a high degree of condensation stands mostly for a stable network and therefore such compounds seem to be favorable for luminescence properties upon doping with Eu^{2+}. This was confirmed by doping of $Li_{24}Sr_{12}Si_{24}N_{47}OF$ and the observed emission at 598 nm after irradiation with blue light. This compound shows an interesting change of luminescence properties induced by the incorporation of F. The emission is narrower and blue-shifted (λ_{em} = 598 nm; FWHM = 81 nm) when compared with the homeotypic compound $Li_2SrSi_2N_4:Eu^{2+}$ (λ_{em} = 613 nm; FWHM = 86 nm). Hence, $Li_{24}Sr_{12}[Si_{24}N_{47}O]F:Eu^{2+}$ is an example of a flexible system, which enables tuning of luminescence properties and widens the group of novel orange to red-emitting systems. By incorporation of F into further host lattices it may be possible to achieve materials of specific properties, precisely tunable pursuant to respective application.

All the shown examples corroborate that the possibilities of this synthetic route are enormous. Surely it would be interesting to further extent this metathesis route by alteration of the starting materials, their composition or by adding additional components as well as the thermal treatment of the samples. This might enable the synthesis of further new lithium (oxo)nitridosilicates, e.g. so far unknown quaternary lithium (oxo)nitridosilicates with Mg might become accessible with this approach. As the compounds $La_6Ba_3[Si_{17}N_{29}O_2]Cl$ as well as $Ba_{1.63}La_{7.39}Si_{11}N_{23}Cl_{0.42}:Ce^{3+}$ are known, also the incorporation of Cl into lithium (oxo)nitridosilicates should be possible as well.

Since lithium (oxo)nitridosilicates might be intriguing as Li^+ ion conductors, the effect of Ca and Mg doping on the ionic conductivity of Li_2SiN_2 was also investigated during this thesis. The preparation of pellets of phase-pure samples of Li_2SiN_2, $Li_2SiN_2:Ca^{2+}$as well as $Li_2SiN_2:Mg^{2+}$ was successful. However, the pellets were not stable during the conductivity

measurements and the determination of conductivity values was not possible so far. Presumably the instability of the pellets is originating from the materials properties of the samples. The exchange of "$Si(NH)_2$" against Si_3N_4 yet improved this problem remarkably. Since doping of Li_2SiN_2 with Ca^{2+} and Mg^{2+} was already achieved, only the stability of the pellets needs to be further optimized in future works to determine the lithium ion conductivity.

In this thesis, a novel synthetic approach for synthesis of nitridosilicates could be established and several new compounds leading to structural expansions could be investigated. Moreover, exceptional luminescence properties of a novel Eu^{2+}-doped lithium nitridosilicatefluoride were presented. The findings of this thesis raise a further incentive to investigate novel compounds in the class of lithium (oxo)nitridosilicates. With the used approach additional structural novelties should be achievable increasing the structural variety of this interesting compound class further on.

References

[1] D. Durach, Doctoral Thesis, Univesity of Munich (LMU), Germany, **2016**.

[2] W. Grochala, P. Edwards, *Chem. Rev.* **2004**, *104*, 1283.

5 Summary

5.1 Investigations into the Synthesis of Ternary and Ouaternary Lithium (Oxo)nitridosilicates

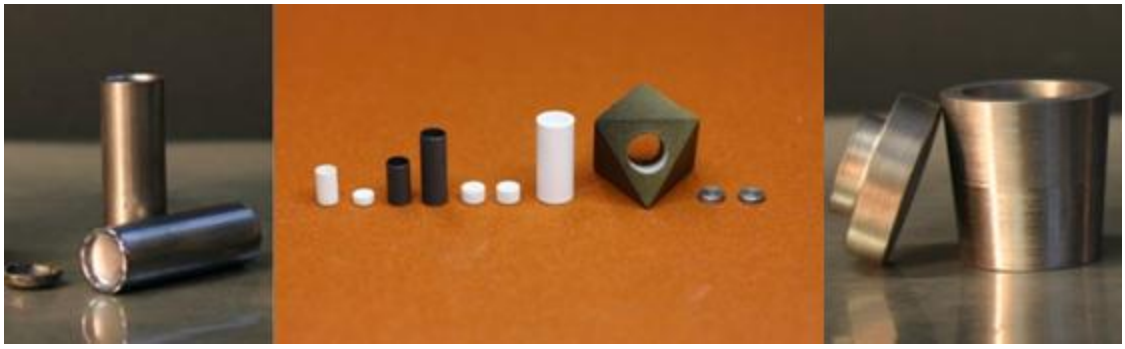

Up to now, there are only few reports of ternary lithium (oxo)nitridosilicates and even no reports of lithium (oxo)nitridosiliciates with barium. Thus, the focus of this thesis was on development of new synthetic strategies enabling access to novel representatives of the mentioned compound classes. Therefore, both starting materials and reaction conditions were modified extensively. These investigations included high temperature reactions in tantalum ampoules, tungsten crucibles and high-pressure reactions as well as the usage of uncommon starting materials. Thereby, various starting materials in varying molecular ratios were used as well as different temperatures, reaction times and cooling rates were investigated. In summary, with all of these conditions and variations, no unknown compounds within the system Li/Si/N and Li/Ba/Si/N were obtained or could not be structurally characterized due to bad crystallinity of the obtained products. In future works high-pressure high-temperature reactions should be pursued since these reactions clearly indicated the formation of an unknown Li/Si/N compound. Finally, the transformation of a synthetic approach - based on halides, hydrides and amides and developed for the synthesis of novel lanthanum (oxo)nitridosilicates – to the system Li/Si/N was also successful for synthesis of novel multinary lithium (oxo)nitridosilicates. With this approach the compound class of lithi-

um (oxo)nitridosilicates was expanded. The different novel members which were obtained are summarized in the following chapters.

5.2 $Ba_{32}[Li_{15}Si_9W_{16}N_{67}O_5]$ – a Ba-containing Oxonitridolitho-tungstosilicate with a Highly Condensed Network Structure

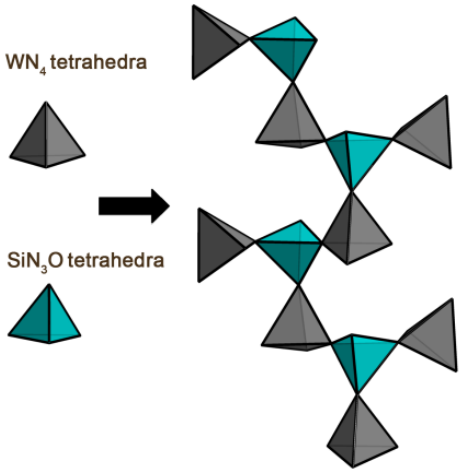

The oxonitridolithotungstosilicate $Ba_{32}[Li_{15}Si_9W_{16}N_{67}O_5]$ was synthesized by means of solid-state metathesis reactions. Block-like orange crystals of the latter one were obtained by heating the reactive starting materials $Si(NH)_2$, $LiNH_2$, LiF and BaH_2 in a tungsten crucible in a radio-frequency furnace at 1000 °C. But also a targeted incorporation of tungsten was possible. Exchange of LiF against WCl_6 in the initial reaction mixture showed that $Ba_{32}[Li_{15}Si_9W_{16}N_{67}O_5]$ is also formed. The crystal structure was successfully solved and refined using single-crystal X-ray diffraction [$P2_1/n$ (no. 14), a = 8.3402(3), b = 8.5465(3), c = 16.6736(6) Å, β = 99.1950(10)°, Z = 1, R_1(all) = 0.0302]. The chemical composition as well as the structural model of the compound was confirmed through X-ray spectroscopy, lattice energy calculations with MAPLE and X-ray diffract. The absence of N-H bonds was proven with IR spectroscopy. Magnetic measurements validated oxidation state +VI for W since these measurements showed diamagnetic behavior. Additionally, the optical band gap of $Ba_{32}[Li_{15}Si_9W_{16}N_{67}O_5]$ was determined by UV-Vis spectroscopy and was estimated to be

~ 2.71 eV according to the light orange body color. The compound is characterized by a highly condensed framework of vertex- and edge-sharing LiN_3O, Li/SiN_3O and SiN_3O tetrahedra as well as vertex-sharing WN_4 units. The tetrahedra are condensed to different kinds of rings. Whereby *fünfer*, *sechser* and *achter* rings form channels along [100] and [010]. The cavities of the structure are filled with Ba^{2+} ions which are coordinated by 6 to 8 anions. An exceptional structural feature is given for the WN_4 tetrahedra. These are part of the three-dimensional network – whereas in other tungsten nitrides isolated $[W^{VI}N4]^{6-}$ tetrahedra anions are common - and are alternating connected with SiN_4 tetrahedra in chains running along [001]. With this contribution, we could show that solid-state metathesis reactions represent a promising and new synthetic approach for novel nitridosilicates. It opens up a wide range of novel possible crystal structures and combined the Si/N and W/N compound classes for the first time. Furthermore, this combination led to an incorporation of Ba into lithium (oxo)nitridosilicates, which was not observed before. Since this incorporation could also not been achieved with the other investigated approaches (chapter 2.2) the presence of W seems to be crucial for it.

5.3 $LiCa_4Si_4N_8F$ and $LiSr_4Si_4N_8F$ – Nitridosilicate Fluorides with a BCT-Zeolite Type Network Structure

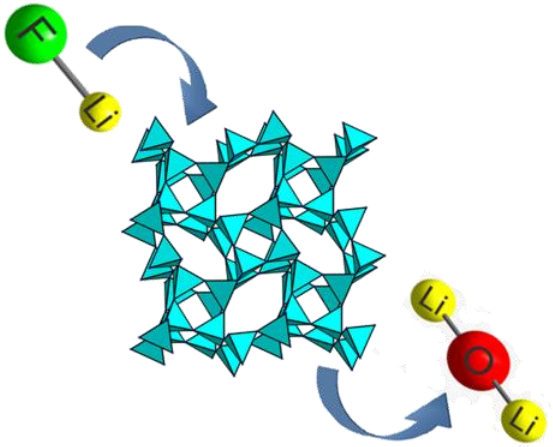

The nitridosilicate fluorides $LiCa_4Si_4N_8F$ and $LiSr_4Si_4N_8F$ were synthesized employing the same solid-state metathesis reaction in a radio-frequency furnace at 1000 °C. The presence of sufficient amounts of LiF within the reaction mixture resulted in the formation of the two new F-containing phases. Both compounds contain the same structural motifs and crystallize in the monoclinic space group $P2_1/c$ ($LiCa_4Si_4N_8F$) and the tetragonal space group $P4nc$ ($LiSr_4Si_4N_8F$). The crystal structures were solved and refined on the basis of single-crystal X-ray diffraction data ($LiCa_4Si_4N_8F$: a = 10.5108(3), b = 9.0217(3), c = 10.3574(3) Å, β = 117.0152(10)°, R_1 = 0.0422, wR_2 = 0.0724, Z = 4; $LiSr_4Si_4N_8F$: a =9.3118(4), b = 9.3118(4), c = 5.5216(2) Å, R_1 = 0.0160, wR_2 = 0.0388, Z = 2) and were confirmed by lattice-energy calculations (MAPLE), EDX measurements and powder X-ray diffraction. IR spectra proves absence of N-H bonds. Both compounds represent nitridosilicates with the same BCT-zeolite analogous network - exclusively built up of vertex-sharing SiN_4 tetrahedra with Ca^{2+}/Sr^{2+}, Li^+ and F^- ions filling the voids - and are homeotypic with $Li_2Sr_4Si_4N_8O$. The crystal structure of $LiSr_4Si_4N_8F$ incorporates LiF instead of the Li_2O units in case of $Li_2Sr_4Si_4N_8O$. In contrast to

$LiSr_4Si_4N_8F$ $LiCa_4Si_4N_8F$ shows a distortion of the BCT-zeolite analogous framework along with different crystallographic sites and coordinations for fluorine. These two novel compounds are the first F-containing lithium alkaline earth nitridosilicates as well as the first multinary nitride-fluorides consisting of a zeolite-related framework. Furthermore, both compounds are additional examples for the benefits of the engaged synthetic route. This route leads on the one hand to the first compounds in the system Li-*EA*-Si-N-F (*EA* = Ca, Sr). On the other hand it enabled the synthesis of new porous nitridosilicates - without any particular precursors like "$Si(CN_2)_2$", "$Si(NH)_2$" or "$Si_2(NH)_3 \cdot 6NH_4Cl$" – as well as the formation of a zeolite-type nitride framework at moderate temperatures. Thus, it appears to be a promising synthesis route leading to further new (oxo)nitridosilicates with further structural features. The title compounds are stable against air and moisture at ambient temperature and include cavities, so substitution and ion exchange are conceivable. Consequently, the presented combination of nitridosilicates and zeolite-like frameworks could possibly lead to advanced materials properties.

5.4 $Li_{24}Sr_{12}[Si_{24}N_{47}O]F:Eu^{2+}$ - Structure and Luminescence of an Orange Phosphor for Warm White LEDs

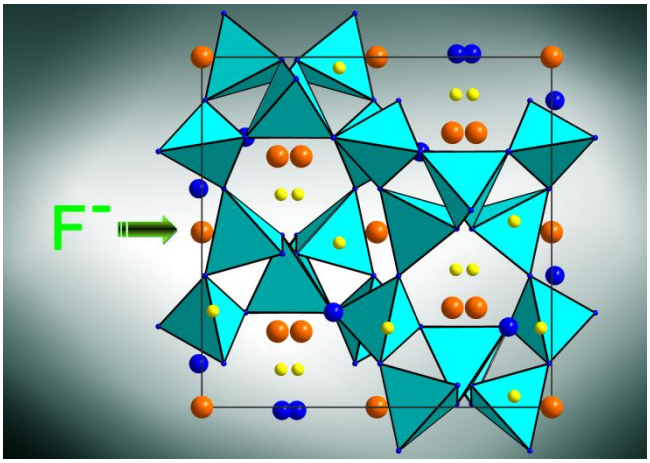

The solid-state metathesis reaction of the reactive starting materials (halides, hydrides, amides) plus the dopant EuF_3 in tungsten crucibles yielded an inhomogeneous sample with orange-colored crystals of $Li_{24}Sr_{12}[Si_{24}N_{47}O]F:Eu^{2+}$. The crystal structure was solved and refined on the basis of single-crystal X-ray diffraction data. $Li_{24}Sr_{12}[Si_{24}N_{47}O]F:Eu^{2+}$ crystallizes in the cubic space group $Pa\overline{3}$ (no. 205) with a = 10.72830(10) Å, R_1 = 0.0401, wR_2 = 0.0885, Z = 1. $Li_{24}Sr_{12}[Si_{24}N_{47}O]F$ is homeotypic with the nitridosilicate $Li_2SrSi_2N_4$. Both compounds are characterized by the identical tetrahedra network topology of vertex-sharing Q^4 type $Si(N/O)_4$ tetrahedra. But $Li_{24}Sr_{12}[Si_{24}N_{47}O]F$ is an oxonitridosilicate and contains an additional F site, which is located at the middle of the cell edges as well as the center of the unit cell. The latter is verified by EDX measurements as well as through calculations with PLATON. The structural motif of the Si(N/O) framework are *siebener* rings build up by four *dreier* rings. One part of the Li^+ and Sr^{2+} ions is located in the channels running parallel to the crystallographic axes of the Si(N/O) network, whereas the remaining part is distributed amongst the voids of the structure. Upon irradiation with blue light, orange to red emission of $Li_{24}Sr_{12}[Si_{24}N_{47}O]F:Eu^{2+}$ (λ_{max} = 598 nm; FWHM = 81 nm) is observed, which differs from that

of $Li_2SrSi_2N_4:Eu^{2+}$ (λ_{em} = 613 nm; FWHM = 86 nm) due to the additional F site. Consequently, the luminescence properties can be easily tuned by further variation of the ratio F/O. Hence, $Li_{24}Sr_{12}[Si_{24}N_{47}O]F:Eu^{2+}$ is an example of a flexible system, which enables tuning of luminescence properties and widens the group of novel orange to red-emitting systems. It has been shown that syntheses based on LiF, hydrides and amides permit a promising synthetic tool - not only concerning the various structural opportunities which were enabled with it - even for the synthesis of novel interesting luminescent materials.

5.5 Li^+ ion Conductivity Investigations of $Li_2SiN_2:Ca,Mg^{2+}$

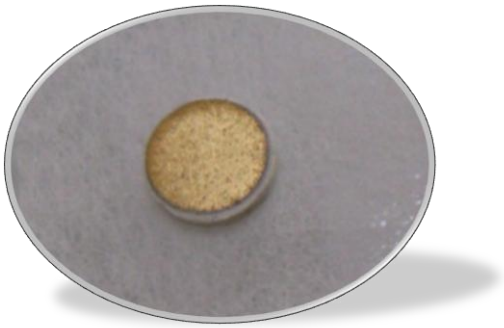

Nitridosilicates are not only interesting regarding their luminescence properties. Ternary lithium nitridosilicates are – due to their lithium ion conductivity - interesting materials for novel solid electrolytes as well. Thus, chemical doping in Li_2SiN_2 with the aim to further improve and optimize the Li^+ ion conductivity in Li_2SiN_2 solid electrolyte was also investigated. Since phase-pure pellets of the samples are indispensible for impedance measurements, intense optimization processes – concerning syntheses as well as pressing of pellets - were performed. Finally, phase-pure samples of Li_2SiN_2, $Li_2SiN_2:Ca^{2+}$and $Li_2SiN_2:Mg^{2+}$ were obtained with Si_3N_4 and were only accessible with double excess of Li_3N and Ca metal or MgH_2, respectively. For pressing pellets under inert conditions, also the starting material "$Si(NH)_2$" had to be exchanged by Si_3N_4. It has not been possible to determine conductivity values so far due to instability of the prepared pellets during the conductivity measurements. Given

that doping of Li_2SiN_2 with Ca^{2+} and Mg^{2+} was successful, only the pellets stability needs to be optimized in future researches to determine the lithium ion conductivity.

6 Appendix

6.1 Supporting Information for Chapter 2.3

Katrin Horky and Wolfgang Schnick, *Eur. J. Inorg. Chem*. **2017**, 1100.

Table S1. Anisotropic displacement parameters (U_{ij} in Å^2) of $Ba_{32}[Li_{15}Si_9W_{16}N_{67}O_5]$ with standard deviations in parentheses.

	U_{11}	U_{22}	U_{33}	U_{12}	U_{13}	U_{23}
W1	0.00467(16)	0.00487(15)	0.00388(15)	0.00080(12)	0.00008(12)	−0.00086(12)
W2	0.00540(15)	0.00386(15)	0.00546(16)	0.00044(12)	0.00170(12)	0.00045(11)
Ba1	0.0098(2)	0.0097()	0.0165(3)	0.00105(19)	0.0042(2)	0.00168(19)
Ba2	0.0179(3)	0.0064(2)	0.0089(2)	−0.00179(19)	−0.0023(2)	0.00132(18)
Ba3	0.0095(2)	0.0089(2)	0.0095(2)	0.00052(19)	0.00010(19)	−0.00126(18)
Ba4	0.0080(2)	0.0077(2)	0.0097(2)	−0.00071(18)	0.00117(19)	0.00162(18)
Si2	0.0107(11)	0.0102(11)	0.0084(11)	0.0004(9)	0.0028(9)	−0.0008(9)

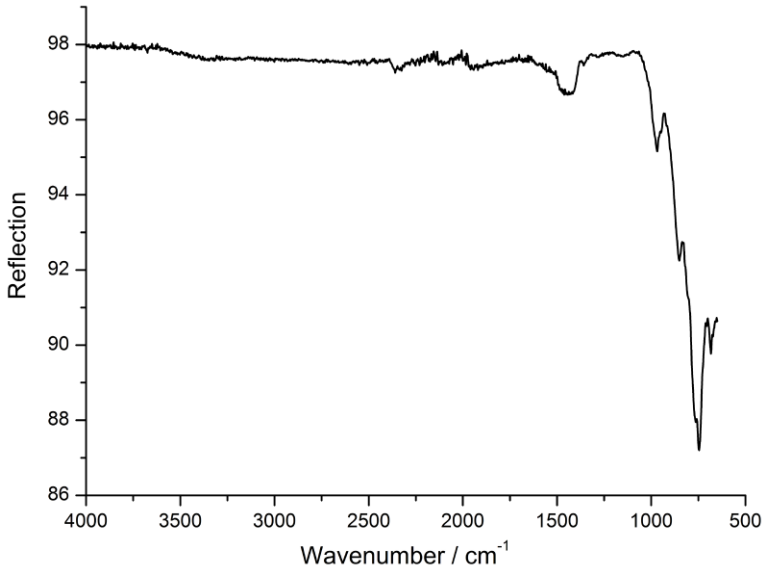

Figure S1. IR spectrum of $Ba_{32}[Li_{15}Si_9W_{16}N_{67}O_5]$.

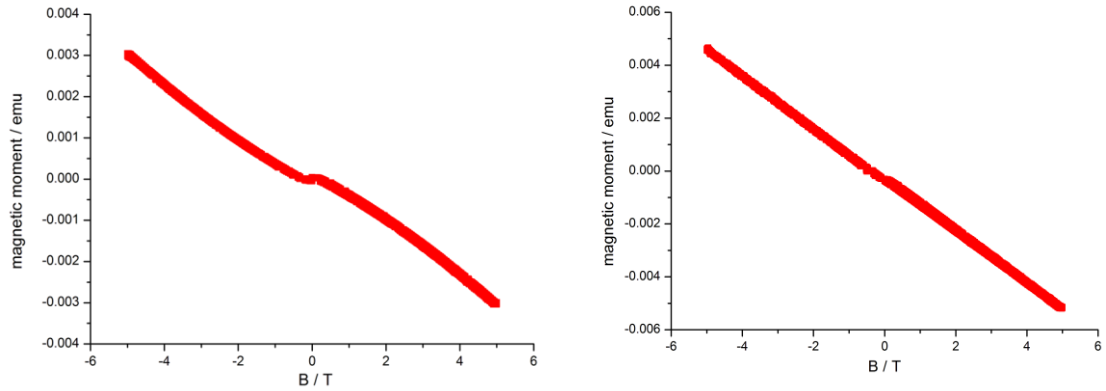

Figure S2. Magnetic moment of $Ba_{32}[Li_{15}Si_9W_{16}N_{67}O_5]$; VSM measurement at 5 K (left) and 295 K (right).

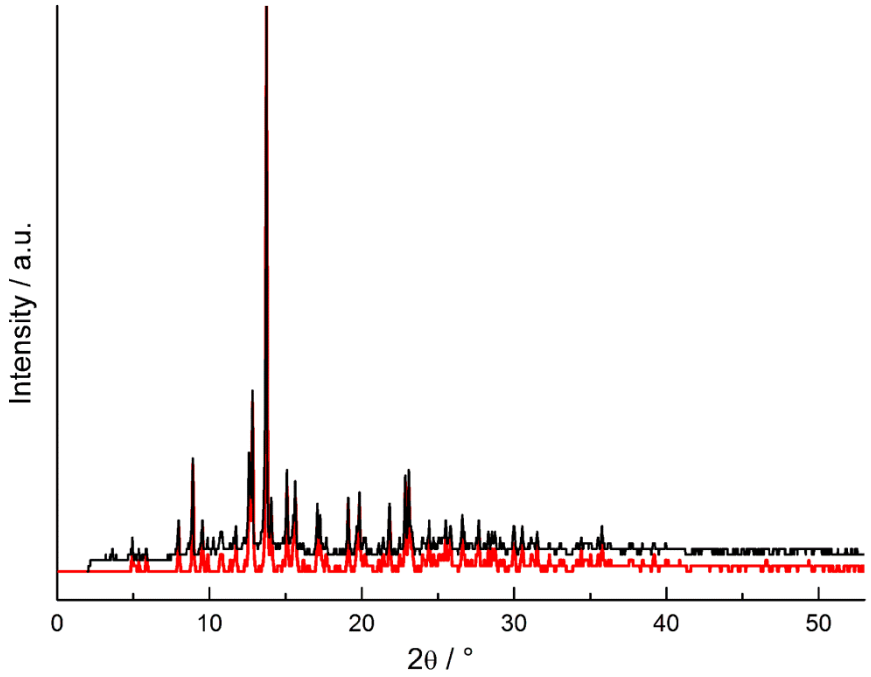

Figure S3. Characteristic section of the experimental powder diffraction pattern (black) of the sample containing $Ba_{32}[Li_{15}Si_9W_{16}N_{67}O_5]$ Red lines describe the simulation of the structural models obtained from single-crystal structure elucidation of the respective compound. Non-described reflections belong to unknown side phases.

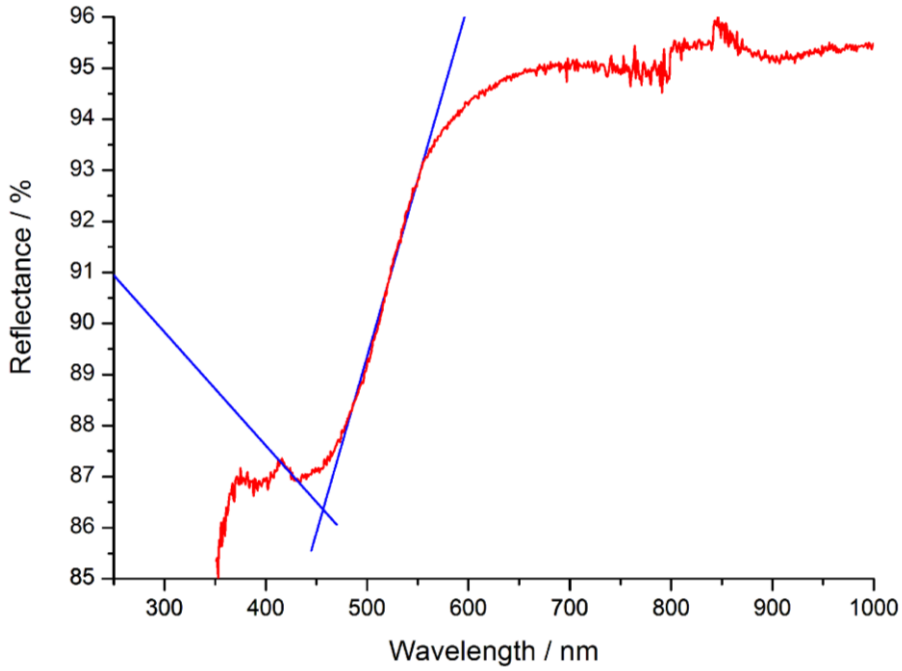

Figure S4. UV-Vis reflectance spectra of $Ba_{32}[Li_{15}Si_9W_{16}N_{67}O_5]$ with plotted tangents to the slope of the reflectance curve (blue).

6.2 Supporting Information for Chapter 2.4

Katrin Horky and Wolfgang Schnick, *Eur. J. Inorg. Chem*. **2017**, 1107.

Table S1. Anisotropic displacement parameters (U_{ij} in Å^2) of $LiCa_4Si_4N_8F$ and $LiSr_4Si_4N_8F$ with standard deviations in parentheses.

	U_{11}	U_{22}	U_{33}	U_{12}	U_{13}	U_{23}
$LiCa_4Si_4N_8F$						
Ca1	0.0080(3)	0.0054(3)	0.0083(3)	0.0001(2)	0.0028(2)	-0.0002(2)
Ca2	0.0058(3)	0.0147(3)	0.0068(3)	-0.0003(2)	0.0036(2)	0.0003(2)
Ca3	0.0077(3)	0.0090(3)	0.0084(3)	-0.0004(2)	0.0057(2)	0.0003(2)
Ca4	0.0083(3)	0.0052(3)	0.0232(3)	-0.0016(2)	0.0043(2)	-0.0002(2)
Si1	0.0039(3)	0.0031(3)	0.0044(3)	0.0007(3)	0.0023(3)	0.0005(3)
Si2	0.0035(3)	0.0038(3)	0.0048(3)	0.0000(3)	0.0025(3)	-0.0001(3)
Si3	0.0034(3)	0.0035(3)	0.0045(3)	0.0001(3)	0.0018(3)	-0.0003(3)
Si4	0.0039(3)	0.0028(3)	0.0053(3)	-0.0004(3)	0.0028(3)	-0.0003(3)
F1	0.0065(12)	0.0220(14)	0.0106(12)	0.0021(11)	0.0033(10)	0.0018(11)
F2	0.0168(15)	0.0099(14)	0.0372(19)	0.0063(13)	-0.0012(13)	-0.0021(12)
N1	0.0076(11)	0.0065(11)	0.0080(11)	-0.0002(9)	0.0055(9)	-0.0011(9)
N2	0.0055(11)	0.0090(11)	0.0065(11)	-0.0008(9)	0.0023(9)	-0.0030(9)
N3	0.0083(11)	0.0051(11)	0.0074(11)	0.0000(9)	0.0055(9)	0.0011(9)
N4	0.0112(11)	0.0043(11)	0.0103(12)	-0.0007(9)	0.0076(10)	-0.0012(9)
N5	0.0063(11)	0.0069(11)	0.0053(11)	-0.0008(9)	0.0026(9)	-0.0004(9)
N6	0.0061(11)	0.0056(11)	0.0053(11)	-0.0003(9)	0.0031(9)	-0.0001(9)
N7	0.0081(11)	0.0079(11)	0.0045(11)	0.0016(9)	0.0029(9)	-0.0001(9)
N8	0.0051(11)	0.0093(11)	0.0078(12)	0.0019(9)	0.0023(9)	-0.0005(9)
Li1	0.018(3)	0.007(2)	0.017(3)	0.002(2)	0.001(2)	0.001(2)
$LiSr_4Si_4N_8F$						
Sr1	0.0033(2)	0.0073(2)	0.0074(2)	-0.0012(12)	0.0001(10)	-0.00015(11)
Si1	0.0025(5)	0.0024(4)	0.0028(6)	0.000(3)	-0.001(3)	0.000
F	0.0107(13)	0.003(6)	0.030(4)	0.000	0.000	-0.0002(3)

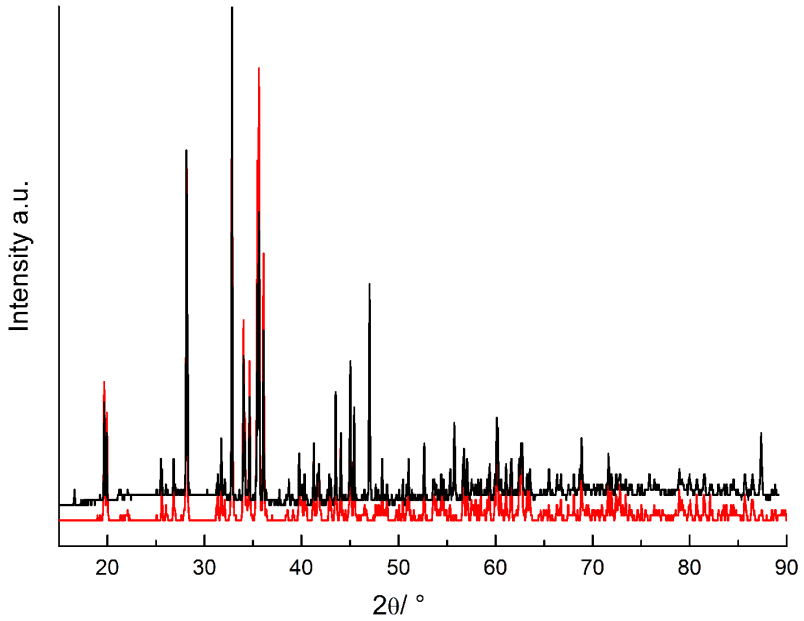

Figure S1. Characteristic section of the experimental powder diffraction pattern (black) of the sample containing $LiCa_4Si_4N_8F$. Red lines describe the simulation of the structural models obtained from single-crystal structure elucidation of the respective compound. Non-described reflections belong to unknown side phases.

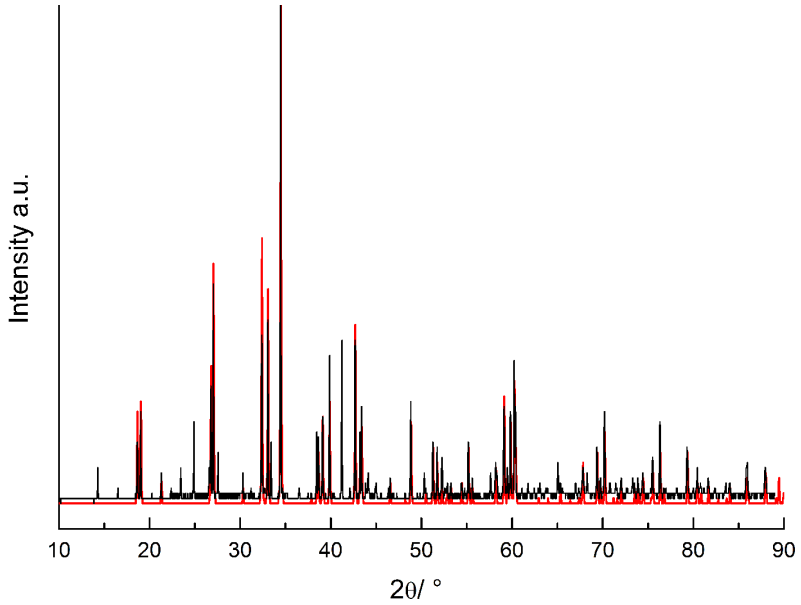

Figure S2. Characteristic section of the experimental powder diffraction pattern (black) of the sample containing $LiSr_4Si_4N_8F$. Red lines describe the simulation of the structural models obtained from single-crystal structure elucidation of the respective compound. Non-described reflections belong to unknown side phases.

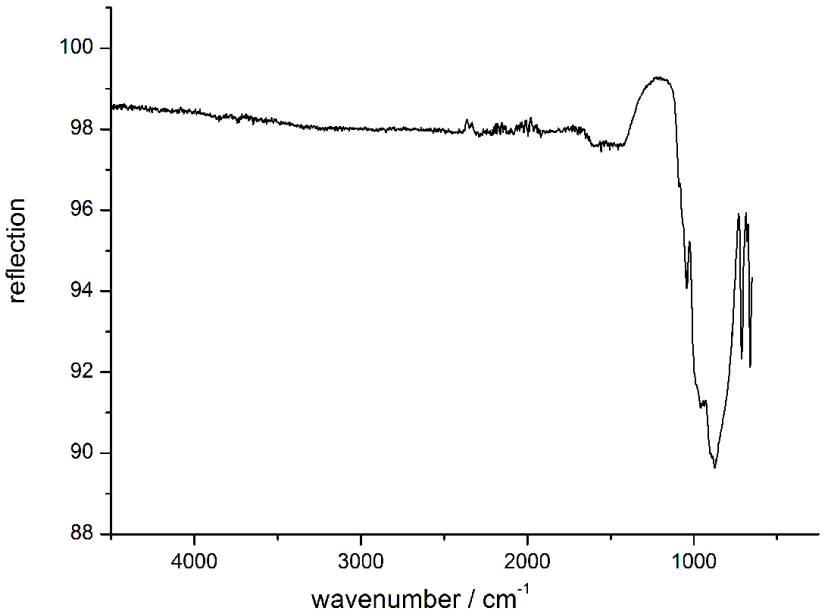

Figure S3. IR spectrum of the sample containing $LiCa_4Si_4N_8F$.

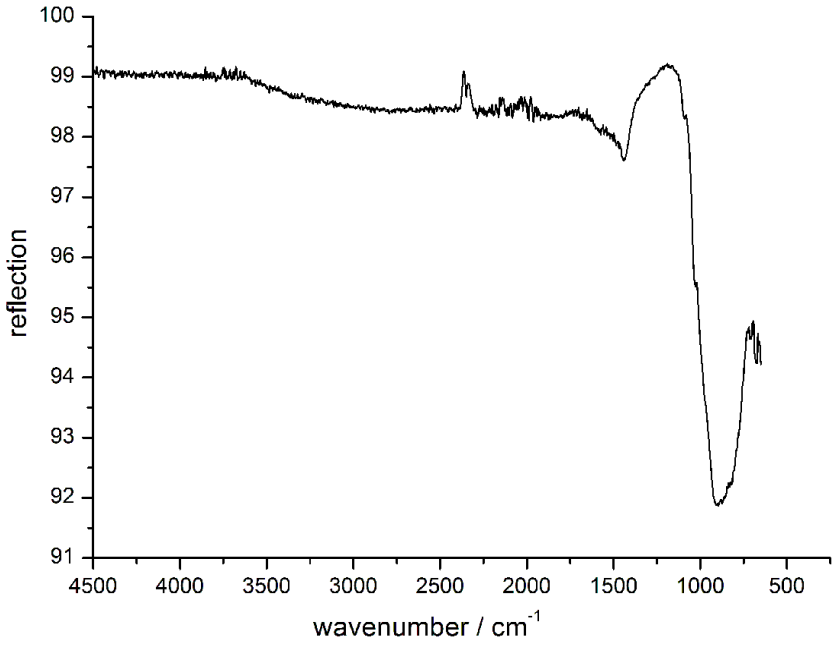

Figure S4. IR spectrum of the sample containing $LiSr_4Si_4N_8F$.

6.3 Supporting Information for Chapter 3.2

Katrin Horky and Wolfgang Schnick, *Chem. Mater.* **2017**, *29*, 4590.

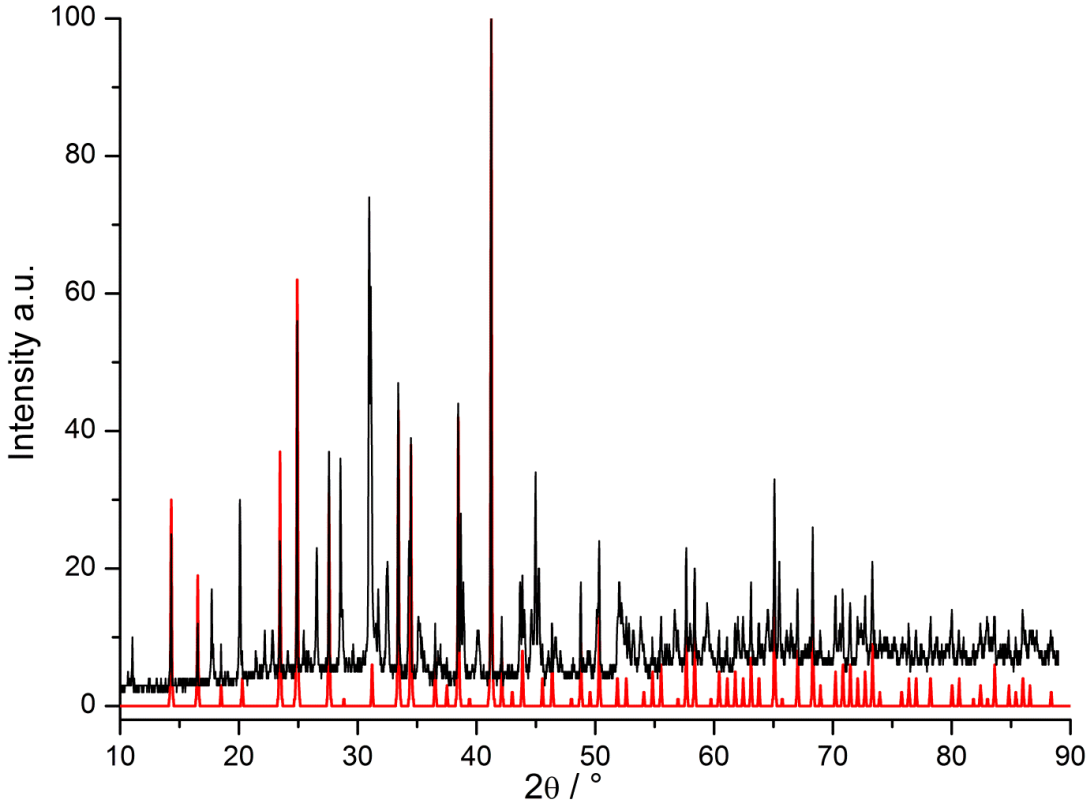

Figure S1. Characteristic section of the experimental powder diffraction pattern (black) of the sample containing $Li_{24}Sr_{12}[Si_{24}N_{47}O]F$. Red lines describe the simulation of the structural model obtained from single-crystal structure elucidation of the respective compound. Non-assigned reflections belong to unknown side phases.

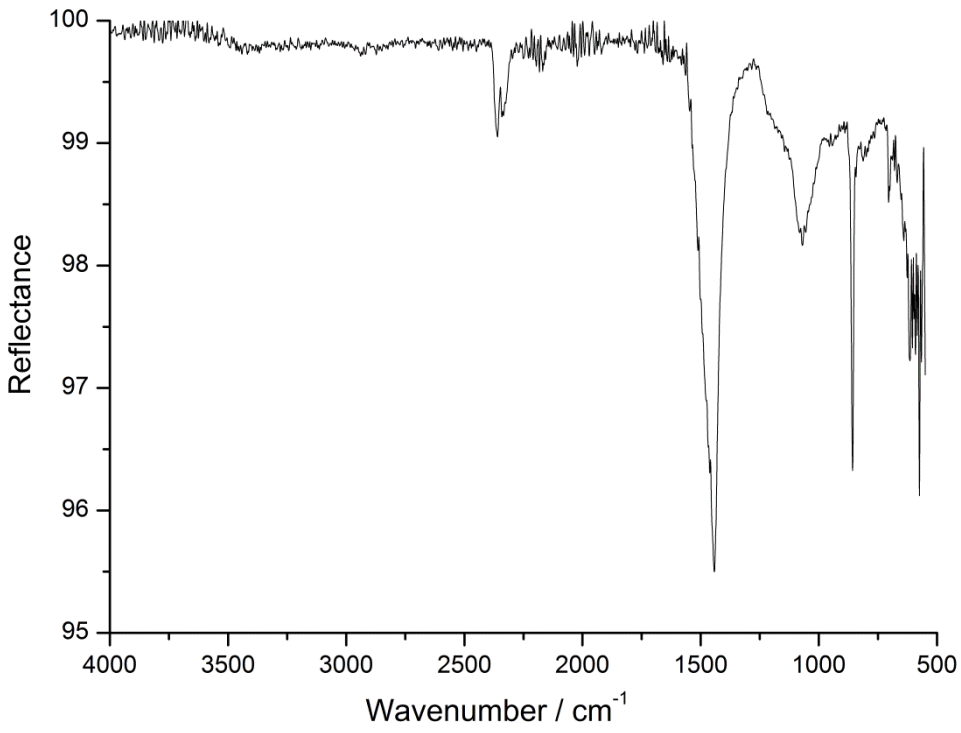

Figure S2. IR spectrum (ATR) of the sample containing $Li_{24}Sr_{12}[Si_{24}N_{47}O]F$.

Table S2. Anisotropic displacement parameters (Uiy, in Å2) (for Sr/Si/NO) of $Li_{24}Sr_{12}[Si_{24}N_{47}O]F$.

atom	U_{11}	U_{22}	U_{33}	U_{23}	U_{13}	U_{12}
Sr1	0.00818(12)	0.00818(12)	0.00818(12)	0.00067(10)	0.00067(10)	0.00067(10)
Sr2	0.01494(17)	0.01494(17)	0.01494(17)	-0.00608(15)	-0.00608(15)	-0.00608(15)
Si1	0.0021(3)	0.0044(3)	0.0022(3)	0.0000(3)	0.0004(2)	-0.0004(2)
N1O1	0.0066(10)	0.0069(10)	0.0039(9)	0.0013(8)	0.0010(8)	0.0005(8)
N2O2	0.0094(11)	0.0131(13)	0.0047(10)	-0.0030(9)	-0.0019(9)	-0.0028(10)

7 Publications

7.1 List of Publications Included in this Thesis

1. **$Ba_{32}[Li_{15}Si_9W_{16}N_{67}O_5]$- a Ba-containing Oxonitridolithotungsto-silicate with a Highly Condensed Network Structure**

Katrin Horky and Wolfgang Schnick

Eur. J. Inorg. Chem. **2017**, 1100.

For this article, writing the manuscript, syntheses of the samples, single-crystal refinements, evaluation of spectroscopic data and MAPLE calculations were performed by K. Horky. W. Schnick supervised the work and revised the manuscript.

2. **$LiCa_4Si_4N_8F$ and $LiSr_4Si_4N_8F$ – Nitridosilicate Fluorides with a BCT-Zeolite Type Network Structure**

Katrin Horky and Wolfgang Schnick

Eur. J. Inorg. Chem. **2017**, 1107.

For this publication, writing the manuscript, syntheses of the samples, single-crystal refinements, evaluation of spectroscopic data and MAPLE calculations were performed by K. Horky. W. Schnick supervised the work and revised the manuscript.

3. $Li_{24}Sr_{12}[Si_{24}N_{47}O]F:Eu^{2+}$ - Structure and Luminescence of an Orange Phosphor

Katrin Horky and Wolfgang Schnick

Chem. Mater. **2017**, *29*, 4590.

In this contribution, writing the manuscript, syntheses of the samples and structure determination based on single-crystals, evaluation of spectroscopic data, investigations with PLATON and MAPLE calculations were performed by K. Horky. W. Schnick supervised the work and revised the manuscript. Luminescence investigations and interpretation of measured values were done in the LDC Aachen by Petra Huppertz and Peter Schmidt.

7.2 Conference Contributions

Lithiumnitridosilicate (talk)

K. Horky, W. Schnick

Obergurgl-Seminar Festkörperchemie, Obergurgl, 2014.

7.3 CSD Numbers

$Ba_{32}[Li_{15}Si_9W_{16}N_{67}O_5]$	CSD - 432182
$LiCa_4Si_4N_8F$	CSD - 432268
$LiSr_4Si_4N_8F$	CSD - 432269
$Li_{24}Sr_{12}Si_{24}N_{47}OF:Eu^{2+}$	CSD - 432550